TELLUS BORDER
Understanding Underground

European Union
European Regional Development Fund
Investing in your future

A project supported by the INTERREG IVA Programme managed by the Special EU Programmes Body

Tellus Border project

Airborne Geophysics Data Processing Report

Version 1

Authors:
J. A. Hodgson, M. D. Ture

Geological Survey of Ireland and Geological Survey of Northern Ireland joint report
2013

Geological Survey of Ireland

The Geological Survey of Ireland is responsible for providing geological advice and information, and for the acquisition of data for this purpose. GSI produces a range of products including maps, reports and databases and acts as a knowledge centre and project partner in all aspects of Irish geology. GSI is a division of the Department of Communications, Energy & Natural Resources (DCENR).

Geological Survey of Ireland

Beggars Bush

Haddington Road

Dublin 4

Ireland

Tel. +353-1-678 2000
Fax +353-1- 668 1782
Email: tellusborder@gsi.ie
Web: www.gsi.ie

Geological Survey of Northern Ireland

The Geological Survey of Northern Ireland is part of the Department of Enterprise, Trade and Investment (DETI). GSNI provides geoscience information and services to inform decision making, promote economic development and assist environmental management in Northern Ireland.

Geological Survey of Northern Ireland

Geological Survey of Northern Ireland

Colby House

Stranmillis Court

Belfast

BT9 5BF

Northern Ireland

Tel: +44 (0)28 9038 8462
Fax: +44 (0)28 9038 8461
Email: gsni@detini.gov.uk
Web: bgs.ac.uk/gsni

The Tellus Border project

Tellus Border is a geo-environmental mapping project which provides data on soils, waters and rocks across the border region of Ireland and integrates these with existing data in Northern Ireland. This cross-border collaboration between the Geological Survey of Ireland, the Geological Survey of Northern Ireland and research partners supports the assessment of natural resources, sustainable environmental management and improvement of geological mapping on the island of Ireland. For more information on Tellus Border please see www.tellusborder.eu.

Tellus Border is funded by the INTERREG IVA development programme of the European Regional Development Fund, which is managed by the Special EU Programmes Body (SEUPB). The SEUPB is a North/South Implementation Body sponsored by the Department of Finance and Personnel in Northern Ireland and the Department of Finance in Ireland. It is responsible for managing two EU structural funds Programmes PEACE III and INTERREG IV designed to enhance cross-border co-operation, promote reconciliation and create a more peaceful and prosperous society. For more information on the SEUPB please visit www.seupb.eu.

Tellus Border is additionally part funded by the Department of Environment, Community and Local Government in Ireland and the Department of the Environment in Northern Ireland.

Disclaimer

Copyright

Document Information

Written by:	**Position**	**Date**
Jim Hodgson	Assistant Project Geophysicist	11th January 2013
Mohammednur Desissa Ture	Project Geophysicist	11th January 2013
Reviewed by:		
Mike Young	Director GSNI	29th January 2013
Mairead Glennon	Assistant Project Manager	30th January 2013
Ray Scanlon	GSI Manager	31st January 2013

Change record

Date	**Author**	**Version**	**Details**
5th February 2013	J. A. Hodgson, M. D. Ture	Version 1	Report on processing and data merging of the magnetic and radiometric data.

Executive Summary

The Tellus Border project is a geochemistry and airborne geophysical survey of the six northern counties of the Republic of Ireland, funded by the INTERREG IVA programme of the European Regional Development Fund. It is an extension of the successful Tellus project of Northern Ireland *(http://www.bgs.ac.uk/gsni/tellus/).* The project objective is to create a seamless cross-border geo-environmental baseline dataset incorporating new and existing data. This report outlines the merging procedure and reviews the main processing carried out to individual geophysical datasets.

The new airborne data was collected within the border counties of Donegal, Leitrim, Sligo, Cavan, Monaghan and Louth in the Republic of Ireland (ROI).Surveying was carried out between October 2011 and July 2012. Previous airborne geophysical surveys were carried out across Northern Ireland (Tellus) in 2005 and 2006 (Beamish *et. al*, 2006 a,b,c) and a pilot study covering parts of the counties of Cavan and Monaghan in the ROI *(*Kurimo*,* 2006*, GSI 2006 Internal report).* All surveys measured magnetic field, electrical conductivity and gamma-radiometric spectrometer data (primarily potassium, thorium and uranium). The same survey specifications were used for each survey to assist in the merging of the different data sets.

Final merged data is to be released in February 2013. However due to need for further processing of the electrical conductivity data version 1 of this report will deal with only the final production of the magnetic and radiometric data. Version 2 of this report will include all data when it becomes available.

As the data falls within different jurisdictions it is subject to different agreements and levels of availability. All data within the ROI except for one area under commercial licence is free to all. Release of data from Northern Ireland is subject to data-licensing, which is free to non-profit organisations.

The full processing reports from the contractors who carried out the surveys are contained in appendices at the end of this report.

Acknowledgements

Dave Beamish's help was crucial in the successful completion of the survey. His hard work in assisting in the operation of the survey, detailed processing and continued advice were greatly appreciated. The contribution of the whole Tellus Border team (Ray Scanlon, Marie Cowen, Shane Carey, Kate Knights, Claire McGinn) all helped in making the geophysical survey such a success. In particular great support was received in the outreach program carried out for the airborne survey, management of the data and making the data available on-line.

Table of Contents

List of Tables

List of Figures

1 Introduction

This report describes the processing of airborne geophysical data of the six northern counties of the Republic of Ireland (Tellus Border) and subsequent merging of this data with existing airborne geophysics data for Northern Ireland (Tellus) and a previous pilot survey (Cavan). The Tellus Border project is funded by the INTERREG IVA programme of the European Regional Development Fund.

The contract for the survey was commissioned by the Central Procurement Directorate on behalf of Geological Survey of Northern Ireland (GSNI), the Lead Partner. The contract is being managed by GSNI with the assistance of the Geological Survey of Ireland (GSI).

The full merged data set of the 12 northern counties of the island of Ireland include data from:

(1) Tellus Border carried out by Sander Geophysics Ltd between 2011 and 2012. An industry survey was completed for Oriel Selection Trust Ltd at the same time as Tellus Border in the Charlestown Block in Co. Mayo. The Charlestown survey data is subject to data release agreement (1st April 2013).
(2) Tellus survey of Northern Ireland carried out by Joint Airborne-geoscience Capability (JAC) joint venture between the Geological Survey of Finland and the British Geological Survey between 2005 and 2006.
(3) Cavan pilot study carried out by JAC in 2006.

Figure 1 shows the areas covered by the different surveys.

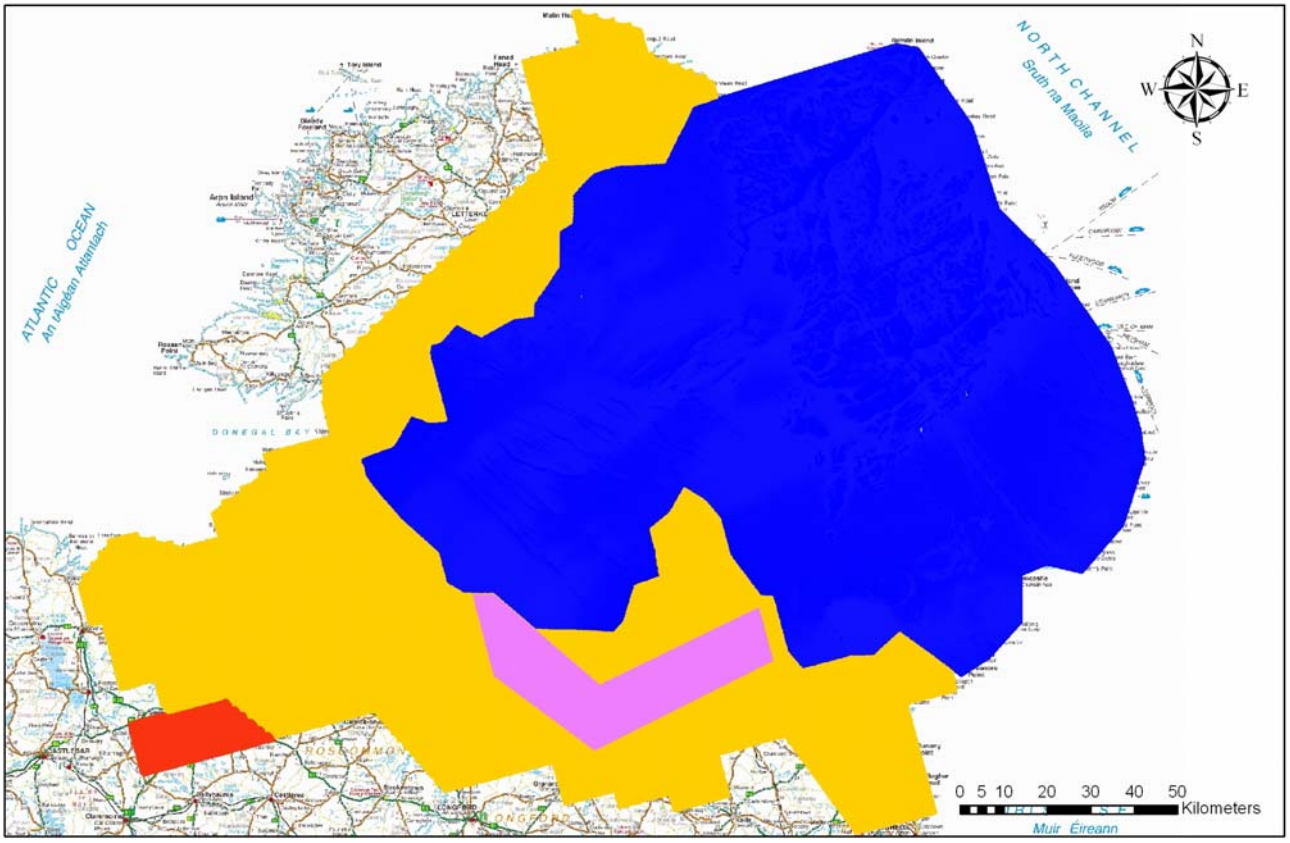

Figure 1: Different Survey areas, *Yellow*-Tellus Border, *Blue*-Tellus, *Pink*-Cavan and *Red*-Charlestown.

The full processing report compiled by Sander Geophysics, including all calibrations for the Tellus Border and Charlestown surveys, is contained within Appendix I. The processing report compiled by JAC for the Tellus and Cavan surveys (Beamish 2006c) can be downloaded from http://nora.nerc.ac.uk/7427/1/IR06136.pdf

Version 1 of this report deals with the final processing and data merging of the magnetic and radiometric data. The electromagnetic conductivity data will be reported in Version 2 following the completion of the data processing and data merging.

2 Survey Details

2.1 Overview

The different geophysical airborne surveys all recorded magnetic, frequency domain electromagnetic and radiometric data. The geophysical systems, on board a De Havilland Twin Otter aircraft, are described by Hautaniemi *et al*., (2004). All data were collected using the same specifications with the exception of electromagnetic data which saw a change in the number of frequencies used between the first and second phase of the Tellus survey (Beamish *et al.* 2006 a,b,c).

2.2 Tellus Border Specifications

The Tellus Border survey was flown between October 2011 and July 2012. A total of 57,681 line km were surveyed. The database includes 1799 survey lines and 154 tie (control) lines. The total area covered by the survey was *c.*10,484 km^2. Survey specifications are shown in Table 1. The Charlestown survey was flown at the same time as the Tellus Border survey and was included within the final data delivery from the contractor. Due to licensing agreements the data is masked from general availability.

Table 1: Tellus Border Survey Specifications

Survey line spacing	200 m
Survey line direction	345 degrees
Tie line spacing	2000m
Tie line direction	75 degrees
Minimum survey altitude (rural)	59 m
Maximum survey altitude (other)	240 m
Typical survey speed	60 m/s
Magnetic sampling	0.1 sec
Electromagnetic sampling	0.1 sec
Radiometric sampling	1.0 sec
GPS positional sampling	1.0 sec
Magnetic/GPS base station sampling	1.0 sec
Radiometric total energy range	0.396-2.808 MeV
Electromagnetic Frequencies	0.912, 3.005, 11.962 & 24.510 kHz

A full account of the survey is given in the Final Processing Report in Appendix I.

2.3 Tellus & Cavan Specifications

The Tellus survey was carried out for the entirety of Northern Ireland with the western half of the country surveyed in 2005 and the eastern half in a second phase in 2006 (Beamish *et al.* 2006, a b,c). A total of 80,458 line km were surveyed along 2,209 lines. Table 2 outlines the main survey specifications.

Table 2: Tellus Survey Specifications

Survey line spacing	200 m
Survey line direction	345 degrees
Tie line spacing	2000m
Tie line direction	75 degrees
Minimum survey altitude (rural)	56 m
Maximum survey altitude (other)	244 m
Typical survey speed	70 m/s
Magnetic sampling	0.1 sec
Electromagnetic sampling	0.25 sec
Radiometric sampling	1.0 sec
GPS positional sampling	1.0 sec
Magnetic/GPS base station sampling	1.0 sec
Radiometric total energy range	0.41-2.81 MeV
Electromagnetic Frequencies (Phase 1)	3.125 & 14.368 kHz
Electromagnetic Frequencies (Phase 2)	0.912, 3.005, 11.962 & 24.510 kHz

The Cavan survey is the smallest of the three datasets and includes 315 lines with a total length of 5,110 km covering an area of 1,006 Km^2. The same survey specifications were used for the Cavan pilot survey as were used for Tellus Phase 2, outlined in Table 2.

3 Data Processing Overview

3.1 Tellus Border

3.1.1 Magnetic Processing

The magnetometer in the left wing was found to be more reliable and less noisy than the magnetometer from the nose and was used in all processing. Standard magnetic survey calibrations and corrections were applied to all data by the contractor. Data processing of the survey data was also carried out by the contractor and comprised (1) height adjustment, (2) tie-line levelling and (3) micro-levelling. A full description of all calibrations, applied corrections and processing steps can be found in Appendix I.

The contractor supplied data in ASCII.xyz and Geosoft grid format. Table 3 outlines all the delivered data.

Table 3: Contractor Supplied Magnetic Data for Tellus Border

No	Name	Units	Comment
1	DATE	-	Date YYYYMMDD
2	DAY	-	Day
3	FLIGHT	-	Flight number
4	LINE	-	Line number
5	TIME	s	UTC seconds
7	RADAR_ALT	m	Radar Altimeter
8	LASER_ALT	m	Laser Altimeter
9	RAW_RADAR	m	Raw Radar
10	RAW_LASER	m	Raw Laser
11	X-IRISH-NG	m	X coordinate,
12	Y-IRISH-NG	m	Y coordinate,
13	X-IRISH-WING	m	X coordinate for wing
14	Y-IRISH-WING	m	Y coordinate for wing
15	MSLHGT	m	Height above mean sea level
16	X-LONG	m	X coordinate,
17	Y-LAT	m	Y coordinate,
18	X-LONG-WING	m	X coordinate,
19	Y-LAT-WING	m	Y coordinate,
20	WGSHGT	m	WGS-84 Altitude
21	HEADING	deg	Aircraft heading
22	DIURNAL	nT	Diurnal correction
23	IGRF	nT	IGRF value

24	RAWMAG2	nT	Raw compensated magnetic values
25	DICMAG2	nT	Diurnally Corrected magnetic value
26	LEVMAG2	nT	Levelled WING magnetic value
27	MICROLEVMAG2	nT	Microlevelled WING magnetic value

Following diurnal corrections all data was IGRF corrected using the date at each point based on 2010 model and DGPS heights above GRS-80 ellipsoid.

Figure 2 below shows the magnetic anomaly map produced from the Tellus Border data after processing.

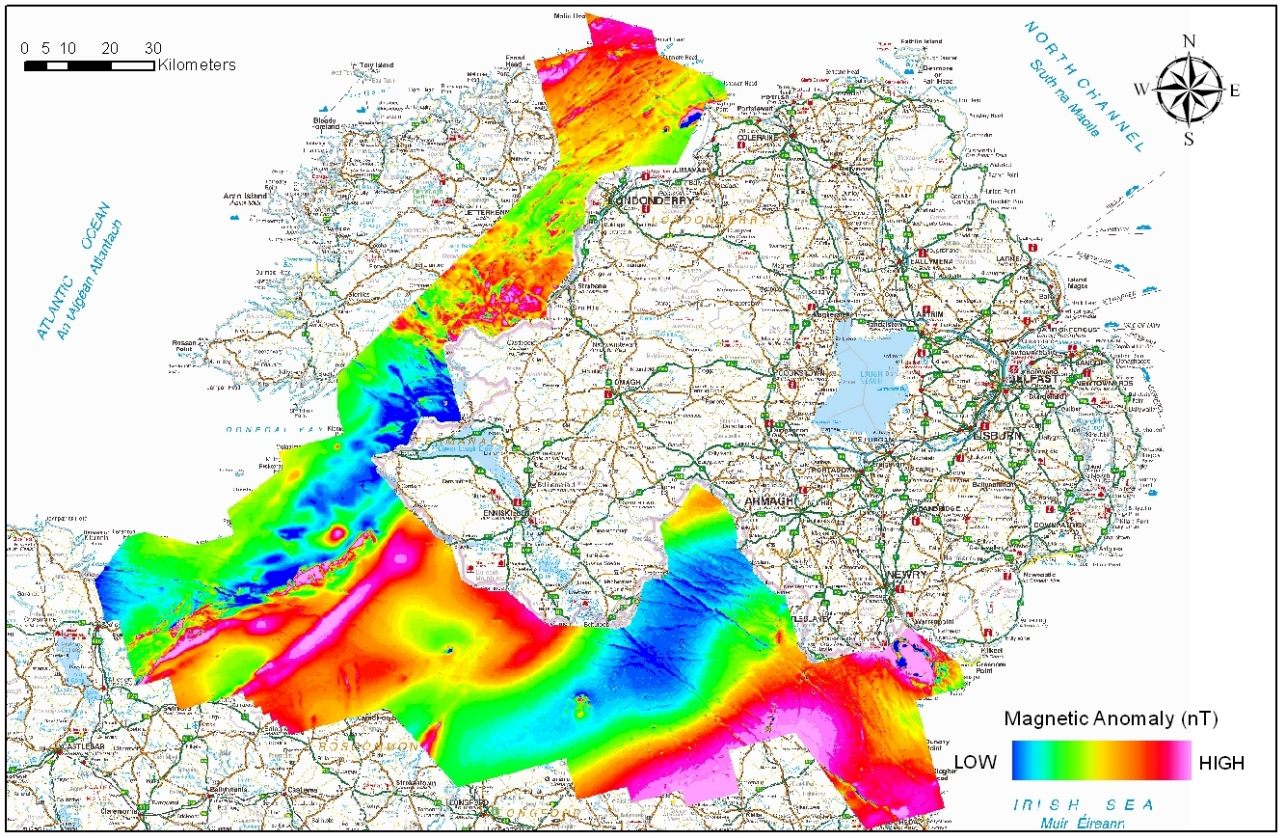

Figure 2: Magnetic anomaly data for Tellus Border

3.1.2 Radiometric Processing

Standard radiometric survey calibrations and corrections were applied to all data by the contractor. Data processing of the survey data was also carried out by the contractor and comprised;

1. Dead time correction
2. Calculation of effective height above ground level

3. Lag correction
4. Height adaptive filter
5. Removal of cosmic and aircraft background radiation
6. Radon background corrections
7. Stripping correction
8. Conversion to radio element concentrations
9. Altitude attenuation corrections
10. Data gridding

A full description of all calibrations, applied corrections and processing steps can be found in Appendix I.

The contractor supplied data in ASCII.xyz and Geosoft grid format. Table 4 outlines all the delivered data.

Table 4: Contractor Supplied Radiometric data for Tellus Border

No	Name	Units	Description	Comment	Comment
1	DATE	-	Date	YYYYMMDD	
2	DAY	-	Day	Julian Day	
3	FLIGHT	-	Flight	number	
4	LINE	-	Line	number	
5	TIME	-	UTC	seconds	past midnight
6	X-IRISH-NG	m	X	coordinate,	Irish National Grid
7	Y-IRISH-NG	m	Y	coordinate,	Irish National Grid
8	MSLHGT	m	Altitude	Mean Sea Level	
9	WGSHGT	m	WGS-84	Altitude	
10	ALTIMETER	m	Altimeter	height	
11	BARO	m	Barometric	Altitude	
12	TEMP	celcius	Temperature		
13	LIVE	msec	Live	Time	
14	COSMIC	counts/s	Recorded	Cosmic	Count
15	UP	counts/s	Recorded	Upward	Uranium count
16	RAW_TOT	counts/s	Recorded	Total	Count
17	RAW_K	counts/s	Recorded	Potassium	Count
18	RAW_U	counts/s	Recorded	Uranium	Count
19	RAW_TH	counts/s	Recorded	Thorium	Count
20	COR_TOT	counts/s	Corrected	Total	Count, de-lagged
21	E_Dose	nGy/hr	Air	absorbed	dose

22	COR_K	%	Corrected	Potassium	Concentration, de-lagged
23	COR_U	ppm	Corrected	Uranium	Concentration, de-lagged
24	COR_TH	ppm	Corrected	Thorium	Concentration, de-lagged
25	C_Uml	ppm	Corrected	Uranium	Concentration, microlevelled
26	COR_TOTL	counts/s	Corrected	Total	Count, de-lagged, minimum limited to 0
27	E_DoseL	nGy/hr	Air	absorbed	dose, minimum limited to 0
28	COR_KL	%	Corrected	Potassium	Concentration, de-lagged, minimum limited to 0
29	COR_UL	ppm	Corrected	Uranium	Concentration, de-lagged, minimum limited to 0
30	COR_THL	ppm	Corrected	Thorium	Concentration, de-lagged, minimum limited to 0
31	C_UmlL	ppm	Corrected	Uranium	Concentration, microlevelled, minimum limited to 0
32	LAT	DEGREE	Latitude		
33	LONG	DEGREE	Longitude		

3.1.2.1 256 Channel and Cs-137 Processing

Caesium-137 data processing was undertaken by Mohammednur Desissa (GSNI) using the PRAGA4 package from Geosoft and following the procedure used by Schreib et al 2010. The standard processing steps are described below. The Geosoft database consisting of 256 by 256 array channels (Down-256 and Up-256) and other necessary channels (radar altimeter, barometer, temperature etc) were created and processed from raw data files supplied by the contractor.

3.1.2.2 Energy Calibration

The lowest energy window used for Cs-137 processing was 400KeV and the maximum was 1860KeV. The natural radionuclide peaks present in the energy window (i.e. nine man made and three natural nuclides) resulting in 12 in total were then used and stacked. This resulted in comparable means from all data sets (Tellus Border, Cavan and Tellus).

3.1.2.3 Spectrum Fitting

Following average spectrum data fitting all natural and man-made nuclides were selected**.** Positions of peak plot were checked and compared with standard positions for peaks of K, not selected would produce false results as their contribution will be attributed to another nuclide. Calibration constants from the contractor's report were used (Appendix I , Beamish 2006c).

3.1.2.4 Background Model

Aircraft and cosmic background models provided with software and the contractor's calibration constants were compared with the survey data and corrections applied.

3.1.2.5 Standard Temperature and Pressure

Standard temperature and pressure (STP) values from a fixed altitude (80m) were calculated. All nuclides were then selected for fitting and model detector responses were interpolated for current STP altitudes.

3.1.2.6 Response Fitting

Response fitting was apples and consisted of inputting the measured responses into a spectrum and sorting the data using least-squares technique, weighted by a variance of the signal across the spectrum. The smoothed spectrum processed by normal windows processing and by Noise Adjusted Single Value Decomposition (NASVD) methods were used for comparison. The NASVD result was shown to be better and this output was used for merging. All results were then output into a new database.

3.1.2.7 Radon Analysis and Removal

Radon removal is one of the most challenging aspects of radiometric data processing as it is often localised and dependant on variations in the weather. Although different processing options are available, the spectral ratio method was applied. The spectral ratio method after Minty (1997), is based on the 609 keV and 1765 keV photo peaks of 214Bi and has been to date the most accepted technique for radon removal. Radon was analysed and removed from the data using smoothed spectrum (windows processing and NASVD).

3.1.2.8 Principal component analysis (PCA)

Twenty five Eigen values were used in PCA processing. A 25, 2N+1 standard approach, where N is number of nuclides considered in the processing was used. After statistics were collected, NASVD was processed (i.e. Eigen vectors computed and stored into project). Results were assessed using functionality included in the Interactive mode of PRAGA4. The signature components were found using PCA which then subtracts the noise. A co-variance matrix of 256 by 256 was used as input for the transformation.

3.2 Tellus & Cavan

Processing of these data are described in Beamish *et al*. (2006), (http://nora.nerc.ac.uk/7427/1/IR06136.pdf)

3.2.1 Magnetic Processing

Standard magnetic survey calibrations and corrections were applied to all data by the contractor. Data processing of the survey data was also carried out by the contractor and comprised (1) tie-line levelling and (2) micro-levelling.

The contractor supplied data in ASCII.xyz and Geosoft grid format. Table 5 outlines all the delivered data.

Table 5: Contractor Supplied Magnetic Data for Tellus and Cavan

No	Name	Units	Comment	Comment
1	X:	m	Grid	Easting
2	Y:	m	Grid	northing
3	LAT:	degrees	WGS84	latitude
4	LONG:	degrees	WGS84	longitude
5	FID:	sum	Numerical	sum
6	Area:	sum	Tellus	survey
7	Flight:	sum	Flight	number
8	DATE:	sum	Date	(YYYYMMDD)
9	Day:	sum	Day	Julian Day
10	Time:	sec	Time	(HHMMSS.SS)
11	DIR:	degrees	Flight	Direction
12	RALT:	m	Radar	altitude
13	GPS_H:	m	GPS	altitude
14	DTM:	m	Digital	Terrain
15	MAG_MID:	nT	Total Field	magnetic
16	BASE:	nT	magnetic	basestation
17	GRAD_PERP:	nT/m	perpendicular	gradient
18	MAG_ML:	nT	microlevelled	magnetic
19	MAG_IGRF:	nT	IGRF	field
20	MAG_RES:	nT	Magnetic	anomaly

Following diurnal corrections all phase 1 data was IGRF corrected using the date of the setup of the base station (01/06/2005) based on the 2005 model, while Cavan data used IGRF calculated on

the start of the survey date (06/06/2006) with GPS_H heights above geoid WGS-84 at latitude, longitude point locations.

Figures 3 & 4 below show the magnetic anomaly map produced from the Tellus and Cavan data after processing.

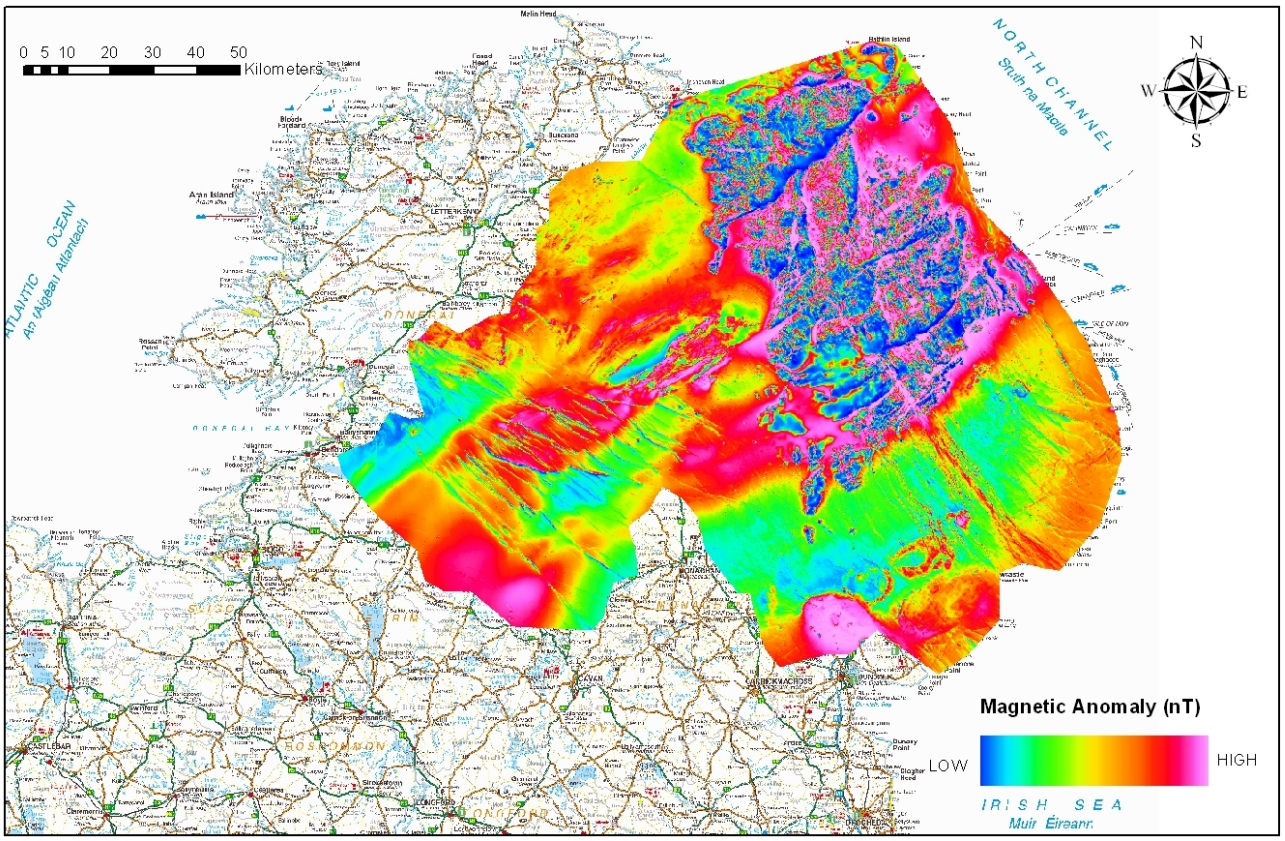

Figure 3: Magnetic Anomaly data for Tellus

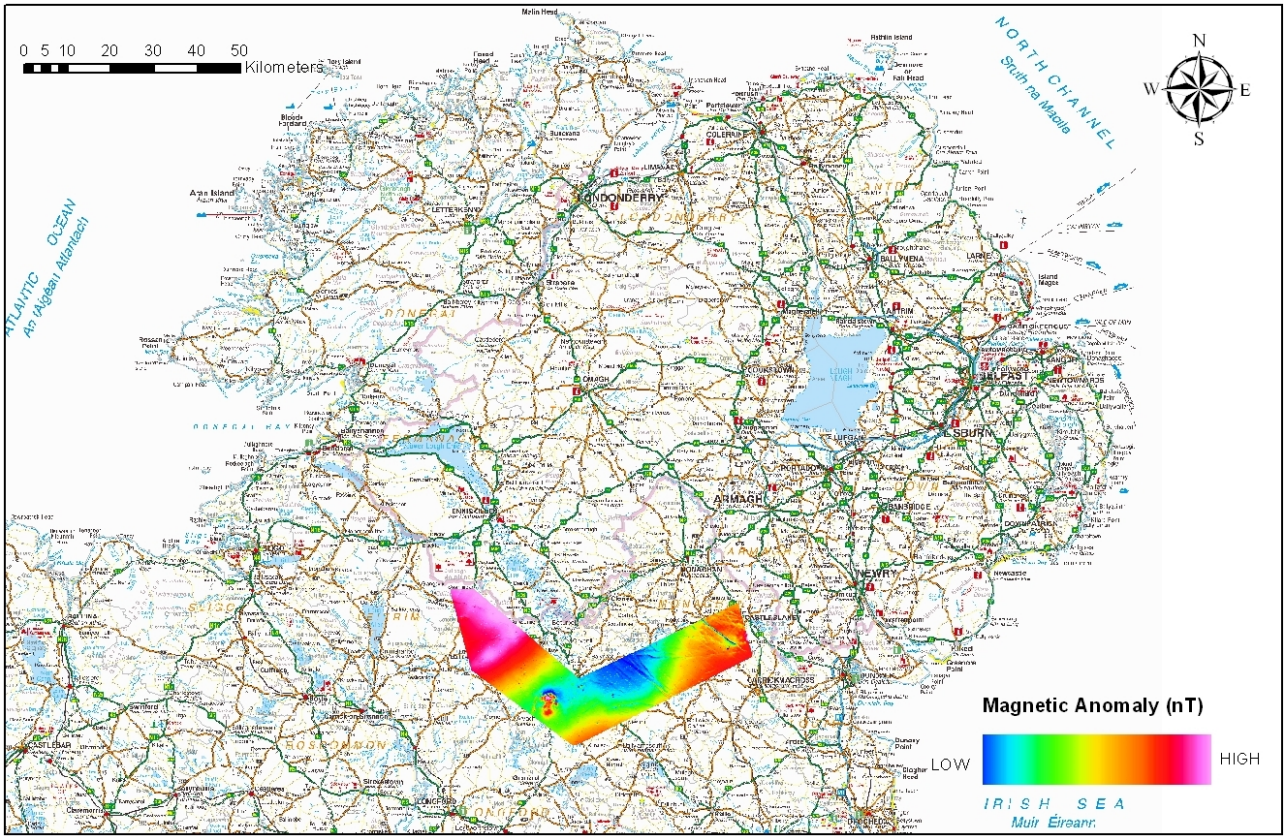

Figure 4: Magnetic anomaly data from Cavan

3.2.2 Radiometric Processing

Standard radiometric survey calibrations and corrections were applied to all data by the contractor using the methods described by Grasty and Minty (1995 a,b) and IAEA (1991, 2003). Data processing carried out by the contractor comprised;

1. Dead time correction
2. Digital filtering before correction
3. Lag correction
4. Effective height and altitude attenuation corrections
5. Removal of cosmic and aircraft background radiation
6. Radon background corrections
7. Stripping Correction
8. Conversion to radio element concentrations
9. Levelling
10. Greens radon levelling
11. Data Gridding

A full description of all calibrations, applied corrections and processing steps can be found in Appendix II and in further detail in Hautaniemi *et al*. 2005.

The contractor supplied data in ASCII.xyz and Geosoft grid format. Table 6 outlines all the delivered data.

Table 6: Contactor Supplied Radiometric Data for Tellus and Cavan

No	Name	Units	Comment	
1	X:	(m)	Easting	Grid
2	Y:	(m)	Northing	Grid
3	LAT:	degrees	latitude	WGS84
4	LONG:	degrees	longitude	WGS84
5	FID:	sum	numerical	
6	Flight:	No	Flight Number	
7	Day:	No	Julian day	
8	Date:	(YYYYMMDD)	Date	
9	Time:	(HHMMSS.SS)	(HHMMSS.SS)	Time
10	DIR:	degrees	direction	Flight
11	RALT:	(m)	altitude	Radar
12	BALT:	(m)	altitude	Barometric
13	TOUT:	degrees	temperature	External
14	GPS_H:	(m)	altitude	GPS
15	DTM:	Model	Terrain	Digital
16	D_TOT_CPS:	Ur	Total Counts	sum of all counts
17	D_TOT_NGY:	nGy/h	Total Counts	Dose Rate
18	D_KAL:	%	Potassium	
19	D_URA:	pp	Uranium	
20	D_THO:	pp	Thorium	

3.2.3 256 Channel and Cs-137 Processing

Caesium-137 values from the Tellus and Cavan data sets were extracted and processed by BGS. The processing is outlined in Beamish 2006c but section 3.1.3 above outlines the main processing steps carried out for the Tellus Border data, which was based on that done for Tellus.

4 Data Merging Overview

4.1 Master Database

One of the project goals of the Tellus Border project was to merge the newly acquired data with existing data from Northern Ireland and Cavan to produce a seamless data set. During the survey design for Tellus Border overlaps with the previous data were planned along with a test line that was flown 5 different times throughout the duration of the survey.

A master database was created from the 3 contractor provided databases

1. Tellus Border (TB)
2. Tellus (TEL)
3. Cavan (CAV)

Not all channels from the contractor-supplied data were deemed necessary for the final master database and therefore for each database (1) magnetics and (2) radiometrics relevant channels were selected (see readme files in section 5). A uniform name was applied to each of the relevant channels for each of the 3 contractor supplied databases.

To allow easy comparison with the original contractor supplied data the original line numbers have been kept with a new prefix of **B** for Tellus Border Line Data, **T** for Tellus Border Tie-Lines, **D** for Cavan and **L** for Tellus data. In addition, to avoid any confusion in identifying the source of the data within the master database a Survey ID (SID) channel has been produced, where;

- **TB** indicates Tellus Border data
- **TEL** indicates Tellus data
- **CAV** indicates Cavan data

Individual databases were trimmed to defined survey polygons, removing all potential overlaps. Then the three databases were merged into one master database using the merge database tool in Geosoft.

The final master database which includes all data has been masked to exclude data from Tellus (not currently free of charge to download) and the Charlestown survey (still within licence restriction dates).

4.2 Magnetic Data Merging

The levelled and IGRF correction data from both Tellus and Cavan datasets were compared to Tellus Border data in the regions of overlap which allowed direct comparison. Consistent offsets were found between the data.

A grid of magnetic anomaly was created for each database using the minimum curvature method and a cell size of 50m. Because there is no overlap between Cavan and Tellus data the 3 grids were knitted together in 2 stages, to create one fully merged grid. The grid knitting was performed using the suture stitching method (Geosoft) and an output grid cell size of 50m. The de-trending method for both grids was set to none.

The final fully merged grid was then re-sampled into the Master database using the sample-a-grid function in Geosoft.

Figure 5 below shows the result of the merged magnetic database.

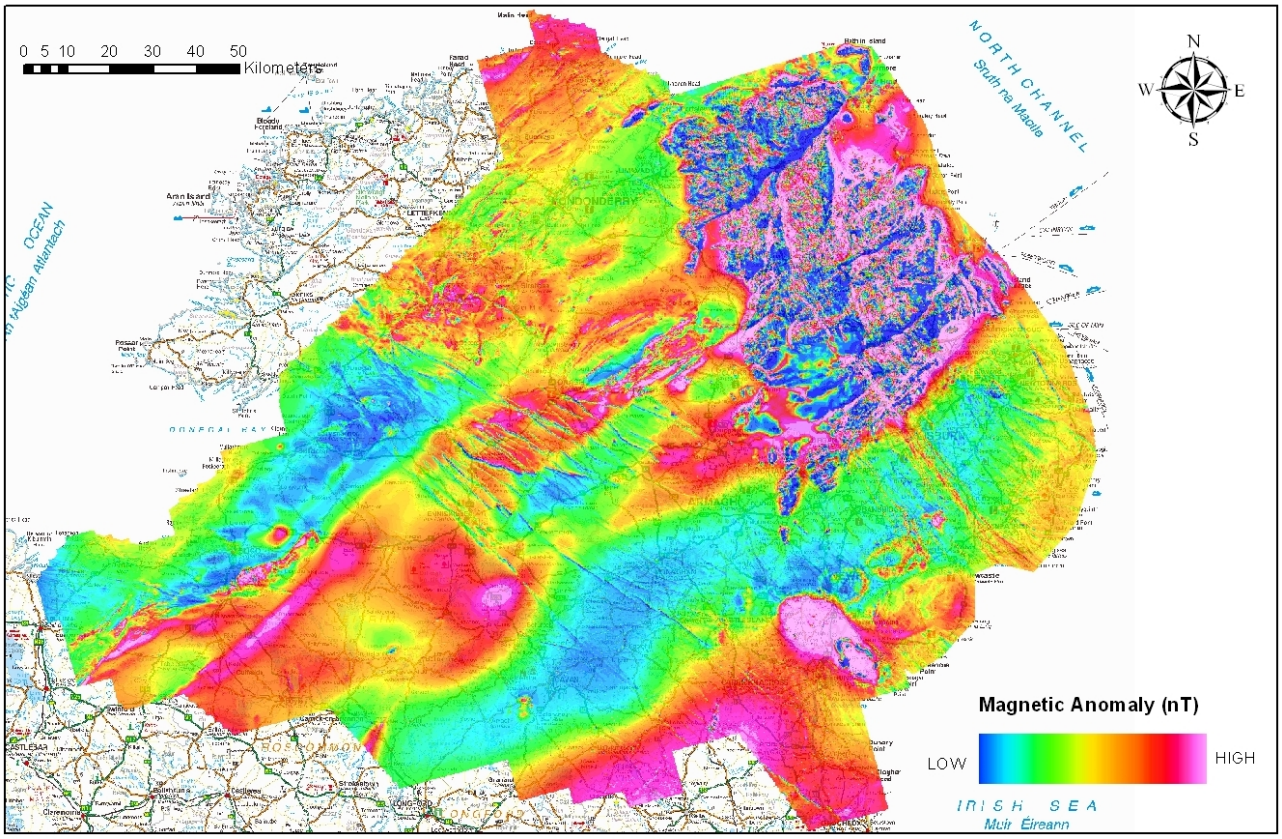

Figure 5: Merged magnetic anomaly image created from merger of Tellus Border (minus Charlestown), Tellus and Cavan datasets

4.3 Radiometric Data Merging

Following detailed assessment of the data it was determined that levels were different between data within the overlap areas. This is understandable in that the surveys were undertaken 6 years apart at different times of the year when seasonal affects can cause local variations. It should also be noted that slight differences in the energy windows were used to measure data which would have a small affect on the measured data.

Tellus Border used energy windows

Total Count	396 keV to 2808 keV
K	1368 keV to 1572 keV
Th	2412 keV to 2808 keV
U	1656 keV to 1860 keV

Tellus Phase 2 / Cavan used energy windows

Total Count	410 keV to 2810 keV

K	1370 keV to 1570 keV
Th	2410 keV to 2810 keV
U	1660 keV to 1860 keV

It was decided that all elements should be corrected to correspond with values measured for the most recent survey, Tellus Border. Further investigation revealed that the Cavan data showed that one correction for the whole block was insufficient to create a good match with the Tellus Border data as zonation with the data occurred. Therefore the data was split into two zones A and B. This split was consistent for all elements. Section A covered the first 50 lines, which show marked differences to the rest of the area, possibly due to seasonal effects. Corrections applied to the different radio-elements for the Tellus data were found to be consistent across the whole area and therefore further subdivisions were not required allowing one correction per element. The following correction factors were applied.

Table 7: Radiometirc correction factors

	Cavan – Polygon A	**Cavan – Polygon B**	**Tellus**
Potassium (%k)	0.875	0.801	0.866
eThorium (ppm)	1.202	1.014	1.064
eUranium (ppm)	0.834	0.946	0.989
Total Count	0.483	0.524	0.553

A new grid was created for each database for each element using the new corrected values using the minimum curvature method (Briggs, 1974) and a cell size of 50m. Because there is no overlap between Cavan and Tellus data the 3 grids were knitted together in 2 stages, to create one fully merged grid. The grid knitting was performed using the suture stitching method and an output grid cell size of 50m. The de-trending method for both grids was set to none. Static grid shifts are described below.

As a test, uncorrected contractor data was stitched together with TB data using the gridknit suture method (Geosoft) with different variations. The manually corrected data showed the best agreement. As a further test a Geosoft derived static merged grid for Tellus Border and Tellus data was removed from a manually derived knitted grid of the same area and showed little or no change.

The final fully merged grid was then re-sampled into the Master database using the sample function in Geosoft.

The DOSE_2012 channel was created using DOSE= (13.078xK) = (5.675xU) + (2.494 x Th) as outlined in IAEA (2003).

Figure 6 below shows an example of the merged potassium map.

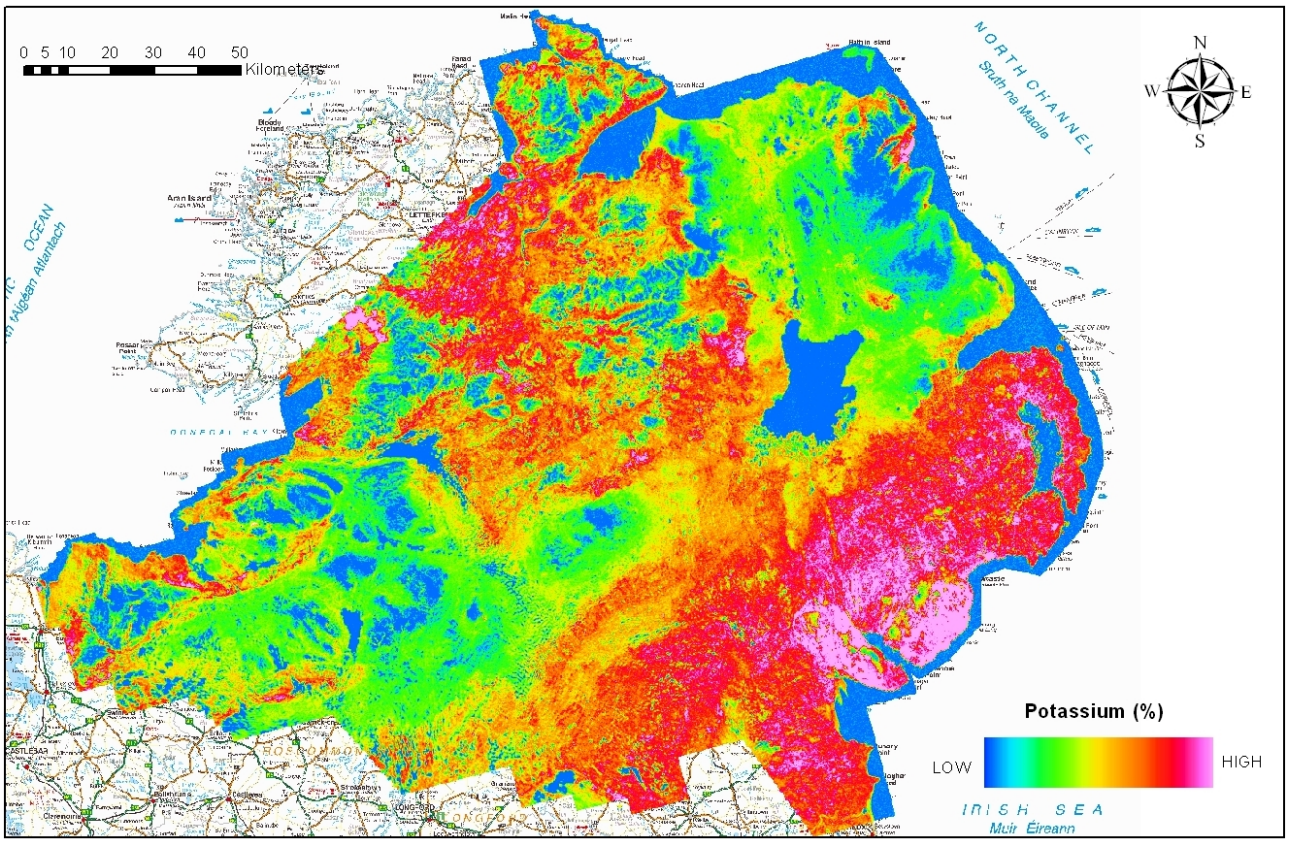

Figure 6: Merged potassium image created by merger of Tellus Border (minus Charlestown), Tellus and Cavan datasets.

4.4 Cs-137 Data Merging

The output from NASVD smoothed spectra was used for merging. The three data sets (CAV, TEL and TB) were checked independently for data quality. Microlevelling was applied when needed.

4.4.1 Temporal variation

The disintegration of a given quantity of any radioactive element can be expressed by the formula $N = N_0 e^{-\lambda t}$ where λ is decay constant and N_0 is number of parent nuclei at time t=0, 2005 is used as t=0 i.e. when Tellus Phase I data was collected. N is number of parent nuclei remain after time t. If t_0 is 2005, t_2 is 2006 (Tellus Phase II) and T_3 is 2012 (TB) then the the following temporal variation was applied to the data before merging.

1. Decay constant (λ) for Cs137 is -0.0231
2. $\frac{TEL2}{TEL1} = e^{-\lambda t} = e^{-0.0231} = 0.977 \Rightarrow TEL2 = 0.977 * TEL1$

   TEL1 and TEL2 were merged as TEL
3. $\frac{TB}{TEL} = e^{-6*\lambda} = e^{-0.1386} = 0.87 \Rightarrow TB = 0.87 * TEL$
4. $\frac{\mathrm{TB}}{\mathrm{CAV}} = \mathrm{e}^{-0.1386} = 0.87 \Rightarrow \quad \mathrm{TB} = 0.87 * \mathrm{CAV}$

A temporal variation was applied as above to TEL1 to bring it to reduce it to the 2006 Cs level. Then the two Tellus data sets were merged together to give the whole Tellus Cs-137 data in 2006 level. A similar correction has been done to CAV data as in equation 4 to bring all old Cs data sets to 2012 level so they can then be merged with Tellus Border data. After the temporal variation was applied to TEL and CAV, each data set was gridded and checked to see if there was a levelling difference. In TEL and TB data severe corrugations were not seen. However, corrugations parallel to survey lines were observed in CAV data and it was subsequently levelled . Figure 7 below shows the results of the merged data.

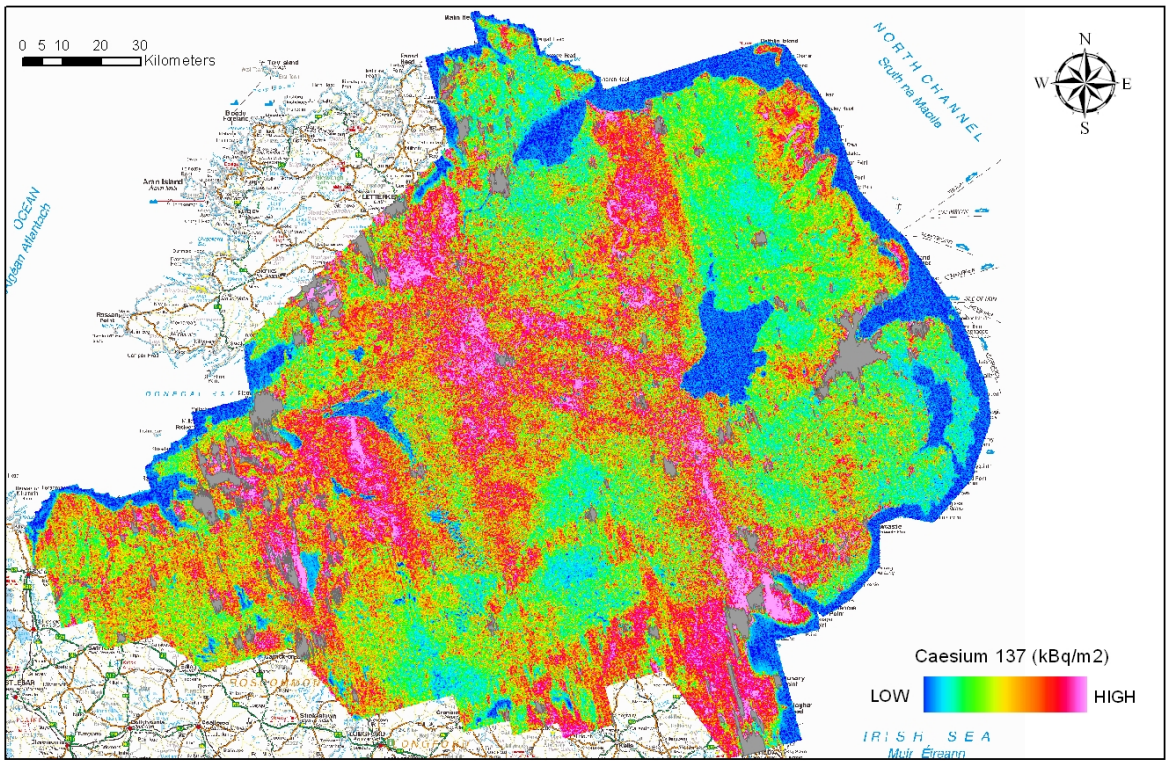

Figure 7: Merged Cs137 data. Gray shade shows altitude greater than 180m.

After individual grids were checked and accepted, two different databases were created: one containing data only for the Republic of Ireland i.e. TB and CAV, and the other including all data TEL, TB and CAV. The TB-CAV database was masked to a polygon that perfectly fit TB and CAV boundaries. The accepted final grid was sampled to the masked and merged database. The merged database consists of 9 channels, which are believed to be helpful for anybody who wants to reprocess the data for his own purposes. The xyz file (Geosoft / spread sheet) was exported from the database so as to allow access to the data in any appropriate software for further processing.

5 Merged Data Delivery

5.1 Overview

The final merged data images can be viewed at www.tellusborder.eu and data from the ROI can also be freely downloaded.

Data is shown in Airy modified 1964 Irish National Grid as well as latitude/longitude. Read me files for the magnetic and radiometric data are shown below, The pre-existing line numbers from the original survey have been kept with the proviso that lines with a prefix **B** indicate Tellus Border (TB) data, **D** indicate Cavan data, **L** indicates Tellus data and a prefix of **T** indicate Tie lines from TB data.

Magnetic merged data

Tellus Border 2012 - Tellus 2005/06 - Cavan 2006

Table 8: Produced merged magnetic data

No	Name	Units	Description
1	X	m	X coordinate, Irish National Grid
2	Y	m	y coordinate, Irish National Grid
3	LAT	Degree	Latitude
4	LONG	Degree	Longitude
5	DATE	YYYYMMDD	Date
6	SID		Survey ID (TB-Tellus Border, TEL – Tellus, CAV - Cavan
7	RALT	m	Altimeter height
8	GPS_H	m	WGS-84 Altitude
9	MAG_RES	nT	Magnetic Anomaly (IGRF & Diurnal corrected, Levelled)
10	Total Field	nT	Total Magnetic Field
11	IGRF	nT	Reference Field at January 1st 2012

Radiometric merged data
Tellus Border 2012 - Tellus 2005/06 - Cavan 2006

Table 9: Produced merged radiometric data

No	Name	Units	Description
1	X	m	X coordinate, Irish National Grid
2	Y	m	y coordinate, Irish National Grid
3	LAT	Degree	Latitude
4	LONG	Degree	Longitude
5	DATE	YYYYMMDD	Date
6	SID		Survey ID (TB-Tellus Border, TEL – Tellus, CAV - Cavan
7	RALT	m	Altimeter height
8	GPS_H	m	WGS-84 Altitude
9	K_Merge	%	Merged Corrected Potassium Concentration
10	TH_Merge	ppm	Merged Corrected Thorium Concentration
11	U_Merge	ppm	Merged Corrected Uranium Concentration
12	TC_Merge	cps	Merged Corrected Total Count
13	Dose_2012	nGy/hr	Air absorbed dose rate

5.2 High Fly Zones

Although the EM system is not discussed in detail here, it is known that this data and to a lesser extent the radiometric data is sensitive to survey altitude (IAEA, 2003). All data should be viewed in respect of the survey altitude. Radar altitude (RALT) is included within the database. As survey altitude increases, data is attenuated resulting in less reliable data.

The Tellus Border survey was issued with a flying permit from the Irish Aviation Authority (IAA) for 59m altitude in non congested (rural areas) areas. However, in upland areas which affected aircraft climb and descend rates and due to the presence of numerous wind farms some areas have been surveyed at higher altitudes. Figure 8 shows altitude greater than 180 m and data in these areas should be deemed to be less reliable.

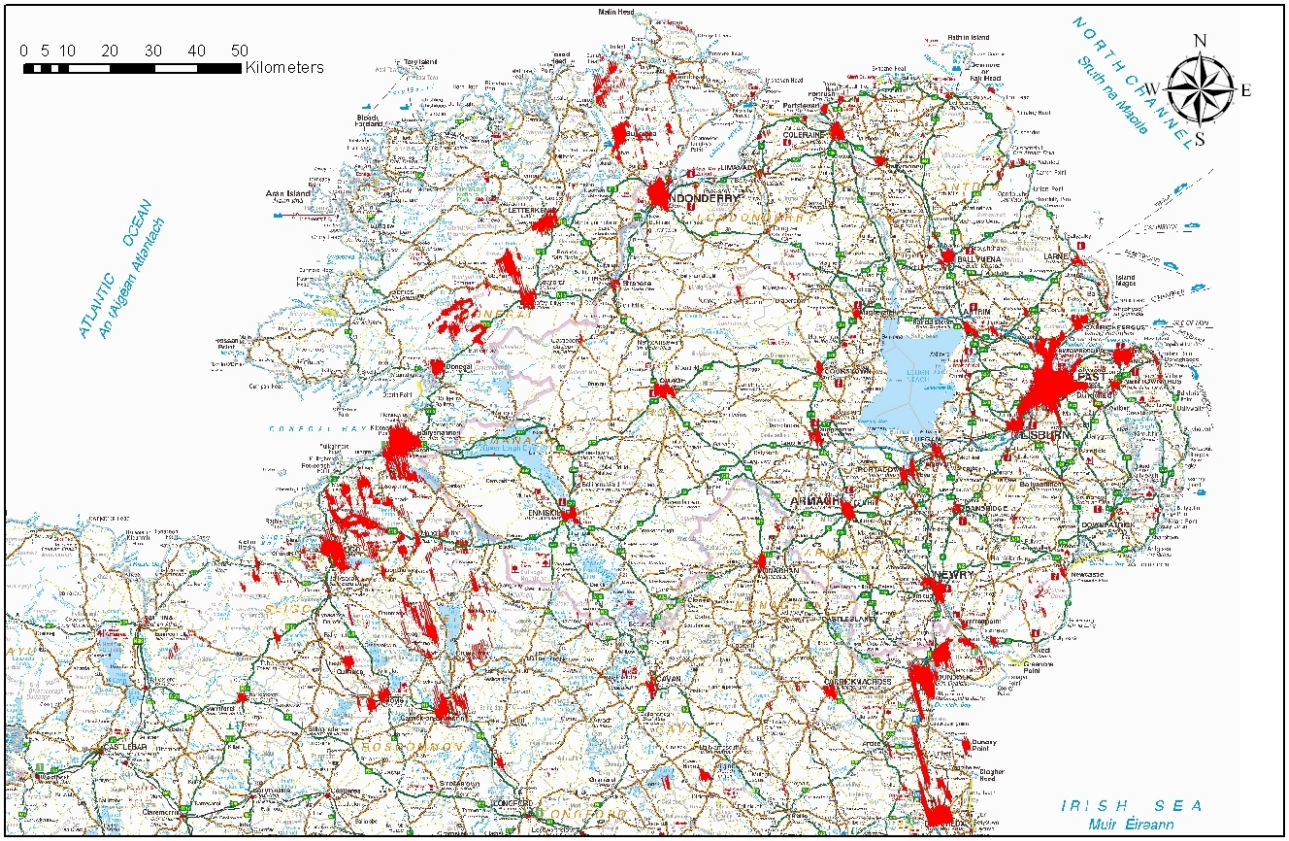

Figure 8: Survey altitude greater than 180m shown in red

As can be seen from Figure 8 the large urban areas of Belfast, Derry, Sligo, Drogheda and Dundalk all correspond with significant high fly zones as expected. However, other significant high fly zones are found along the M1 motorway in the southeast of the survey area and over hilly terrain in the west.

6 Noise Levels

6.1 Magnetic Noise

Magnetic data was measured using a Scintrex Cs-2 and Geomatrics G-822A caesium vapour instruments which have a sensitivity of 0.005nT.

Taking airborne system tests (Magnetic Compensation which provides a Figure of Merit or FOM) for the wing magnetometer during the Tellus Border survey shows FOM values of 0.4 nT to 1.16 nT. These values are corrected within the standard processing sequence but indicate possible background noise levels of FOM/10 i.e. better than ~0.1 nT within the measured data.

Figure 9 is a histogram of the magnetic anomaly data from the merged dataset and shows a mean value of 0.66 nT on a bi-model / normal distribution. A standard deviation of 143.4 nT is calculated.

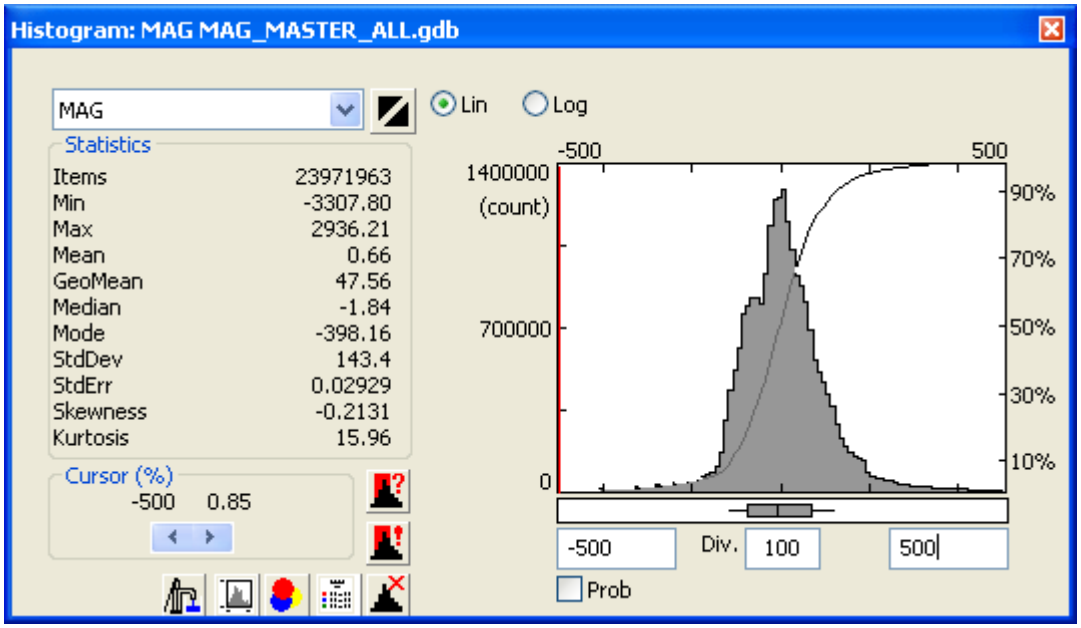

Figure 9: Histogram of magnetic anomaly for merged dataset

Cultural interference is the main source of noise affecting the data. Cultural interference from anthropogenic sources such as houses, farm buildings, roads, power lines etc. create spikes throughout the data. A system of deculturing (Lahti *et al.,* 2007) was carried out for Tellus data. Both automatic and manual processes were used to help assess individual anomalies and using

airphotographs / buildings databases to remove affected data points. Tellus Border and Cavan datasets were not subjected to deculturing.

A number of well developed smoothing procedures are available for potential field methods. The upward continuation method is widely used and it does not produce mathematical artefacts. This method could be used to minimize high frequency cultural noise in the magnetic data.

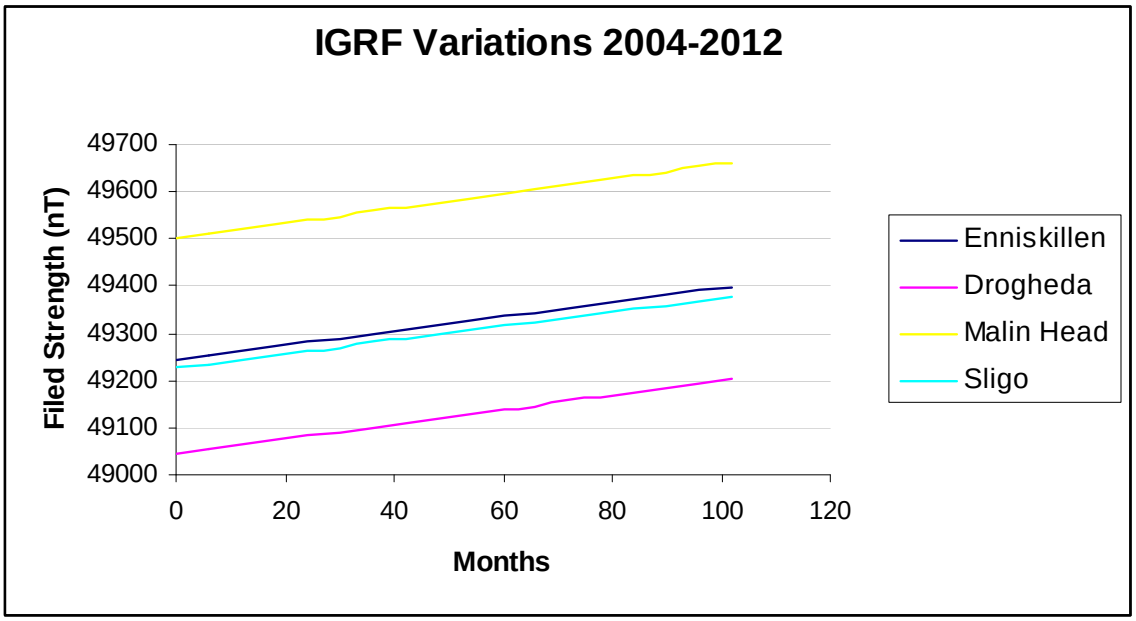

Figure 10: Secular variation across survey area between 2004 and 2012

Figure 10 shows the variation in the calculated IGRF field over the period 2004 to 2012. Malin Head in Co. Donegal, to the north show greater values of ~ 450nT than in Drogheda in the south east of the survey area. The yearly increase at each location is of the order of 18nT.

6.2 Radiometric Noise

To assist in the assessment of the Tellus Border radiometric data, a 6 km test line flown throughout the duration of the survey. The test line was flown 5 times and during each flight the line was surveyed at 7 different nominal altitudes 56, 60, 65, 70 75, 85 and 90 m (Figure 11). The line crossed from sea to land.

The test line data once re-sampled allows direct comparisons at the same locations to be made over the duration of the survey giving insight into the sensitivity of the system and any environmental impacts. Looking at total count data along the test line shows that readings vary by

factors of 0.98 to 1.06 from their calculated means. This would therefore indicate that measured values vary by up to 6% from the mean.

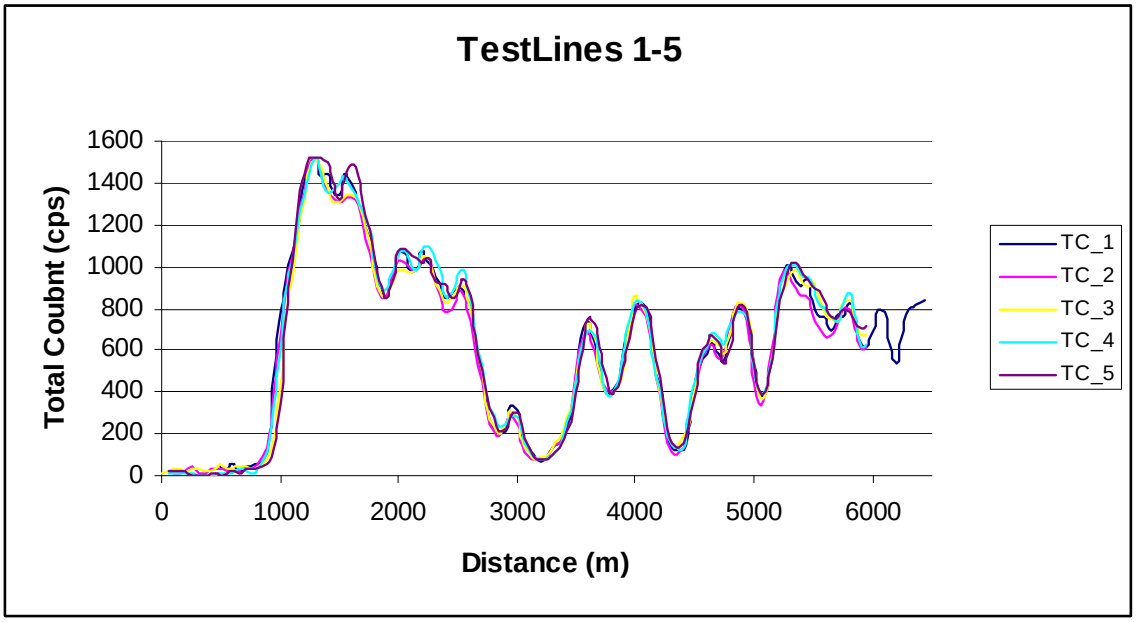

Figure 11: Total count variations along test line at 60m altitude for 5 flights

Noise levels can also be assessed by reviewing measured values over water where data should be zero. The survey included data over sea water in three areas: Dundalk Bay, Lough Foyle and Donegal Bay. Data from the three areas have been averaged and the statistics for the different elements are shown in Table 10.

Table 10: Statistics from radiometric elements over sea water. The survey mean refers to the statistics of the whole Tellus Border survey.

K	Mean	Min	Max	SD	Survey mean
AVE	*0.030*	*-0.068*	*0.377*	*0.134*	0.691
Th	**Mean**	**Min**	**Max**	**SD**	**Survey mean**
AVE	*0.039*	*-0.777*	*1.233*	*0.192*	3.281
U	**Mean**	**Min**	**Max**	**SD**	**Survey mean**
AVE	*-0.043*	*-0.589*	*0.451*	*0.099*	0.736
TC	**Mean**	**Min**	**Max**	**SD**	**Survey mean**
AVE	*-2.088*	*-48.768*	*185.978*	*15.592*	726.63

As can be seen from Table 10 the data oscillates close to zero but not all values over sea water return zero values as theory predicts (Minty, 1997). Therefore one standard deviation, from the calculated sea averages can be taken as a general system noise level for the radiometric data.

Rainfall data was taken from the Finner Meterological Station in Co. Donegal which lies approximately 7 km to the NW from the test line to assist in the assessment of seasonal effects. Plotting total count variations against rainfall from the reference flight shows a negative relationship whereby for every ~1 mm increase in rainfall, total count values decrease by about 0.8 %. Rainfall data was taken for each day of the flight as well as over a 3 day average and 14 day average. Taking rainfall only on the day of each flight may have lead to errors as the measurement was for the entire day and flights may have occurred before any measured rainfall for that day. The 3 and 14 day averages may indicate the degree of saturation of the ground. Recent studies have investigated how both soil and bedrock type together with the degree of saturation of the ground can influence the attenuation of gamma rays (Beamish, 2013 and Beckett, 2008).

6.3 Caesium-137 Noise

Caesium-137 data is affected by high fly zones and data above 180m is masked to avoid severe noise effects. Comparing statistics between the individual datasets within the region show similar means, suggesting reasonable confidence in the data. Other factors such as the land use can affect the absorption and storage/distribution of Cs-137.

Caesium 137 has a half-life of approximately 30 years and temporal corrections need to be considered and have been applied to all merged data collected at different periods.

References

Beckett, K., 2008.Multspectral processing of high-resolution radiometric data for soil mapping. Near Surface Geophysics, 6, 281-287.

Beamish, D., Cuss, R.J., and Lahti, M., 2006a. The Tellus airborne geophysical survey of Northern Ireland: Phase 1 Logistics report. *British Geological Survey Technical Report* IR/06/032. A report prepared for DETI, Belfast. http://nora.nerc.ac.uk/7184/

Beamish, D., Cuss, R.J., and Lahti, M., 2006b. The Tellus airborne geophysical survey of Northern Ireland: Phase 2 Logistics report. *British Geological Survey Technical Report* IR/06/104. A report prepared for DETI, Belfast.

Beamish, D., Cuss, R.J. and Lahti, M., Scheib, C, Tartaras, E., 2006c. The Tellus Airborne Geophysical Survey of Northern Ireland: Final Processing Report. *British Geological Survey Technical Report* IR/06/136. A report prepared for DETI, Belfast. http://nora.nerc.ac.uk/7427/1/IR06136.pdf

Beamish, D., 2013. Gamma ray attenuation in the soils of Northern Ireland, with special reference to peat. Journal of Environmental Radioactivity, 115, 13-27.

Briggs, I,. 1974. Machine contouring using minimum curvature. Geophysics, v39 No 1, p39-48.

Grasty, R.L. and Minty, B.R.S., 1995a. A guide to the technical specifications for airborne gamma-ray surveys. Australian Geological Survey Organisation, Record, 1995/20.

Grasty, R.L. and Minty, B.R.S., 1995b. The standardisation of airborne gamma-ray surveys in Australia. Exploration Geophysics, 26, 276-283.

Hautaniemi, H., Kurimo, M., Multala, J., Leväniemi, H. and Vironmäki, J. 2005. The 'three in one' aerogeophysical concept of GTK in 2004. In: Airo, M-L. (ed.) *Aerogeophysics in Finland 1972-2004:*

Methods, System Characteristics and Applications. Geological Survey of Finland, Special Paper 39, 21-74.

IAEA, 1991. *Airborne gamma ray spectrometer surveying,* International Atomic Energy Agency, Technical Report Series, No. 323.

IAEA, 2003. *Guidelines for radioelement mapping using gamma ray spectrometry data.* International Atomic Energy Agency, Technical Report Series, No. 1363. http://www-pub.iaea.org/mtcd/publications/pdf/te_1363_web.pdf

Kurimo M,. 2006. High Resolution aerogeophysical survey, Ireland. Internal report for the Geological Survey of Ireland.

Lahti, M., Beamish, D., Cuss, R.J., and Williams, J., 2007. Deculturing of the Northern Ireland Tellus magnetic data. *British Geological Survey Technical Report* IR/07/147. A report prepared for the DETI, Belfast. http://nora.nerc.ac.uk/7570/

Minty, B., 1997. *Fundamentals of airborne gamma-ray spectrometry.* AGSO Journal of Australian Geology and Geophysics, 17, 39-50.

Scheib, Cathy; Beamish, David. 2010. High spatial resolution observations of 137Cs in northern Britain and Ireland from airborne geophysical survey. *Journal of Environmental Radioactivity*, 101 (9). 670-680. 10.1016/j.jenvrad.2010.03.010 http://nora.nerc.ac.uk/12929/

Appendix I Tellus Border Contractor Processing Report

Technical Report by Sander Geophysics Ltd

Technical Report

**Fixed-Wing High-Resolution Aeromagnetic,
Gamma-ray Spectrometric and
Frequency-Domain Electromagnetic Survey**

Tellus Border
2011-2012

for

Geological Survey of Ireland and
Geological Survey of Northern Ireland

Sander Geophysics Limited
260 Hunt Club Road
Ottawa, ON Canada K1V 1C1

Tel: +1 613.521.9626
Fax: +1 613.521.0215
www.sgl.com

Malcolm Argyle, P.Geo

Martin Bates, Ph.D.
Monika Pal, B.Sc.
Sol Meyer, B.Sc.

TABLE OF CONTENTS

FIGURES

TABLES

APPENDIX

INTRODUCTION

Sander Geophysics Limited (SGL) conducted a fixed-wing high-resolution aeromagnetic, gamma-ray spectrometric, and frequency-domain electromagnetic survey in the Republic of Ireland for the Geological Survey of Ireland (GSI) and the Geological Survey of Northern Ireland (GSNI). Please refer to *Appendix I* for a Company Profile of SGL.

The survey was conducted using SGL's De Havilland DHC-6 Twin Otter, registration C-GSGF. Production flights commenced on October 26, 2011 and were completed on July 15, 2012. A total of 177 flights were flown during the survey to complete the planned 57,682 line kilometres. The survey operations were conducted from Enniskillen Airport (EGAB).

The traverse lines are oriented N15ºW and spaced at 200 m, while the control lines are oriented at N75ºE and spaced at 2,000 m. The target clearance was 59 m above ground level, based on the IAA permit. The target average ground speed was 59 m/s, or 115 knots.

SURVEY AREA

The survey area is an irregular polygon that composes a significant portion of the 6 northern counties of the Republic of Ireland. Enniskillen, County Fermanagh, Northern Ieland, where operations were based, is approximately in the middle of the survey boundaries, although is not within the survey area. The survey area covers mostly rural areas which are essentially comprised of farmland. A small fraction of the planned lines were over offshore areas. The terrain is generally rolling hills for most of the survey area with high cliffs along the west coastline, varying from approximately 0 m above mean sea level (MSL) to approximately 700 m above MSL. The weather in the region is mild and wet, with temperatures averaging 12°C over the survey period. Low cloud, rain and fog were common.

The survey was flown as a single block. *Figure 1* shows the geographical location of the survey area. The Planned Lines are listed in *Appendix II.*

Figure 1: Survey Area Map

SURVEY EQUIPMENT

SGL provided the following instrumentation for this survey, see *Appendix IV* for further details:

Frequency Domain Electromagnetic System

JAC AEM05 four frequency (1) EM System (0.9, 3, 12, 24.5 kHz)

SGL's DHC-6 Twin Otter is configured with a four-frequency, wingtip mounted Frequency Electromagnetic (FEM) system that operates at four frequencies, 912, 3005, 11962 and 24510 Hz. This configuration results in a large transmitter-receiver coil separation which improves the signal to noise ratio. The transmitter-receiver coil pairs are mounted in a vertical-coplanar orientation which reduces noise by minimizing coupling with the wingtip surface. Additionally, the coils in any one set (transmitter or receiver) are axially offset and are kept adequately separated from each other. The system also comes equipped with a 50/60 Hz power line monitor which becomes particularly useful in identifying cultural interference when surveying in urban settings. The system has a 40 Hz sampling rate which is later decimated to 10 Hz in the processing.

Aerial and Ground Magnetometers

Scintrex CS-2

Until flight 057, the airborne system used only Scintrex magnetometers. One airborne sensor was mounted in a fibreglass stinger attached to the nose of the aircraft and a second sensor was housed in the left FEM pod attached to the left wingtip. Following this flight the nose magnetometer was changed to a Geometrics magnetometer. The Scintrex magnetometers use self-oscillating split-beam Cesium vapour. They have a sensitivity of 0.005 nT and a range of 20,000 to 100,000 nT with a sensor noise of less than 0.02 nT. Total magnetic field measurements were recorded at 160 Hz in the aircraft then later decimated to 10 Hz in the processing.

Geometrics G-822A

The nose airborne magnetometer (following flight 057) and the ground systems used a non-oriented (strap-down) optically-pumped cesium split-beam Geometrics sensor. These magnetometers have a sensitivity of 0.005 nT and a range of 20,000 to 100,000 nT with a sensor noise of less than 0.02 nT. Total magnetic field measurements were recorded at 160 Hz in the aircraft then later decimated to 10 Hz in the processing. The ground systems recorded magnetic data at 11 Hz.

Magnetic Compensation System

RMS AADC II Magnetic Compensator

The AADC magnetic compensator removes the effects of the aircraft and its manoeuvres from the recorded magnetic data. This system records the magnetic field measured by the two airborne total field intensity magnetometers, as well as the three axis output of a fluxgate magnetometer. These data are recorded for post processing. Coefficients to be used for compensation are derived by processing the calibration flight data. The compensation coefficients are applied to data recorded during normal survey operations to produce compensated magnetic data.

Gamma Ray Spectrometer System

Exploranium GR820 with Crystal Detector Packs GPX-1024/256
(2 packs, 10 crystals)

The Exploranium spectrometer system includes an on-board computer for real-time signal processing and analysis, which allows automatic gain control for individual crystals using the natural thorium peak, and multi-channel recording and analysis. The system utilizes a NaI(Tl) detector volume of 42.0 L consisting of 8 downward-looking and 2 upward-looking parallelepiped crystals of 4.2 L each, housed in two detector packs. Data were recorded in 256 channel spectral mode and windowed data mode at an interval of 1 s.

Airborne Navigation and Data Acquisition System

Sander NavDAS

The NavDAS is the latest version of airborne navigation and data acquisition computers developed by SGL. It displays all incoming data on a flat panel screen for real-time monitoring. The data are recorded in database format on a solid-state internal hard drive and a removable hard drive simultaneously for transfer of data to the field office. The computer incorporates a magnetometer coupler, an altimeter analogue to digital converter and a GPS multi-frequency receiver NovAtel OEMV-V3 tracking 14 GPS Satellites, 12 GLONASS Satellites, 2 SBAS and 1 L-Band which automatically provides the UTC time base for the recorded data. In addition to providing essential post-mission positional data, the NavDAS computer processes user-received GPS or real-time differentially corrected GPS (RDGPS) data and compares the data to the coordinates of a theoretical flight plan in order to guide pilots along the desired survey line in three dimensions.

Reference Station Acquisition System

SGRef

The reference station system SGRef, consists of a ground data acquisition computer with a Sander magnetometer frequency counter to process the signal from the magnetometer sensor and from the GPS receiver. The noise level of the station magnetometer is less than 0.1 nT. The time base (UTC) of both the ground and airborne systems is automatically provided by the GPS receiver, ensuring proper merging of both data sets. All data are displayed on an LCD flat panel monitor. The magnetic data, sampled every 0.5 sec and GPS data, sampled at 11 Hz, are recorded on the internal hard drive of the computer and the removable hard drive simultaneously for transfer to the processing computers in the field office. The entire reference data acquisition system is fully automatic and was set for unattended recording.

Reference Station Gps Receiver

NovAtel Millennium , 12-channel, dual-frequency

The NovAtel Millennium, 12-channel, dual-frequency receiver forms an integral part of the SGRef system. It provides averaged position and raw range information of all satellites in view, sampled every 0.1 s. The comparative navigation data supplied during all production flights allows for post-processed differential GPS (DGPS) corrections for every survey flight.

Digital Video System

SGDIS - Sander Geophysics Digital Imaging System

The video camera is mounted in the floor of the aircraft and oriented to look vertically below while in flight. Real time text annotation of position, flight information and fiducial

marking are incorporated for flight path verification. The data are stored, by flight line, in avi format, viewable by any commercial media player.

Altimeters

SGLas-P - Riegl LD90-3300VHS-FLP Laser Rangefinder

The Riegl laser altimeter is an eye safe laser, has a range of 400 m, a resolution of 0.01 m with an accuracy of 5 cm and a 10 Hz data rate.

Collins AL-101 Radar Altimeter

The Collins radar altimeter has a resolution of 0.5 m, an accuracy of 5%, a range of 0 to 2500 ft, and a 10 Hz data rate. This system is actively employed for survey guidance and data acquisition.

Honeywell Barometric Pressure Sensor

The barometric pressure sensor measures static pressure to an accuracy of ± 4 m and resolution of 2 m over a range up to 30,000 ft above sea level. The barometric altimeter data is sampled at 10 Hz.

Omega RTD-805 Outside Air Temperature Probe

The outside air temperature is measured at 10 Hz with a resolution of 0.1º C. The temperature sensor has a range of +/-100º C and an accuracy of +/-0.2º C. The temperature sensor is mounted in an air inlet duct at the point where the wing strut attaches to the right hand wing.

Survey Aircraft

De Havilland DHC-6 Twin Otter (C-GSGF)

The De Havilland DHC-6 Twin Otter (C-GSGF) is an all metal, high-wing, twin-engine, short takeoff and landing (STOL) aircraft. It is powered by two Pratt & Whitney Canada PT6A-27 engines that run a constant speed, fully feathering, reversible propeller. The PT6 turbine engines provide ample power for climbing over steep terrain, working at altitudes up to 7,000 m and can withstand frequent rapid power changes. The aircraft is highly maneuverable, rugged in design and can be flown at speeds from 80 to 160 knots. The low stall speeds and abundant available power make the Twin Otter a safe and effective aircraft for surveys requiring flying over rough topography, low air speeds or flights at high altitude. The aircraft has fixed gear, extendable flaps and manually adjustable trim tabs on the primary controls for the roll and pitch axes and full rudder trim for the yaw axis. The aircraft is equipped with full de-icing equipment and sufficient avionics for instrument flying, including a flight control system. Supplementary fuel can be added for transoceanic flight. The Twin Otter is certified for IFR flights in known icing conditions.

The SGL Twin Otter is fully equipped for airborne magnetic, radiometric and frequency-domain Electromagnetic (FEM) surveys. EM fields are measured with the SGL frequency-domain EM system (SGFEM). The four-frequency FEM transmitter is located in the right wingtip FEM pod, and the receiver is located in the left wingtip FEM pod. The magnetic field is measured by up to two sensors allowing for horizontal gradient with one sensor in the composite nose stinger and one in the left wingtip FEM pod. The Twin Otter can carry up to 63 litres of detector crystals for gamma-ray spectrometer surveys. The aircraft conforms to Canadian aeronautical regulations in survey configuration.

Data Processing Hardware and Software

Processing was performed on high performance desktop computers optimized for processing tasks. SGL's proprietary geophysical software was used for data processing.

Picture 1: SGL's De Havilland DHC-6 Twin Otter (C-GSGF) survey aircraft

SURVEY SPECIFICATIONS

Data Recording

In the aircraft:

- GPS positional data (time, latitude, longitude, altitude and raw range from each satellite being tracked) recorded at 10 Hz;
- Altitude as measured by the barometric altimeter at intervals of 0.1 s;
- Terrain clearance as measured by the radar altimeter at intervals of 0.1 s;
- Terrain clearance as measured by the laser rangefinder at a sampling rate of 3.3 Hz;
- Total magnetic field recorded at 160 Hz;
- Airborne spectrometer data recorded in windowed and 256 channel spectral format with a 1.0 s sampling rate;
- Outside air temperature recorded at intervals of 0.1 s;
- Digital Video recording at 30 Hz.
- Electromagnetic in-phase and quadrature components for four frequencies (912, 3005, 11962 and 24510 Hz) recorded at 40 Hz.

At the base and remote magnetic/GPS reference stations:

- Total magnetic field recorded at 11 Hz;
- GPS positional data (time, latitude, longitude, and raw range from each satellite being tracked) recorded at 10 Hz.

Technical Specifications

The following technical specifications were used to define when repeat (in-fill) flight lines will be flown:

- Where flight line spacing is greater than 130% of the nominal spacing over a distance of 2km or more or over any distance where flight line spacing is greater than 150% of the nominal spacing (except where ground conditions dictate otherwise, for example to avoid radio-masts etc).*
- Where terrain clearance exceeds +/- 20 metres from the nominal survey height for more than 5 continuous kilometres or +/- 50% of nominal survey height at any time on any line, unless local topography makes this unavoidable.*
- Where the nominal survey flying speed is exceeded by more than 30% for more than 5 continuous kilometres.*
- Where the noise envelope of the magnetic records exceeds 0.1nT as determined by the normalised fourth difference.
- If, during data acquisition, magnetic variations recorded at the local base magnetometer exceed 12nT over any 3 minute chord or exceed 2nT over any 30 second chord, on flight lines or tie lines. These limits may be revised by agreement in the light of experience gained during the first few weeks of data acquisition. The base magnetometer must be fully operational during all on-line data collection.
- Where the average line gamma spectra for any line appears anomalous by comparison with previously acquired data then the data of that line will be investigated in detail and re-flown if necessary.
- If the calibration of the EM system deviates significantly from the norm. The exact specification to be used will depend on the system proposed by the Contractor, who should propose appropriate limits in the Tender.
- If the calculated PDOP is greater than 6 or if less than four satellites are available.
- If both primary and secondary GPS base stations fail to record for 30 minutes or more, simultaneously.

- If both primary and secondary magnetic base stations fail to record for 30 minutes or more, simultaneously.

*These conditions may be exceeded without re-flight where such constraints would breach air regulations, or in the opinion of the pilot, put the aircraft and crew at risk. All such exceptions shall be logged.

The following lines were re-flown:

Table 1: Reflights list

Original Flight		Re-Flights		
Line	Flight	Line	Flight	Reason
105.00	56	105.01	57	FEM drifting due to rain.
110.00	19	110.01	28	FEM drifting due to rain.
110.10	57	110.11	58	FEM drifting due to rain.
118.00	63	118.01	72	Partial due to fuel.
119.00	55	119.01	61	Partial due to M1 highway.
119.00	55	119.02	72	Partial due to M1 highway.
119.02	72	119.03	165	FEM drifting due to rain.
128.10	48	128.11	69	FEM drifting due to rain.
129.00	45	129.01	72	Partial due to weather.
133.00	72	133.01	138	FEM drifting due to rain.
134.00	72	134.02	146	FEM drifting due to rain.
135.00	72	135.01/ 135.02	147	FEM drifting due to rain.
141.00	135	141.01	175	FEM drifting due to rain.
143.00	135	143.01	175	FEM drifting due to rain.
155.10	131	155.11	167	FEM drifting due to rain.
158.00	112	158.01	113	Partial due to weather.
170.00	124	170.01	173	FEM drifting due to rain.
1015.00	138	1015.01	167	FEM drifting due to rain.
1022.00	141	1022.01	175	FEM drifting due to rain.
1023.00	141	1023.01	167	FEM drifting due to rain.
1027.00	141	1027.01	175	FEM drifting due to rain.
1030.00	141	1030.01	175	FEM drifting due to rain.
1032.00	141	1032.01	167	FEM drifting due to rain.
1034.00	141	1034.01	167	FEM drifting due to rain.
1040.00	143	1040.01	175	FEM drifting due to rain.
1088.00	151	1088.01	167	FEM drifting due to rain.
1089.00	151	1089.01	167	FEM drifting due to rain.
1112.00	141	1112.01	175	Magnetometer blackout.
1121.00	143	1121.01	175	FEM drifting due to rain.

Original Flight		Re-Flights		
Line	**Flight**	**Line**	**Flight**	**Reason**
1123.00	143	1123.01	167	FEM drifting due to rain.
1127.00	143	1127.01	167	FEM drifting due to rain.
1136.00	136	1136.01	153	FEM drifting due to rain.
1137.00	136	1137.01	153	FEM drifting due to rain.
1138.00	136	1138.01	153	FEM drifting due to rain.
1160.00	76	1160.01	153	FEM drifting due to rain.
1161.00	76	1161.01	153	FEM drifting due to rain.
1162.00	76	1162.01	153	FEM drifting due to rain.
1163.00	76	1163.01	156	FEM drifting due to rain.
1164.00	76	1164.01	156	FEM drifting due to rain.
1165.00	76	1165.01	156	FEM drifting due to rain.
1166.00	76	1166.02	175	FEM drifting due to rain.
1167.00	76	1167.01	153	FEM drifting due to rain.
1168.00	76	1168.01	153	FEM drifting due to rain.
1169.00	73	1169.01 1169.02	134 153	FEM drifting due to rain.
1170.00	73	1170.01	156	FEM drifting due to rain.
1170.01	156	1170.02	167	FEM drifting due to rain.
1171.00	73	1171.01	156	FEM drifting due to rain.
1171.01	156	1171.02	167	FEM drifting due to rain.
1172.00	73	1172.01	167	FEM drifting due to rain.
1173.00	73	1173.01	177	FEM drifting due to rain.
1174.00	73	1174.01	177	FEM drifting due to rain.
1175.00	73	1175.01	177	FEM drifting due to rain.
1176.00	73	1176.01	177	FEM drifting due to rain.
1177.00	73	1177.01	177	FEM drifting due to rain.
1178.00	73	1178.01	177	FEM drifting due to rain.
1193.00	77	1193.01	175	FEM drifting due to rain.
1197.00	77	1197.01	175	FEM drifting due to rain.
1199.00	77	1199.01	175	FEM drifting due to rain.
1201.00	77	1201.01	175	FEM drifting due to rain.
1202.00	77	1202.01	175	FEM drifting due to rain.
1203.00	82	1203.01	116	Partial due to weather.
1212.00 1212.01	83 101	1212.02	116	Partial due to complaint. Partial due to weather.
1220.00	89	1220.01	116	FEM drifting due to rain.
1220.01	116	1220.02	175	FEM drifting due to rain.

Original Flight		Re-Flights		
Line	**Flight**	**Line**	**Flight**	**Reason**
1231.00	97	1231.01	175	FEM drifting due to rain.
1232.00	97	1232.01	175	FEM drifting due to rain.
1235.00	97	1235.01	175	FEM drifting due to rain.
1239.00	97	1239.01	175	FEM drifting due to rain.
1240.00	97	1240.01	175	FEM drifting due to rain.
1241.00	97	1241.01	175	FEM drifting due to rain.
1243.00	114	1243.02	175	FEM drifting due to rain.
1247.00	116	1247.01	116	Partial due to weather.
1248.00	116	1248.01	175	FEM drifting due to rain.
1260.00	113	1260.01	127	Partial due to weather..
1260.01	127	1260.02	129	FEM drifting due to rain.
1263.01	130/131	1263.02	165	Magnetometer black-out.
1264.00	110	1264.02	175	FEM drifting due to rain.
1266.01	131	1266.02	165	FEM drifting due to rain.
1281.00	109	1281.02	165	FEM drifting due to rain.
1283.00	109	1283.01 1283.02	136 165	FEM drifting due to rain.
1284.00	109	1284.01	165	FEM drifting due to rain.
1285.00	109	1285.01	175	FEM drifting due to rain.
1291.00	104	1291.02	175	FEM drifting due to rain.
1291.01	133	1291.02	175	FEM drifting due to rain.
1307.00	104	1307.02	166	FEM drifting due to rain.
1309.00	104	1309.01	120	FEM drifting due to rain.
1311.00	104	1311.01	120	FEM drifting due to rain.
1311.01	120	1311.03	166	FEM drifting due to rain.
1317.01	120	1317.02	129	FEM drifting due to rain.
1323.00	99	1323.01	120	FEM drifting due to rain.
1324.00	99	1324.01	175	FEM drifting due to rain.
1347.00	93	1347.01	99	FEM drifting due to rain.
1353.10	60	1353.11	173	FEM drifting due to rain.
1354.00	86	1354.01	165	FEM drifting due to rain.
1358.00	86	1358.01	165	FEM drifting due to rain.
1359.00	86	1359.01	165	FEM drifting due to rain.
1360.00	86	1360.01	165	FEM drifting due to rain.
1360.10	60	1360.11	173	FEM drifting due to rain.
1363.10	60	1363.11	173	FEM drifting due to rain.
1367.10	60	1367.11	173	FEM drifting due to rain.

Original Flight		Re-Flights		
Line	**Flight**	**Line**	**Flight**	**Reason**
1370.00	84	1370.01	91	FEM drifting due to rain.
1371.00	84	1371.01	91	FEM drifting due to rain.
1372.00	84	1372.01	91	Partial due to weather.
1373.00	84	1373.01	91	Partial due to weather.
1374.00	84	1374.01	165	FEM drifting due to rain.
1375.00	84	1375.01	165	FEM drifting due to rain.
1378.00	84	1378.01	165	FEM drifting due to rain.
1379.10	61	1379.11	173	FEM drifting due to rain.
1380.00	69	1380.01	165	FEM drifting due to rain.
1390.10	66	1390.11	119	Partial due to weather.
1391.10	66	1391.11	119	Partial due to weather.
1392.10	66	1392.11	119	Partial due to weather.
1395.10	66	1395.11	119	Partial due to weather.
1396.10	66	1396.11	119	Partial due to weather.
1417.00	46	1417.01	165	FEM drifting due to rain.
1419.10	101	1419.11	122	Partial due to weather.
1419.11	122	1419.12	173	FEM drifting due to rain.
1420.10	106	1420.11	107	FEM drifting due to rain.
1421.10	107	1421.11	173	FEM drifting due to rain.
1425.00	44	1425.01	46	Partial due to weather.
1433.10	115	1433.11	173	FEM drifting due to rain.
1436.10	115	1436.11	173	FEM drifting due to rain.
1437.10	115	1437.11	173	FEM drifting due to rain.
1438.10	116	1438.11	173	FEM drifting due to rain.
1439.10	116	1439.11	173	FEM drifting due to rain.
1441.10	116	1441.11	173	FEM drifting due to rain.
1445.10	115	1445.11	173	FEM drifting due to rain.
1446.10	115	1446.11	173	FEM drifting due to rain.
1450.10	112	1450.11	115	Partial due to weather.
1456.10	107	1456.11	173	FEM drifting due to rain.
1464.10	115	1464.11	173	FEM drifting due to rain.
1465.10	115	1465.11	173	FEM drifting due to rain.
1466.10	116	1466.11	173	FEM drifting due to rain.
1472.10	118	1472.11	173	FEM drifting due to rain.
1481.10	115	1481.11	174	FEM drifting due to rain.
1490.10	115	1490.11	174	FEM drifting due to rain.
1492.10	115	1492.11	174	FEM drifting due to rain.

Original Flight		Re-Flights		
Line	Flight	Line	Flight	Reason
1498.20	119	1498.21	174	FEM drifting due to rain.
1499.20	119	1499.21	177	FEM drifting due to rain.
1500.20	119	1500.21	177	FEM drifting due to rain.
1501.20	120	1501.21	174	FEM drifting due to rain.
1523.20	120	1523.21	174	FEM drifting due to rain.
1525.20	120	1525.21	174	FEM drifting due to rain.
1544.10	31	1544.11	39	Accidental reflight.
1545.00	40	1545.01	59	Partial due to weather.
1546.20	106	1546.21	174	FEM drifting due to rain.
1547.20	106	1547.21	174	FEM drifting due to rain.
1572.20	122	1572.21	174	FEM drifting due to rain.
1576.00	36	1576.01	38	Gap in GPS.
1585.20	126	1585.21	174	FEM drifting due to rain.
1604.20	127	1604.21	171	FEM drifting due to rain.
1638.20	132	1638.21	174	FEM drifting due to rain.
1639.20	132	1638.21	174	FEM drifting due to rain.
1640.20	132	1640.21	174	FEM drifting due to rain.
1641.20	132	1641.21	171	FEM drifting due to rain.
1642.20	132	1642.21	171	FEM drifting due to rain.
1643.20	132	1643.21	171	FEM drifting due to rain.
1644.20	132	1644.21	171	FEM drifting due to rain.
1645.20	132	1645.21	171	FEM drifting due to rain.
1646.20	132	1646.21	171	FEM drifting due to rain.
1647.20	132	1647.21	171	FEM drifting due to rain.
1648.20	132	1648.21	171	FEM drifting due to rain.
1649.20	132	1649.21	171	FEM drifting due to rain.
1650.20	132	1650.21	171	FEM drifting due to rain.
1651.20	132	1651.21	171	FEM drifting due to rain.
1654.10	12	1654.11	166	FEM drifting due to rain.
1665.20	132	1665.21	137	FEM drifting due to rain.
1666.20	137	1666.21	171	FEM drifting due to rain.
1683.00	17	1683.01	17	Accidental reflight.
1692.00	17	1692.01	17	Accidental reflight.
1693.20	154	1693.21	171	FEM drifting due to rain.
1694.20	154	1694.21	171	FEM drifting due to rain.
1695.20	154	1695.21	171	FEM drifting due to rain.
1696.10	26	1696.11	33	Partial due to weather.

Original Flight		Re-Flights		
Line	**Flight**	**Line**	**Flight**	**Reason**
1732.00	33	1732.01	34	Accidental reflight.
1751.10	163	1751.11	167	Accidental reflight.
1770.00	21	1770.01	22	Partial due to weather.
1771.00	21	1771.01	22	Partial due to weather.
1818.00	49	1818.01	55	FEM drifting due to rain.
1822.00	48	1822.01	55	FEM drifting due to rain.
1823.00	48	1823.01	55	FEM drifting due to rain.
1824.00	48	1824.01	55	FEM drifting due to rain.
1825.00	48	1825.01	55	FEM drifting due to rain.
1827.00	49	1827.01	55	FEM drifting due to rain.
1829.00	48	1829.01	55	FEM drifting due to rain.
1835.00	51	1835.01	55	Partial due to aircraft maintenance issue.
1835.01	55	1835.02	57	Partial lines 1835.00 and 1835.01 did not overlap.
1847.00	55	1847.01	58	FEM drifting due to rain.
1881.00	61	1881.01	63	FEM drifting due to rain.
1887.00	57	1887.01	67	FEM drifting due to rain.

Flight Line Specifications

The survey area flight line specifications were as follows (line direction is with respect to the UTM zone reference frame):

Table 2: Flight Lines Specification

	Line Direction	Line Spacing (m)
Traverse Lines	N15ºW	200 m
Control Lines	N75ºE	2000 m

Terrain Clearance

Flying guidance was provided primarily by SGNav, a flexible and simple navigation system specifically designed by SGL for the airborne geophysical environment. Following the pre-planned survey lines, SGL's SGNav system guides the pilots from their point of departure to the start of a specific line, directs them along the survey line, and then to the next line or any other line of their choosing. While flying along a line, the SGNav system shows the pilots the correct x and y location and their altitude on a small LCD screen mounted in the pilot's line of vision.

Additional navigation parameters are displayed, such as DTS (distance to start of line), DTE (distance to end of line), TMG (track made good), SPD (aircraft ground speed), XHT (up/down error), DTK (desired heading), TTS (time to start of line), TTE (time to end of

line), TKE (track error). A screen shot of the navigation display is presented in the picture below.

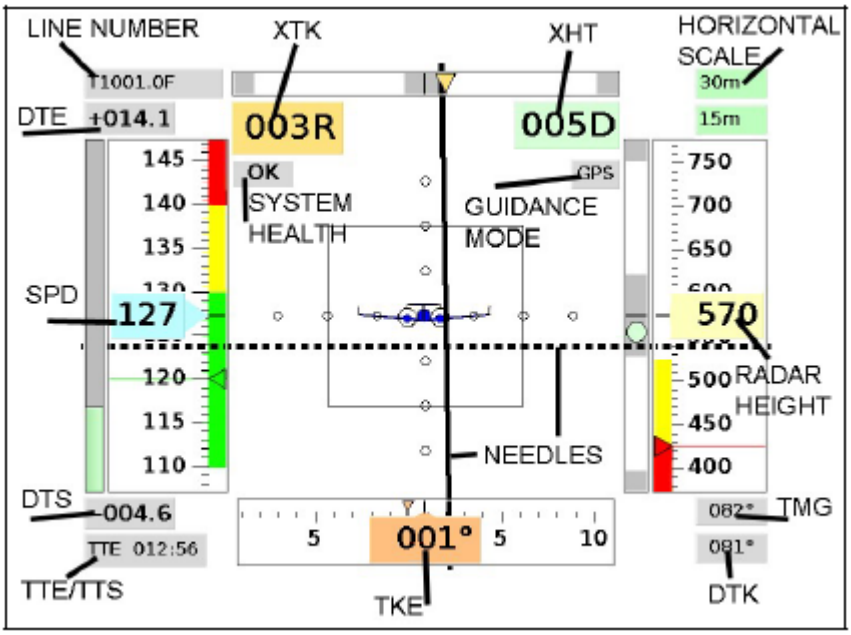

Figure 2: SGNav Navigation Display

For the Tellus Border survey, the target height was set to 59 meters above ground level in accordance with the IAA permit. The altitude measurments were provided by an aviation radar altimeter. The system is equipped with a safety pull up mode that warns the pilots if the clearance is below a pre-determined height, set at 38 meters above ground level in this case. This is illustrated in the image below.

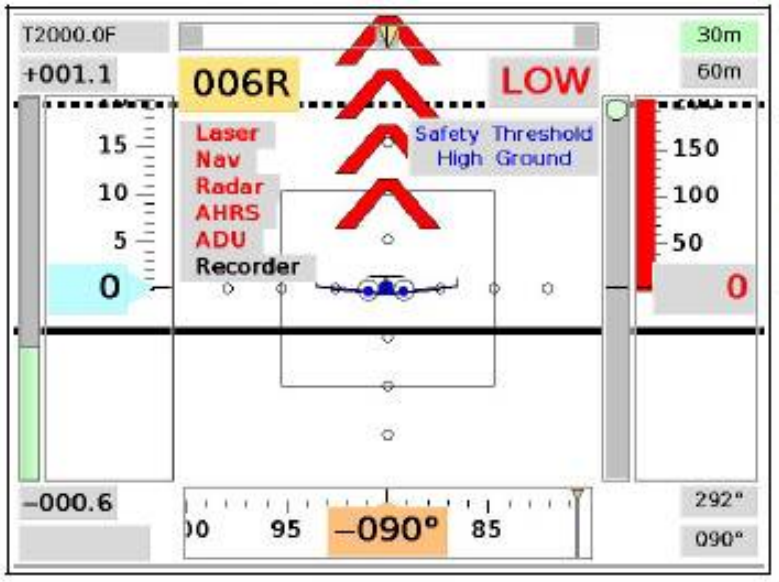

Figure 3: SGNav Secondary Guidance System Display

A second guidance system used by the pilots for this survey was a Garmin GNS430/530 with dual receiver navigation that uses a Jeppesen NavData database system. One was

installed on each pilot's yoke. This displayed the survey lines and also let the pilots know which lines have already been flown. Another important use for this GPS systems was to mark pre-determined areas that pilots had to avoid. This includes farms, equestrian centres, etc. These areas were marked with a polygon with a 2 nautical mile (3.7 km) radius around it (measured from the centre of the polygon). Once the pilots passed this radius they received a warning to begin climbing. The method for dealing with areas to be avoided is discussed in more detail in the *Public Relations and Flying* section below.

Public Relations and Flying

A public relations campaign was set in place by GSI and GSNI to inform the public about the Tellus Border survey. A website was set up showing the survey area and the layout of the flight lines, along with some information about the survey. Each week the website was updated with lines that SGL planned to fly that week. This information was submitted to the PR representatives each week by the crew. There was also a phone hotline set up where the public could call with concerns, usually issues related to low flying. People also had the option to become a 'notify' or an 'avoid'. The people on the notify list were notified before each day that SGL planned to fly over their property. The people on the 'avoid' list were generally not notified but the plane flew at 800 feet over their property to avoid disruption of people and animals. In such a case the person gave the GPS coordinates of their property to the PR group, who in turn passed it along to the crew. This polygon was then input into the Garmin GPS along with a 2 nautical mile radius from the center of the polygon. This allowed the pilots to see the areas they needed to avoid during the flight and plan accordingly. Avoid polygons were also made for large towns and cities without previous request from any specific person, and the pilots also tried to avoid flying low over built up areas during their flight to avoid complaints from the public. By the end of the survey, there were around 120 different avoid polygons.

SYSTEM TESTS

This section outlines the results of the geophysical system tests and calibrations that were performed prior to survey project commencement. The following outlines the results of the various test performed in Ottawa, Canada.

Magnetic Compensation

The compensation flight was flown on September 6, 2011 and was performed at high altitude (roughly 10,000ft) to limit the contribution of ground magnetic signal as much as possible. The compensation boxes were flown on survey line headings with all geophysical systems powered and operating as they would during normal survey data acquisition. A series of pitch (+/- 5º), roll (+/- 10º) and yaw (+/- 5º) maneuvers were performed along all four headings and the largest peak to peak differences (P2P) in the compensated magnetic signal for each maneuver on each heading (total of 12 measurements) were summed to compute the Figure Of Merit (FOM). The following table outlines the FOM calculations for both sensors.

Nose Magnetometer		**Wing Magnetometer**	
Maneuver	**P2P (nT)**	**Maneuver**	**P2P (nT)**
PITCH	0.140	PITCH	0.020
ROLL	0.096	ROLL	0.035
YAW	0.234	YAW	0.140
PITCH	0.120	PITCH	0.110
ROLL	0.076	ROLL	0.035
YAW	0.210	YAW	0.125
PITCH	0.075	PITCH	0.053
ROLL	0.120	ROLL	0.070
YAW	0.270	YAW	0.100
PITCH	0.130	PITCH	0.070
ROLL	0.110	ROLL	0.053
YAW	0.130	YAW	0.132
FOM 1.71 nT		**FOM 0.94 nT**	

Note: P2P = Peak to Peak variation in magnetic signal.

The next figures show the reduction in maneuver noise in the compensated data when compared to the uncompensated data.

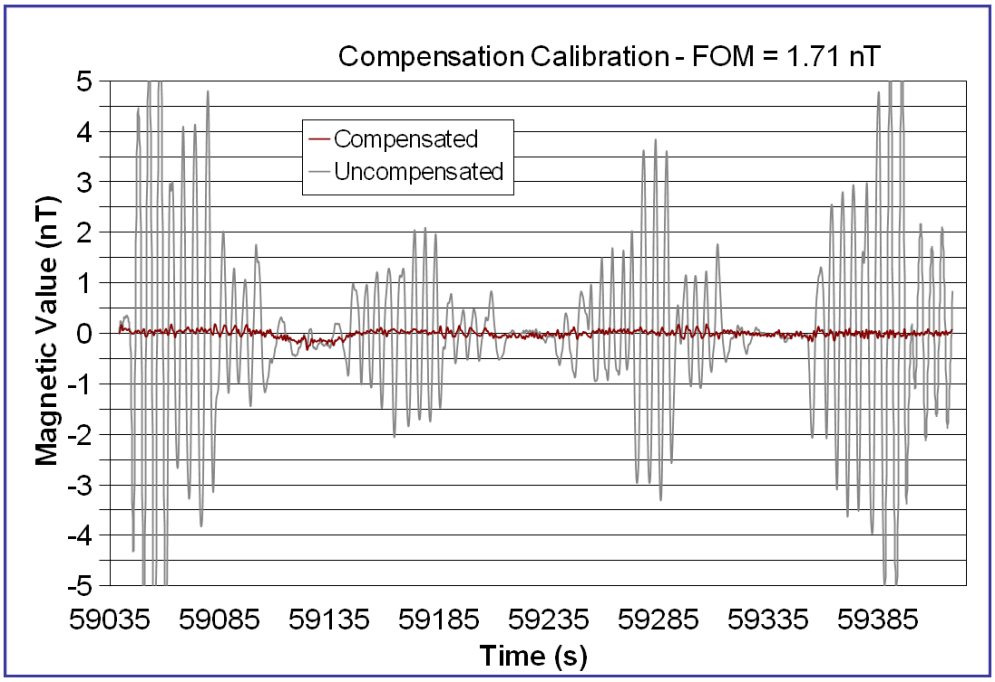

Figure 4: Compensated and Uncompensated Maneuver Noise of Nose Magnetometer

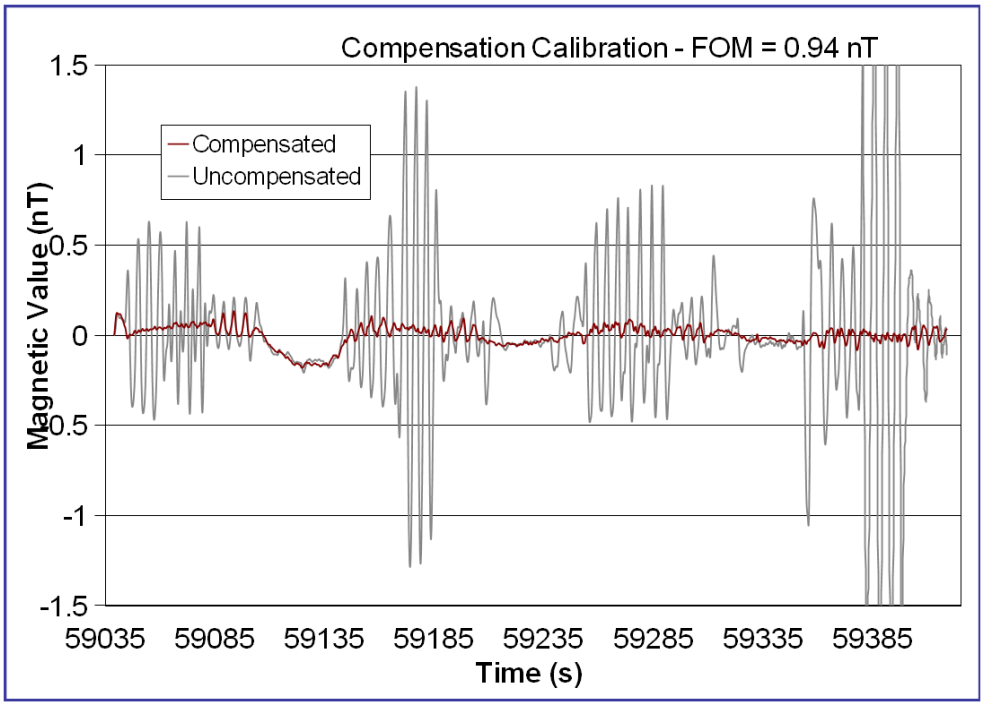

Figure 5: Compensated and Uncompensated Maneuver Noise of Wing Magnetometer

Heading Error Determination

The Heading test was flown on September 5, 2011. The test consists of flying a set of 2 orthogonal lines (North-South and East-West) crossing each other at the midpoint. By comparing the magnetic value at the midpoint between lines flown in reciprocal directions (eg. North vs. South) the error based on heading direction can therefor be established. The following tables outlines the results of the the heading test for both nose and wing magnetometers.

Nose Magnetometer		Wing Magnetometer	
Direction	**Diurnally corrected mag (nT)**	**Direction**	**Diurnally corrected mag (nT)**
N	-339.24	N	-307.43
S	-334.40	S	-307.40
E	-338.77	E	-308.09
W	-337.82	W	-307.68
N-S error	**-4.84 nT**	N-S error	**-0.03 nT**
E-W error	**-0.95 nT**	E-W error	**-0.40 nT**

Magnetic Lag Test

The lag test was flown on September 6, 2011. The lag test measures the offset in time between the detection of a magnetic anomaly and when it is actually registered by the airborne acquisition system. This lag is dominated by 2 factors; the electronic lag which remains constant, and the physical separation between the survey GPS antenna and the magnetic sensors. This last factor is therefore dependent on the speed of the aircraft. The lag test consists of flying over a known sharp magnetic anomaly (an old railway bridge in this case) in reciprocal directions. The uncorrected data will show an offset when plotted in space but should be resolved over the same location once the lag correction is applied. The following figures show the effectiveness of the lag correction for both sensors.

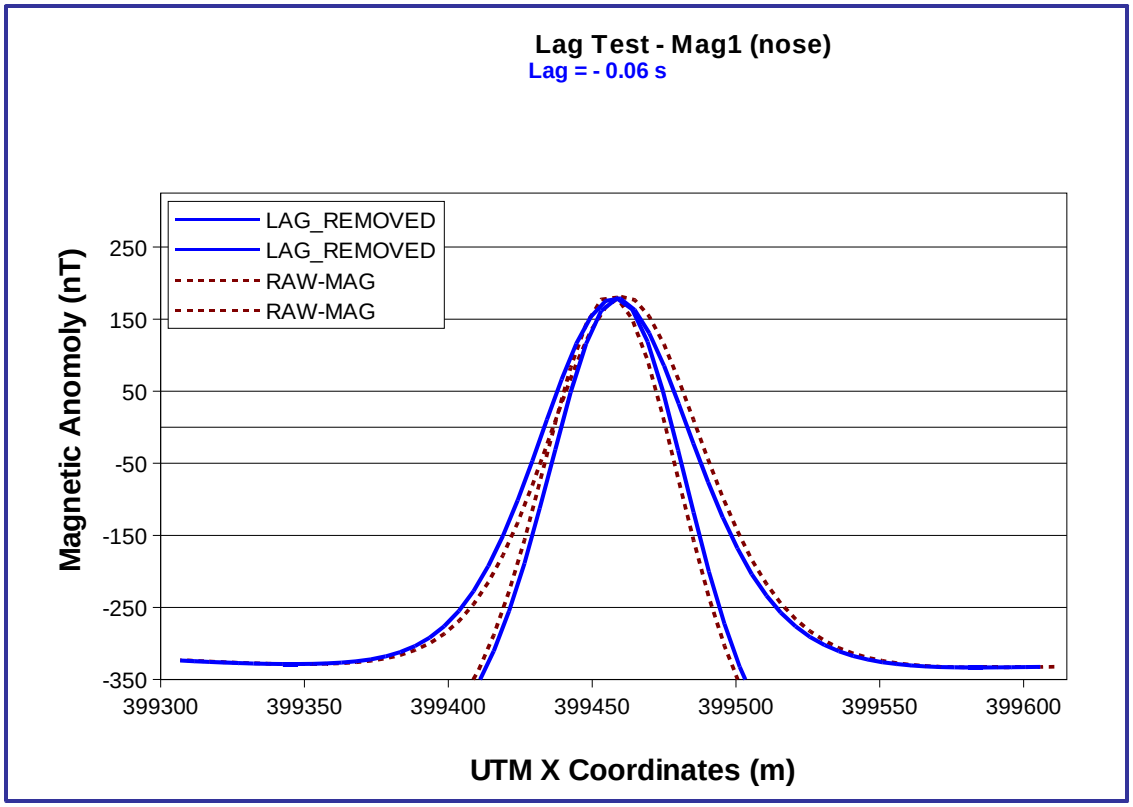

Figure 6: Lag Test Result for Nose Magnetometer

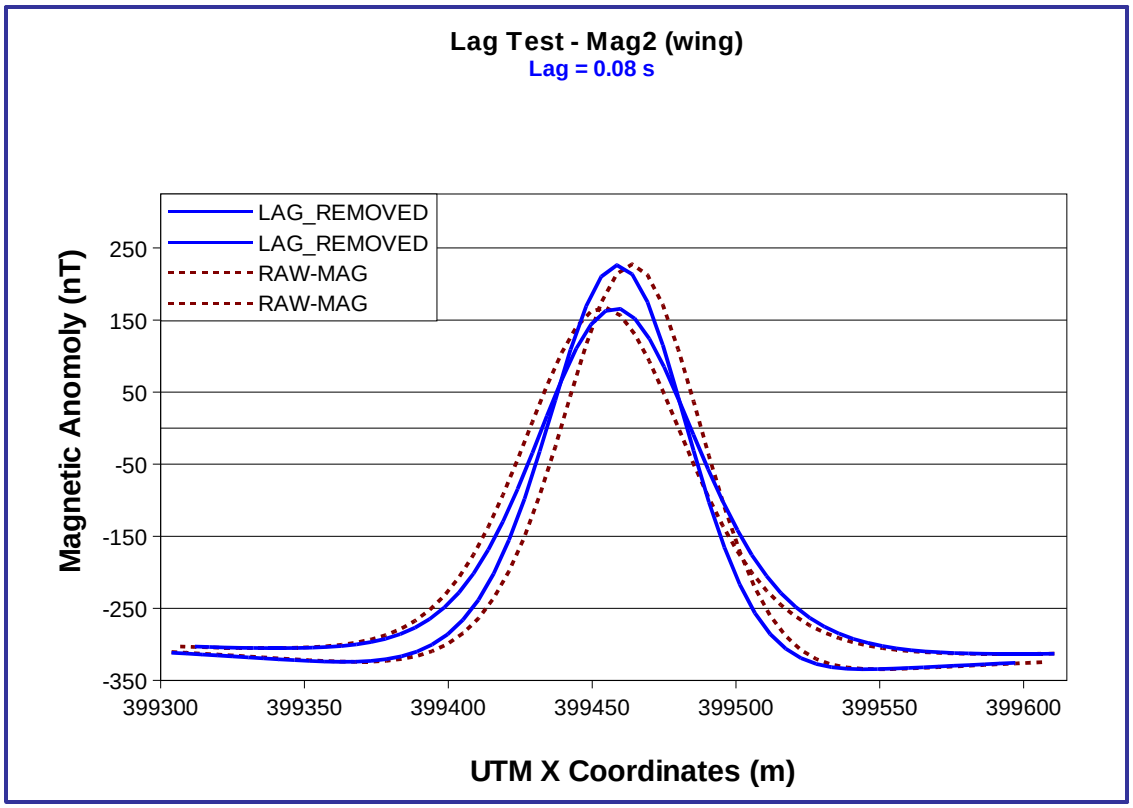

Figure 7: Lag Test Result for Wing Magnetometer

Altimeter / Barometer Calibration

The altimeter test is carried out to ensure proper functioning of the aircraft altimeters by comparing their output to that of GPS height. The test is performed by flying over a flat surface (an airport runway in this case) at several fixed altitudes above ground. Since GPS height is referenced to the WGS-84 ellipsoid a taxi of the entire runway is also included in the test as a means of correcting for that offset. The Collins radar was calibrated for the lowest heights in order to be as precise as possible within the range of heights in which the aircraft will be surveying. The results of the test were used to calibrate the Collins radar altimeter and bring it in alignment with the GPS records.

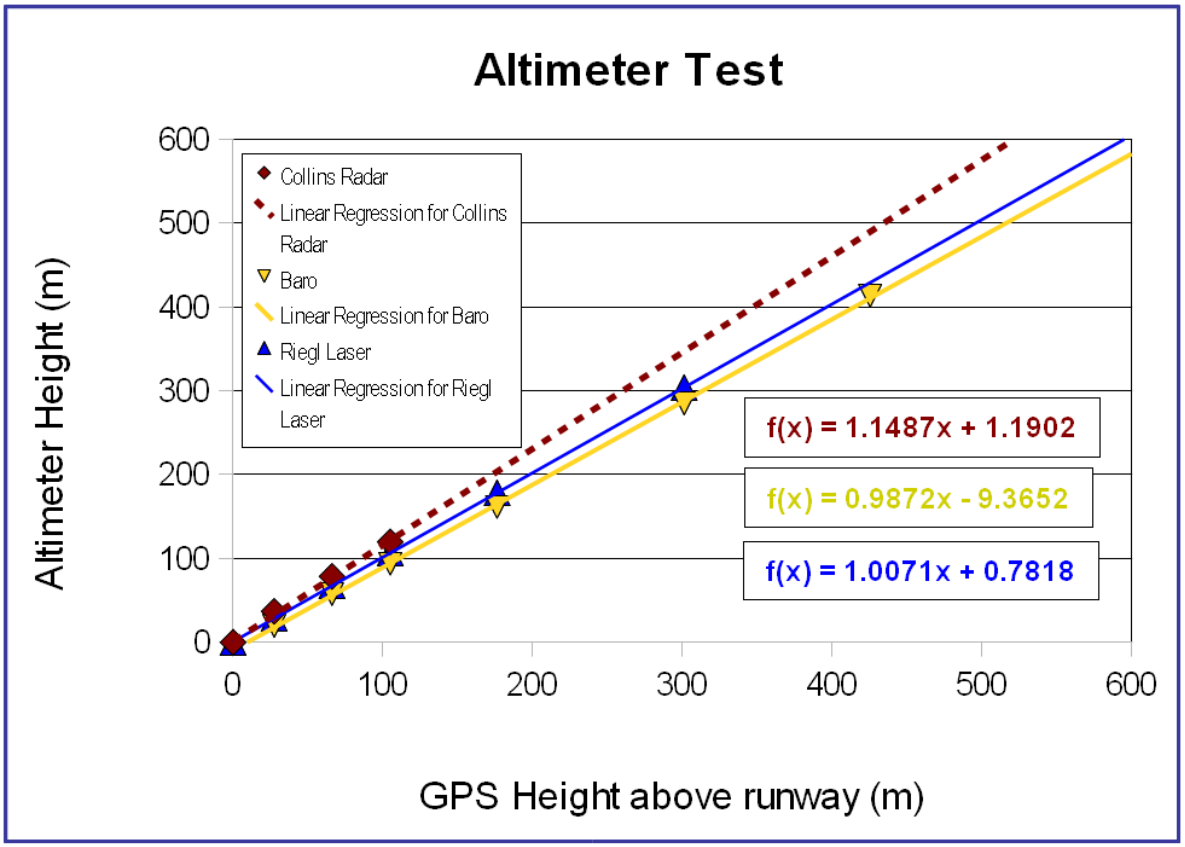

Figure 8: Altimeter Test Results for Laser, Barometer and Radar Altimeter wrt/GPS Height

Altimeter Lag Test

The steel railway bridge that was used for the magnetic sensor lag test was also used to correct the radar altimeter data for lag effect. This test was flown in Ottawa on September 6, 2011. The following figure show the effectiveness of the lag correction for the radar altimeter.

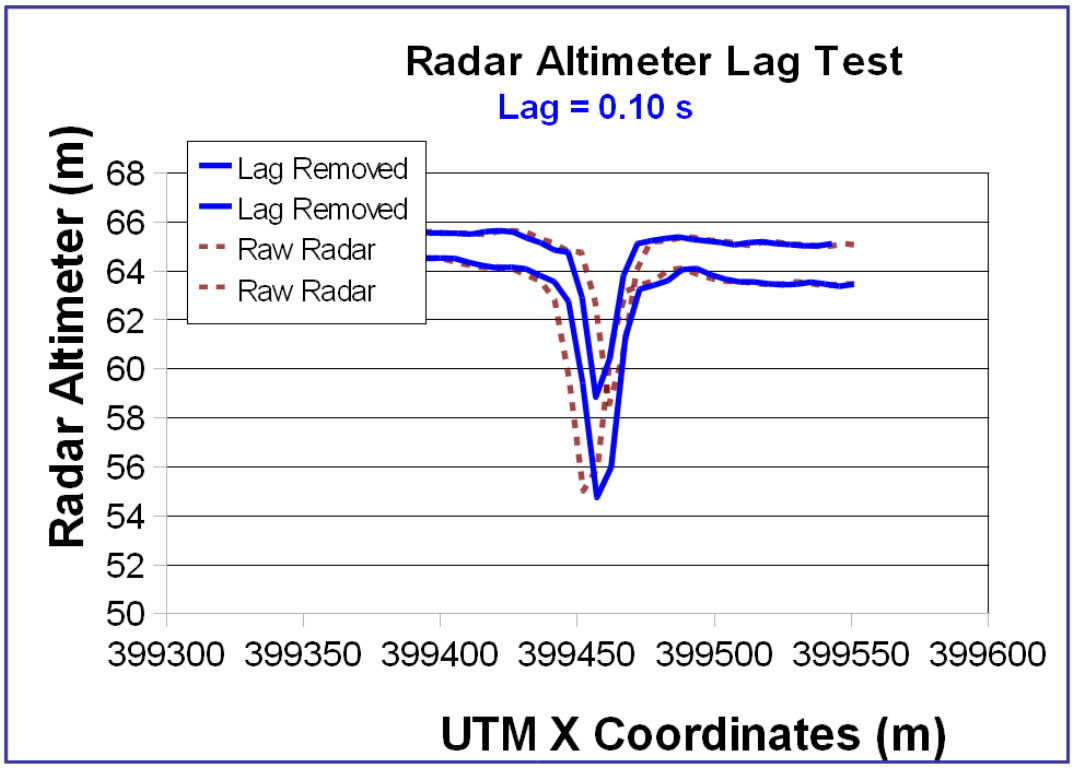

Figure 9: Radar Altimeter Lag Test Results

The FEM lag test was also performed in Ottawa, on September 6, 2011, over the same steel railway bridge that was used for the magnetic and radar lag test. The results are found in the following figure.

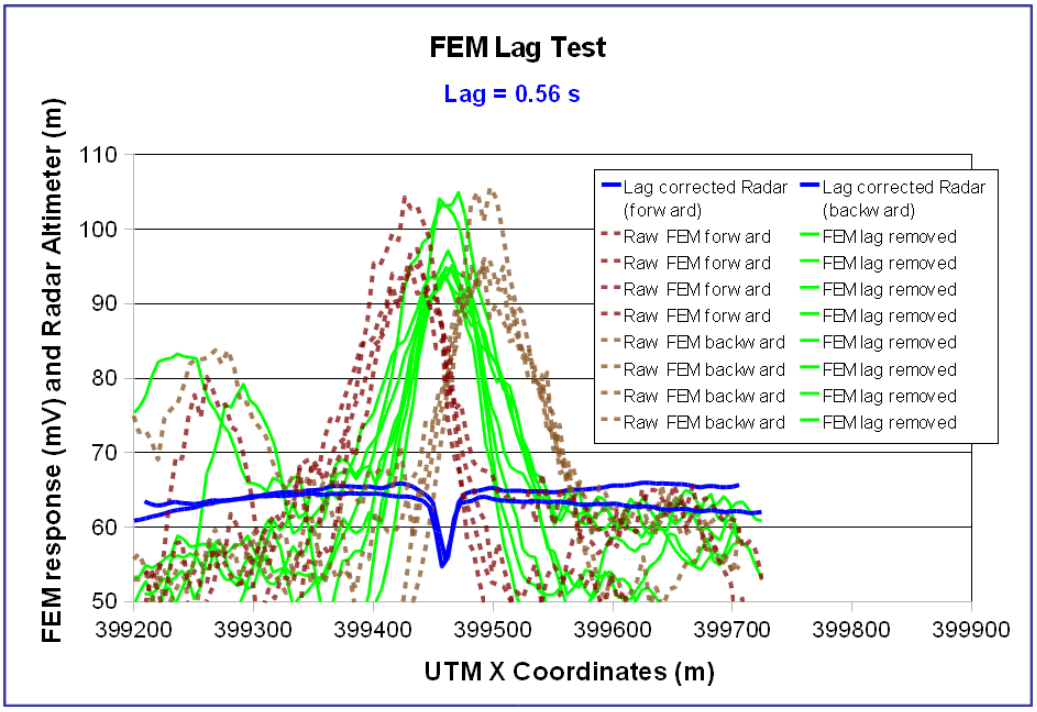

Figure 10: FEM system Lag Test Results

Radiometric Calibrations – Stripping Ratios

The stripping ratios describe how much radiation appears in the lower windows from higher energy sources due to Compton scatter of gamma-rays to lower energy, plus a smaller effect from the resolution of the spectrometer that results in lower and higher energy gamma-rays being recorded in higher and lower energy windows and vice versa. Alpha, Beta and Gamma are the main stripping ratios and they describe the scatter of gamma-rays from Thorium into Uranium, Thorium into Potassium and Uranium into Potassium. A, B and G describe the reverse relationship and are normally much smaller in comparison since they only result from the resolution limits of the spectrometer. The calibration was performed in Ottawa using the Geological Survey of Canada calibration pads. The results are as follows:

Crystal Pack A

TH INTO U (ALPHA = A23/A33):	**0.2562**
TH INTO K (BETA = A13/A33):	**0.3880**
U INTO K (GAMMA = A12/A22):	**0.7489**
U INTO TH (A = A32/A22):	**0.0466**
K INTO TH (B = A31/A11):	**-0.0016**
K INTO U (G = A21/A11):	**0.0042**

Crystal Pack B

TH INTO U (ALPHA = A23/A33):	**0.2547**
TH INTO K (BETA = A13/A33):	**0.3731**
U INTO K (GAMMA = A12/A22):	**0.7372**
U INTO TH (A = A32/A22):	**0.0448**
K INTO TH (B = A31/A11):	**-0.0037**
K INTO U (G = A21/A11):	**0.0026**

Overall System

TH INTO U (ALPHA = A23/A33):	**0.2555**
TH INTO K (BETA = A13/A33):	**0.3806**
U INTO K (GAMMA = A12/A22):	**0.7431**
U INTO TH (A = A32/A22):	**0.0457**
K INTO TH (B = A31/A11):	**-0.0027**
K INTO U (G = A21/A11):	**0.0034**

Attenuation and Sensitivity

The attenuation coefficients determine how the measurements vary with effective height and are used to standardize all of the measurements to the target survey height above ground. The system sensitivities relate the fully corrected airborne count rates to actual ground concentrations. These two calibrations were carried out simultaneously by taking ground measurements at the Breckenridge test range near Ottawa, Canada while the aircraft was flying over that same test range for the purpose of the attenuation calibration.

The cosmic, aircraft background and radon corrections for the attenuation calibration were performed by overflying the Ottawa river next to the calibration site and directly subtracting those counts from the over land data.

The attenuation coefficients obtained are as follows:

Total Count	**-0.006905**
Potassium	**-0.008507**
Uranium	**-0.007583**
Thorium	**-0.007022**

The system sensitivities were determined to be the following:

Potassium	**105.4191 pulses/s/%K**
Uranium	**12.1078 pulses/s/eU ppm**
Thorium	**5.6641 pulses/s/eTh ppm**

ENNISKILLEN CALIBRATIONS

Upon mobilization to Enniskillen, Northern Ireland, and at various points during the survey, a number of test flights were performed to calibrate the various geophysical equipment installed on the survey aircraft. Details are provided below.

Magnetic Compensation

The first compensation flight was performed on October 19, 2011 and was performed at high altitude (roughly 10,000ft), over Lower Lough Erne, to limit the contribution of ground magnetic signal as much as possible. The following tables outlines the FOM calculations for both sensors.

Nose Magnetometer		Wing Magnetometer	
Maneuver	**P2P (nT)**	**Maneuver**	**P2P (nT)**
PITCH	0.21	PITCH	0.06
ROLL	0.25	ROLL	0.03
YAW	0.21	YAW	0.07
PITCH	0.23	PITCH	0.09
ROLL	0.17	ROLL	0.06
YAW	0.19	YAW	0.16
PITCH	0.12	PITCH	0.06
ROLL	0.22	ROLL	0.06
YAW	0.34	YAW	0.13
PITCH	0.15	PITCH	0.06
ROLL	0.18	ROLL	0.07
YAW	0.11	YAW	0.12
FOM	**2.36 nT**	**FOM**	**0.98 nT**

During the week of February 6, 2012, the right engine was changed. Following this, a new compensation flight was required. It was performed on March 7, 2012, in the same conditions as before. The following tables outlines the FOM calculations for both sensors.

Nose Magnetometger		**Wing Magnetometer**	
Maneuver	**P2P (nT)**	**Maneuver**	**P2P (nT)**
PITCH	0.20	PITCH	0.05
ROLL	0.20	ROLL	0.05
YAW	0.43	YAW	0.10
PITCH	0.10	PITCH	0.13
ROLL	0.15	ROLL	0.05
YAW	0.16	YAW	0.23
PITCH	0.12	PITCH	0.04
ROLL	0.09	ROLL	0.04
YAW	0.26	YAW	0.16
PITCH	0.06	PITCH	0.08
ROLL	0.10	ROLL	0.08
FOM	**1.95 nT**	FOM	**1.09**

On May 4, 2012 the nose magnetometer sensor was changed. Following this, a new compensation flight was required. It was performed on May 8, 2012, in the same conditions as before. The following table outlines the FOM calculation for the new nose sensor.

Nose Magnetometer	
Maneuver	**P2P (nT)**
PITCH	0.21
ROLL	0.03
YAW	0.33
PITCH	0.32
ROLL	0.09
YAW	0.29
PITCH	0.08
ROLL	0.01
YAW	0.30
PITCH	0.09
ROLL	0.17
YAW	0.28
FOM 2.18 nT	

On May 29, 2012 the left generator was changed. Following this, a new compensation flight was required. It was performed on June 4, 2012, in the same conditions as before. The following tables outlines the FOM calculations for both sensors.

Nose Magnetometer		Wing Magnetometer	
Maneuver	**P2P (nT)**	**Maneuver**	**P2P (nT)**
PITCH	0.22	PITCH	0.08
ROLL	0.11	ROLL	0.10
YAW	0.28	YAW	0.08
PITCH	0.03	PITCH	0.11
ROLL	0.24	ROLL	0.06
YAW	0.03	YAW	0.13
PITCH	0.10	PITCH	0.08
ROLL	0.11	ROLL	0.05
YAW	0.19	YAW	0.17
PITCH	0.07	PITCH	0.12
ROLL	0.12	ROLL	0.05
YAW	0.15	YAW	0.14
FOM	**1.64 nT**	**FOM**	**1.16 nT**

Heading Error Determination

The Heading test was flown on December 7, 2011. It was performed over Lower Lough Erne, at an altitude of about 10,000 ft. The test consists of flying a set of 2 orthogonal lines (at survey heading 345 and 075) crossing each other at the midpoint. The following tables outlines the results of the heading test for both nose and wing magnetometers.

Nose Magnetometer		Wing Magnetometer	
Direction	**Diurnally corrected mag (nT)**	**Direction**	**Diurnally corrected mag (nT)**
N	-59.03	N	-169.02
S	-61.61	S	-169.43
E	-57.23	E	-169.95
W	-60.52	W	-168.43
N-S error	**2.58 nT**	N-S error	**0.41 nT**
E-W error	**3.29 nT**	E-W error	**-1.51 nT**

Radiometric Calibrations – System Resolution

The resolution of the spectrometer was measured by stabilizing on a Cs-137 source and then on a Th-232 source for the downward facing crystals. The upward facing crystals are always stabilized by a small, permanently attached Cs-137 source. After stabilizing for at least 2 hours for each stabilization, the resolution of the relevant peaks on each crystal was noted. The position of the peaks and the applied gains was also noted as a measure of overall system health. This check is performed before every flight using Th-232 as a source for stabilizing. The following tables contain examples of each stabilization. Crystals A1 to B4 are downward facing, whilst crystals D1 and D2 are upward facing.

Cs.							
Crystal	Peak	Res	Gain	Crystal	Peak	Res	Gain
A1	55.1	8.4	111				
A2	55	7.7	124				
A3	55	7.8	131				
A4	54.9	8	103				
B1	55.1	7.9	102	D1	55.1	9.5	120
B2	55	8.4	115	D2	55.1	8.8	119
B3	54.9	8.6	114				
B4	55.1	8	121				
Overall	55	8.2		Overall	55	9.1	

Th.							
Crystal	Peak	Res	Gain	Crystal	Peak	Res	Gain
A1	218	5	112				
A2	217.7	4.7	120				
A3	218.2	4.6	131				
A4	217.7	4.5	106				
B1	217.9	4.6	101	D1	55	9.3	120
B2	218	4.7	115	D2	55	7.9	116
B3	218.2	5	113				
B4	217.7	4.5	119				
Overall	217.9	4.7		Overall	55.1	8.5	

Radiometric Calibrations – Cosmic and Aircraft Background

This calibration determines the relationship of the counts in the cosmic ray window to the cosmic-ray background in the other windows. The cosmic window measures gamma-rays of 3 MeV or more, which is independent of terrestrial sources. The relationship between the cosmic window and the cosmic radiation in each spectral window is determined. The test also determines the constant aircraft background count rate for each window. On flight 904 a series of lines over land were flown at heights varying from 2000 to 3800 m. The linear regression between the mean count rates of the cosmic window and each window of interest describes the varying relationship between the cosmic window and the other windows (slope) as well as the aircraft background radiation in each window (constant). The following table summarizes the resulting cosmic coefficients for each window.

Windows	Background	Linear
Total	51.99	0.7012
Potassium	7.11	0.0426
Uranium	0.47	0.0336
Thorium	0.31	0.0365
Uranium upward	0.13	0.0085

FEM Transmitter Noise

The effect of the FEM transmitter on the magnetic response was verified for both sensors, while flying at high altitude (about 10,000 ft). This was achieved by turning the transmitter OFF, then back ON. The next figure shows that the FEM transmitter induces no effect on the wing sensor (red), and a slight shift of less than 1 nT on the nose sensor (green). This contribution of the FEM transmitter to the overall aircraft's magnetic response is mostly corrected by the compensation correction since the compensation calibration flight is performed in survey configuration (FEM transmitter in operation).

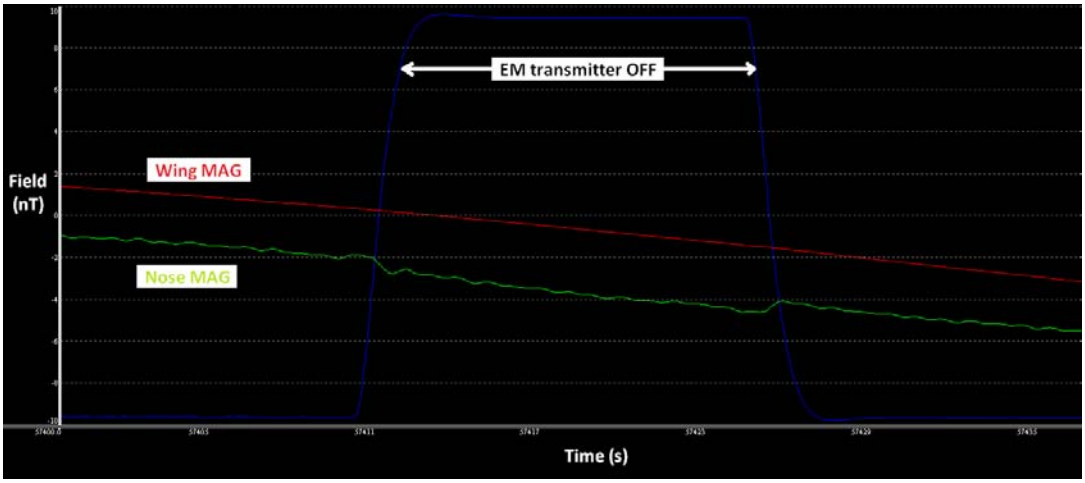

The normalized 4th difference proves that the FEM transmitter induced noise is negligible for both sensors, as shown in the following figure.

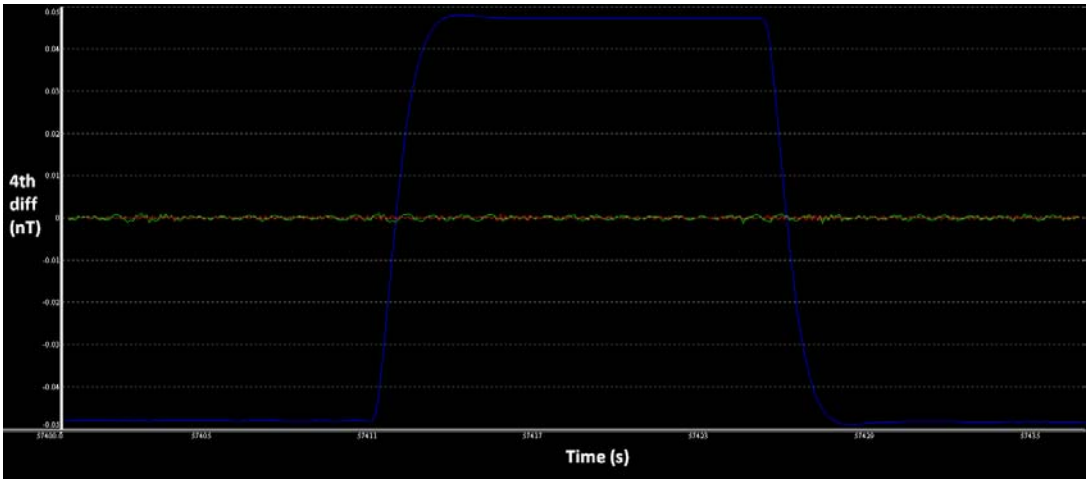

FEM Over-Water Calibration

The frequency domain electromagnetic system was calibrated following procedures described by Hautaniemi et al. (2005). A test site was chosen over Donegal Bay, in an area where water conductivity and temperature have been measured several times over the years, at every meter from surface to sea floor, by the Irish Marine Institute. The water depth reaches over 60 m, ensuring that the bottom sediments do not contribute to the EM response. Conductivity data from two different stations taken at three different years were analyzed, and proved conductivity profiles to be consistent in between the two stations. The calibration line location (in red) and the two sampling stations (CE10003_056 and CE10003_057) are shown in the following figure. This 4.5 km long calibration line was flown on October 26, 2011, at several heights from 25 to 100 m.

Figure 11:FEM Calibration Line over Donegal Bay

The conductivity data was analyzed to estimate the conductivity variation with depth.

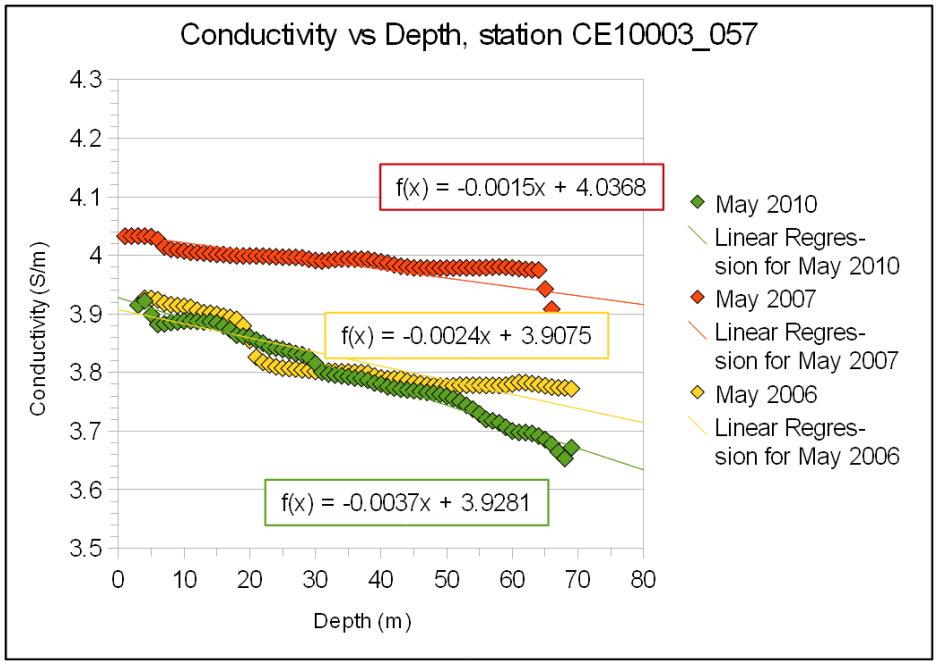

Figure 12: Conductivity vs. Depth, Station CE10003_057

As well, the conductivity change with respect to surface temperature was analyzed over three different years.

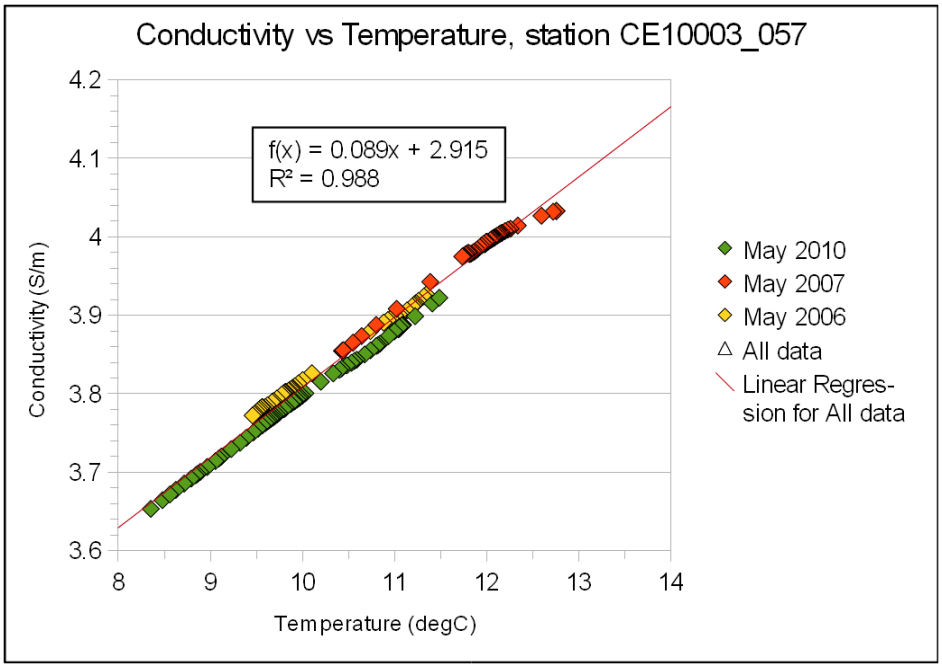

Figure 13: Conductivity vs Temperature, station CE10003_057

Surface water temperature measured on the same day the calibration flight took place (12.4 °C, published by the the Irish Marine Institute) enabled the estimation of the water conductivity close to surface ([0.089 S/m°C* 12.4 °C] + 2.915 S/m = 4.02 S/m). Based on the average conductivity decrease with depth observed over the three years, it was possible to estimate the water conductivity at a depth of 30m ([-0.0025 S/m^2 * 30 m] + 4.02 S/m = 3.94 S/m), and the average conductivity between the surface and a depth of 30 m at the calibration site (3.98 S/m). This conductivity was used to create a single layer model (half-space), which was employed to calculate the EM response for each component of each frequency, for the range of altitudes covered during the calibration flight. The calculation was performed with the software Airbeo, developed by AMIRA. The results are shown in the following figure.

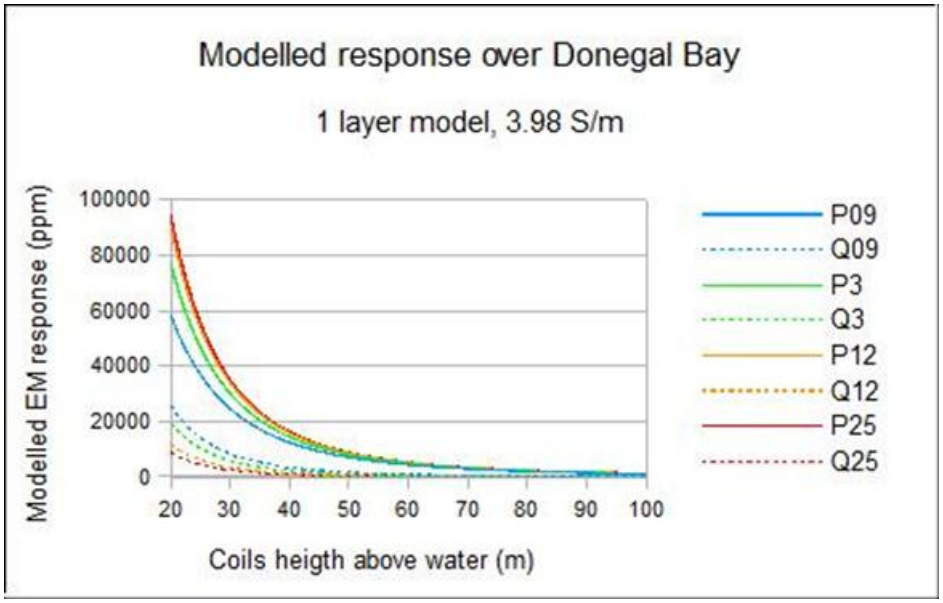

Figure 14: Modelled EM Response over Donegal Bay

This shows how sensitive the EM response is with respect to separation distance between the system and the water. It is therefore important to use accurate clearance information to perform the calibration. The radar altimeter was calibrated over the Enniskillen airport runway, and corrected for lag effect. Moreover, the altimeter data was corrected for the distance between the radar system and the EM coils. Given the wide footprint of the radar, the use of the strongest return when recording altitude, and the relatively low flying altitude, attitude corrections were deemed negligible. The FEM data was also corrected for lag effects.

The receiver measured voltage (mV units) recorded along the calibration line were plotted against the theoretical secondary to primary field coupling ratio (ppm units), and the calibration coefficients (ppm/mV units) were obtained through a linear regression. In order to ensure that the measured in-phase data used for the calibration is indeed entirely in-phase, the in-phase/quadrature orthogonality was verified before and after the calibration flight and confirmed to be good. This particular post-flight orthogonality test

result is shown in the following image. The orthogonality check procedure is described in more details in the section *FEM system orthogonality.*

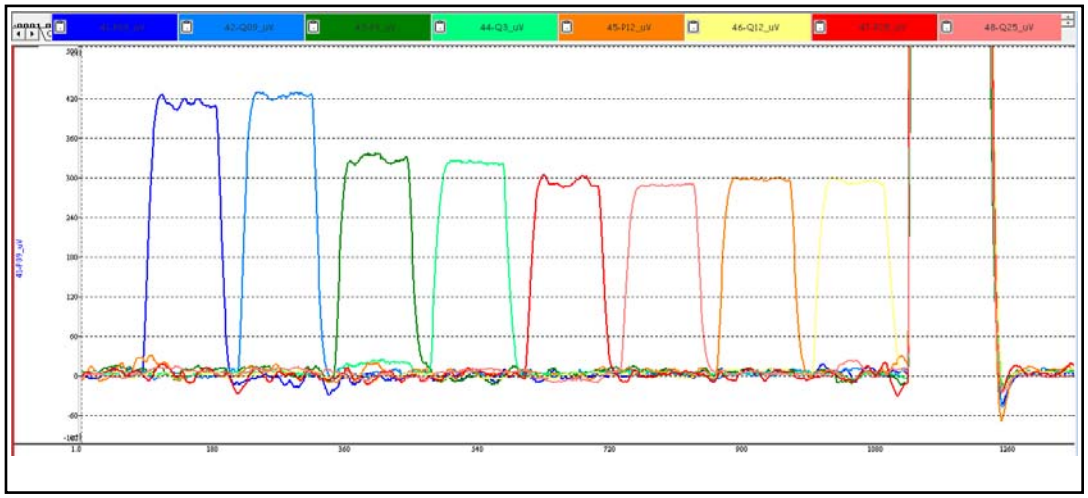

Figure 15: Post-flight Orthogonality Test

The coefficients obtained for each frequency are outlined in the following table. These coefficients were used for flight 1 to 14. The plots showing the fit obtained for the in-phase response at each frequency are presented in the following figures. Only the in-phase component is used as it provides a much stronger response over sea water than the quadrature component, with a much better distribution of points, therefore allowing for a more accurate fit.

Frequency	912 Hz	3005 Hz	11962 Hz	24510 Hz
Coefficient	4.87	6.44	7.00	6.88

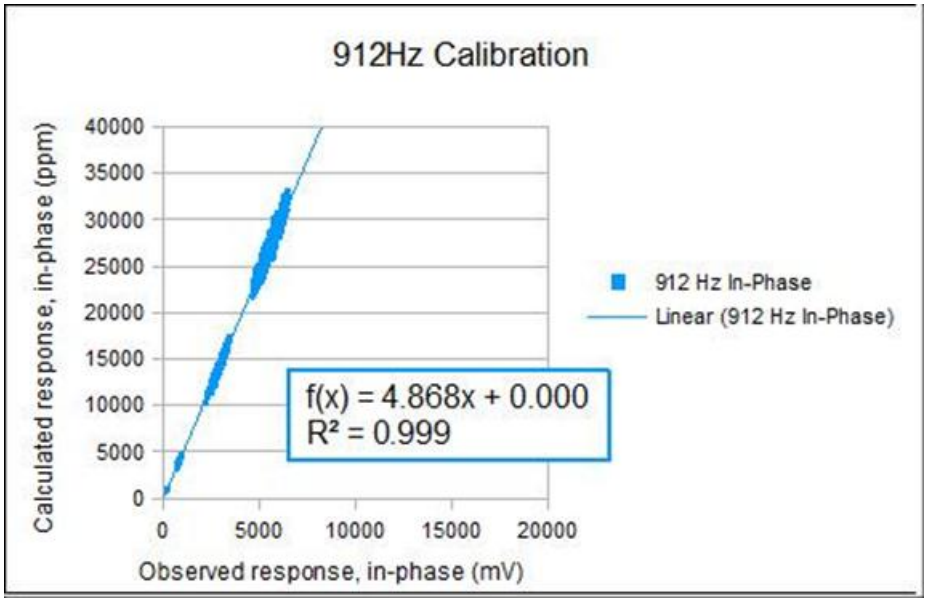

Figure 16:Fit obtained for the In-phase Response of the 912 Hz Frequency

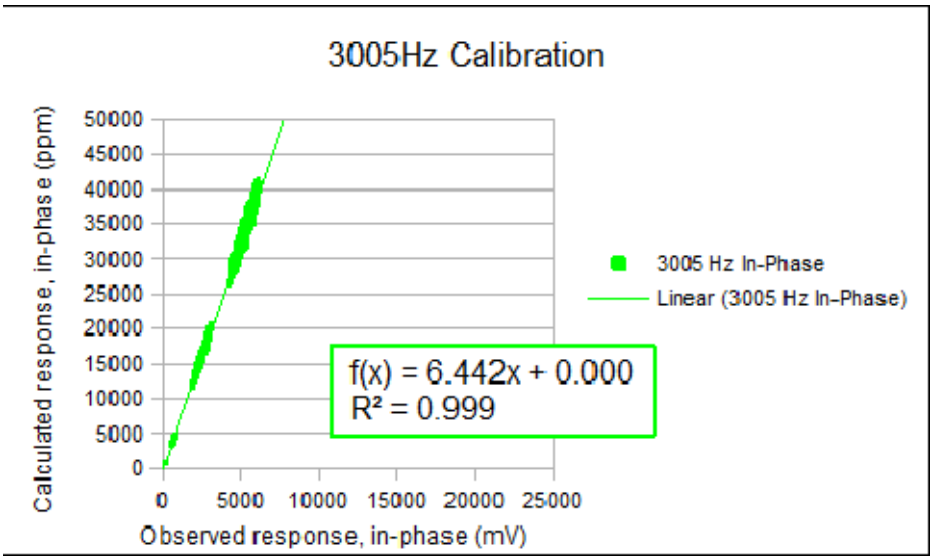

Figure 17: Fit obtained for teh In-phase Response of the 3005 Hz Frequency

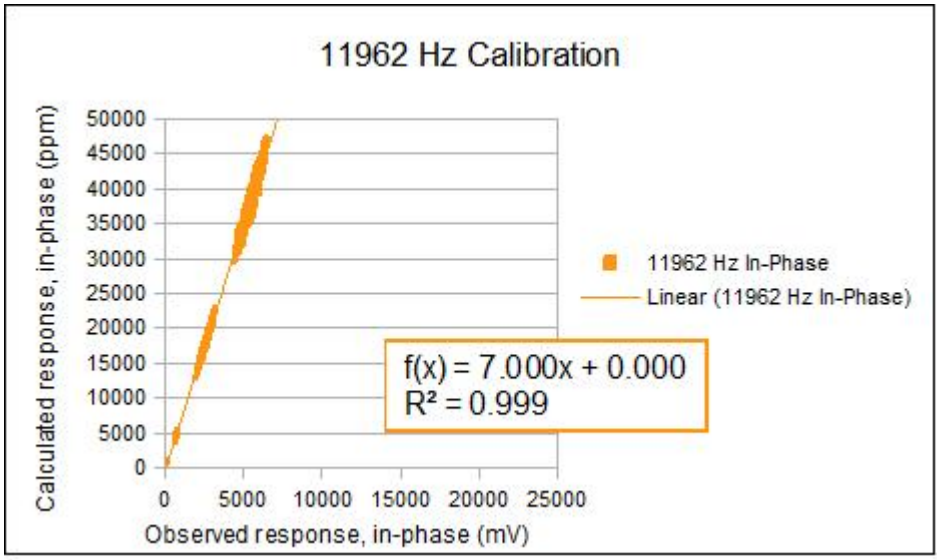

Figure 18: Fit obtained for the In-phase Response of the 11962 Hz Frequency

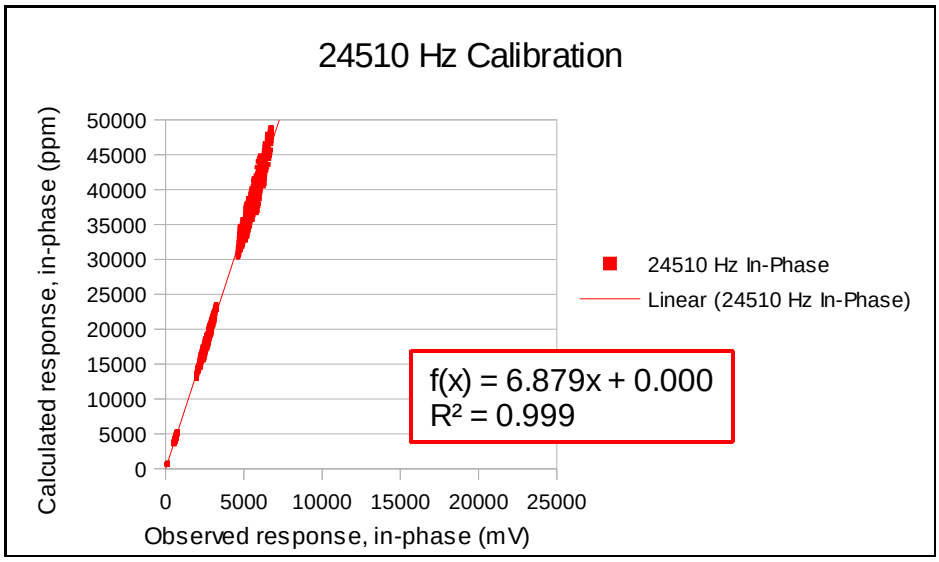

Figure 19: Fit obtained for the In-phase Response of the 24510 Hz Frequency

Prior to flight 15 cooling winter temperature trends necessitated an adjustment of the transmitter power for two frequencies, 3005 Hz and 24510 Hz, and a new calibration flight was performed on December 10, 2011. The same calibration method as outlined above was used. The surface water temperature was 10.8 °C, and the estimated average conductivity between the surface and a depth of 30 m (3.84 S/m) was used for the half-space model. The calibration coefficients used for flight 15 onward are found in the following table. Note that the coefficients for the non-adjusted frequencies, 912 Hz and 11962 Hz, have changed by 1% or less, confirming the repeatability of the calibration and the validity of the procedure used.

Frequency	912 Hz	3005 Hz	11962 Hz	24510 Hz
Coefficient	4.82	5.92	7.03	5.48

Prior to flight 129, the transmitter power was adjusted again for the 24510 Hz frequency, and a new calibration flight was performed on May 8, 2012. The same calibration method as outlined above was used. The surface water temperature was 10.2 °C, and the estimated average conductivity between the surface and a depth of 30 m (3.79 S/m) was used for the half-space model. The calibration coefficients used for flight 129 onward are found in the following table. Note that the coefficients for the non-adjusted frequencies, 912 Hz, 3005 Hz and 11962 Hz, have changed by 1% to 5%, which is to be expected considering the amount of time that has passed since the last calibration.

Frequency	912 Hz	3005 Hz	11962 Hz	24510 Hz
Coefficient	4.76	6.25	7.39	6.27

FEM System Orthogonality

Prior to each flight, the phase shift between the in-phase and quadrature parts of the EM response is verified and adjusted if required. For each frequency, two pulses of constant amplitude are artificially generated, the first being perfectly in-phase with the primary field, and the second being phase shifted by 90 degrees. Therefore, when the phase orthogonality is properly adjusted, no quadrature response should be observed during the first pulse, and vice versa during the second. This test is performed at an altitude, usually above 300 m, sufficient to avoid any EM response from the ground and to minimize cultural interference. The compensation of the primary field, enabling FEM data to be recorded with reference to an arbitrary zero-level low enough to ensure that the full range of the receiving device can be utilized, is also verified to ensure the system is functioning properly. The orthogonality check is also performed following the flight, while ferrying back to the base. An example of the orthogonality check is shown here.

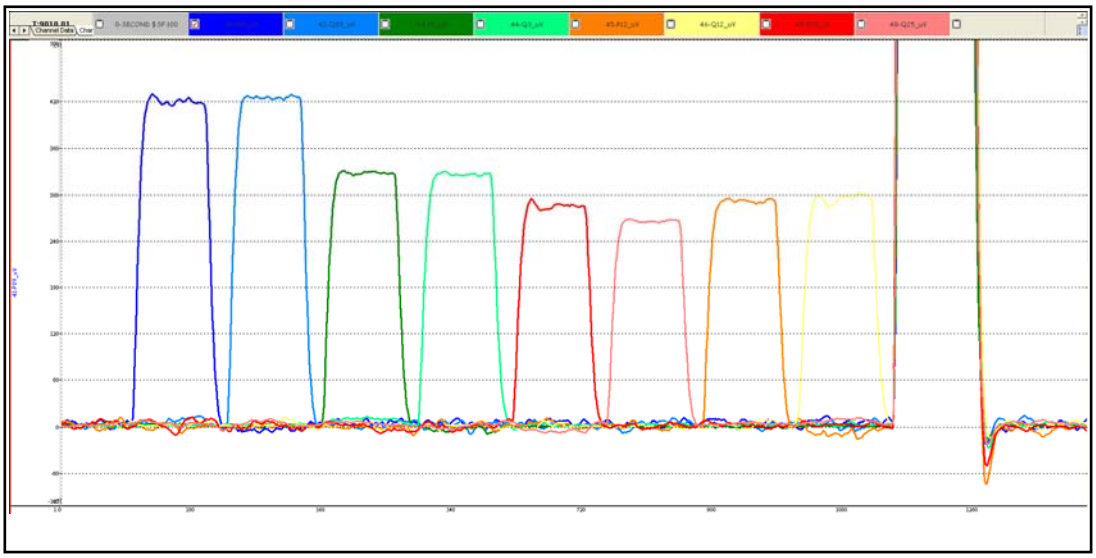

Figure 20: Example of Orthogonality check

Daily Magnetic Diurnal Drift

The average values of all daily ground magnetic field recordings for production days are plotted in the graph below. The average was determined by first correcting for the International Geomagnetic Reference Field (IGRF) using the year 2010 model extrapolated forwards to the present date and using the fixed ground station location and recorded date for each flight. All corrected readings were combined to obtain an average value for the survey. The graph reflects the deviation of each production day from the average value.

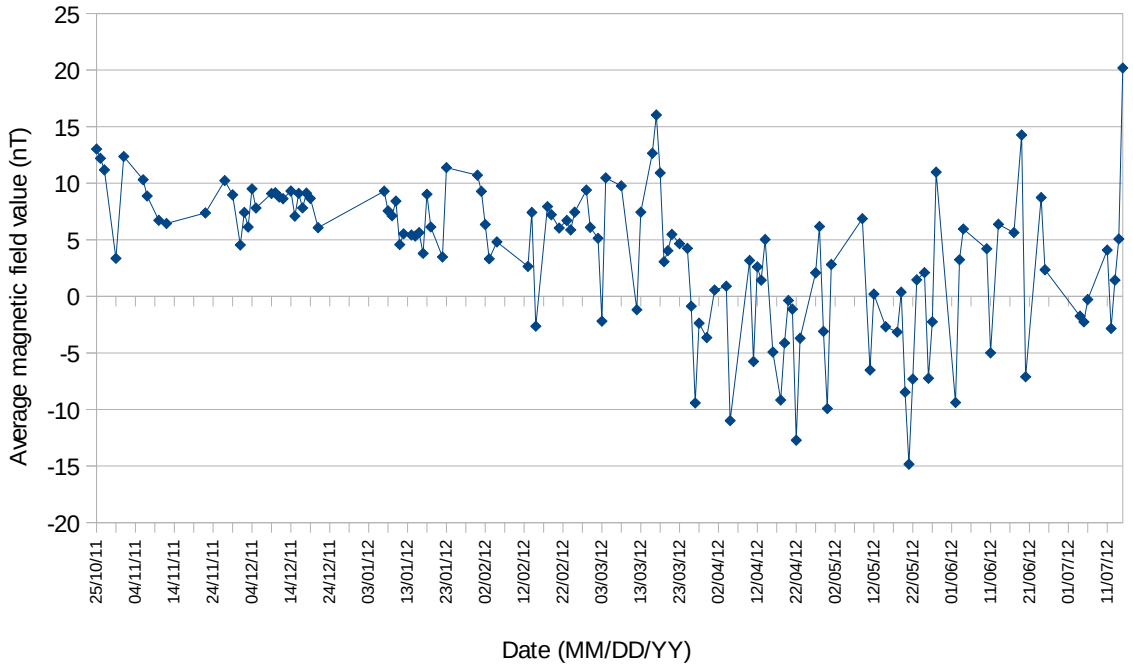

Figure 21: Average Daily Ground Magnetic Field Recordings. Only data from days when survey flights were performed is displayed.

DGPS Closure Error

The aircraft's location is compared pre and post flight as a positional check of the aircraft's parking location. A pre and post flight static period of 5 to 10 minutes is analyzed by our differential processing software after each flight. This difference between the pre and post flight average static positions or "closure error" is then recorded on daily basis. These results are presented in *Appendix 3*.

Daily Source Test

Source tests are carried out using Thorium and Uranium sources before and after each flight. Each source is left under the detector for a minimum of 2 minutes and the average counts in each window is recorded. The dead time and background corrected counts for Thorium and Uranium are then plotted post flight to ensure consistency. The corrected counts should fall within +/- 5% of the running average. These results for Thorium, Uranium and total counts are illustrated in the graphs below. The normal position of the thorium and uranium pucks was changed prior to flight 23 and again prior to flight 160, resulting in different averages over those periods.

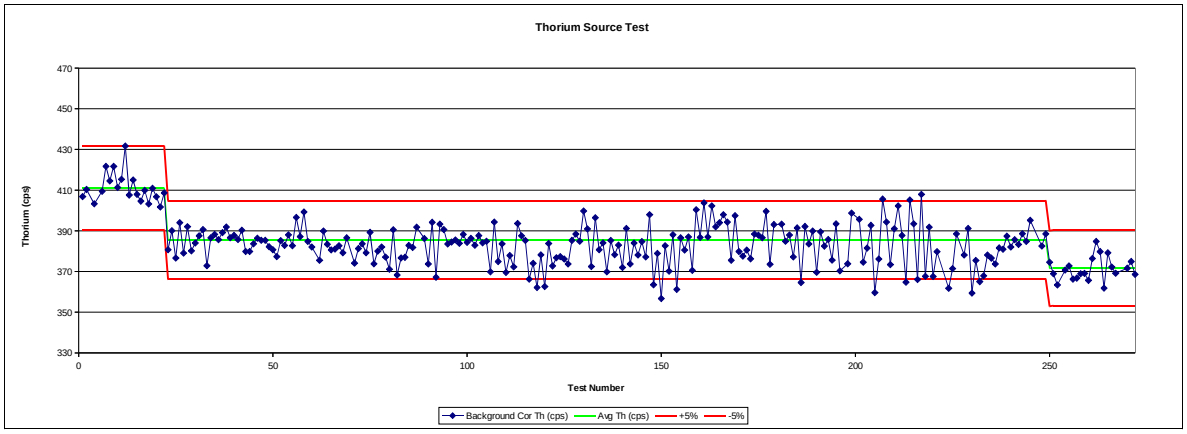

Figure 22: Thorium Source Test

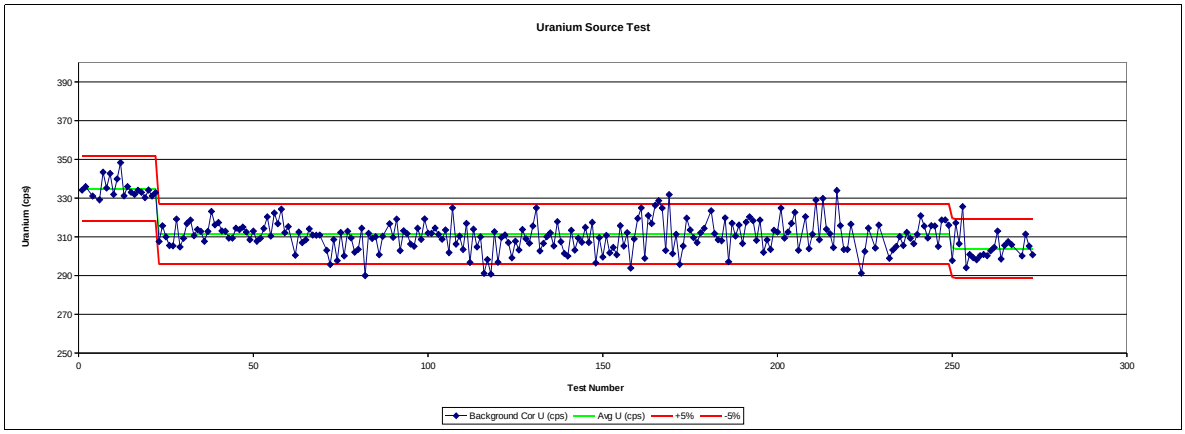

Figure 23: Uranium Source Test

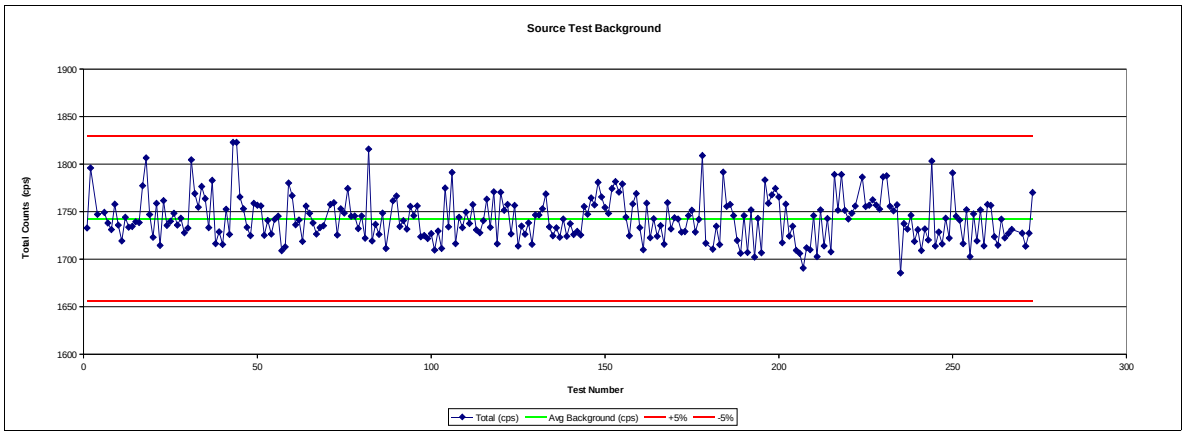

Figure 24: Source Test Background

FIELD OPERATIONS

The field base for the project was located at the Enniskillen airport, with flight operations for the survey conducted from the airport. Power to the aircraft was supplied by cables run from the hangar owned by London Helicopters. The field office was at the airport, and the principle crew accommodations were in rented houses, primarily in Irvinestown, Fermanagh. A dual frequency GPS reference station, GND1, was installed in a farmers field behind London Helicopters hangar at the airport, and a magnetic sensor was installed about 50 meters further into the field. The computer was housed inside a London Helicopter store room. Prior to flight 175 the owner of the field requested that the equipment be moved, and the GPS antenna was relocated to the roof of the hangar. GND2 was located behind a farmers house in Irvinestown, and consisted of a dual frequency GPS reference station and magnetic sensor. Both antennas were differentially corrected prior to the survey.

The aircraft was parked beside the hangar for the duration of the survey. Each survey flight departed and returned to this location. The position of the aircraft was (Irish National Grid datum, Transverse Mercator True origin N53.5):

Parking Location	X	Y	Elevation
1	223056.32	349806.94	56.87 m

GND2 reference station was located in a magnetically quiet environment. Diurnal corrections were therefore applied using GND2 data. GND1 was recording only for redundancy and in case of a failure of GND2.

The position of the GND1 reference station GPS antenna was differentially corrected using data from four International GPS Service (IGS) reference stations HERS (Hailsham, UK), HERT (Manila, Hailsham, UK), HOFN (Hoefn, Iceland) and MORP (Morpeth, UK), using data recorded on days 269, 270, 271 and 272 of 2011. Base station GND2's position was differentially corrected using data from GND1 on the same days.

The positions of the GPS antennas after differential correction were (Irish National Grid datum, Transverse Mercator True origin N53.5):

Table 3: Reference stations location

Station	X	Y	Elevation
GND1	223005.3057	349891.3534	52.19 m
GND2	222609.7512	355529.5518	59.19 m

Operational Issues

Rain in the survey block, as well as frequent low cloud and fog forced occasional production delays. See *Appendix VI* for the Weekly Reports.

Field Personnel

The following technical personnel of SGL participated in field operations:

Field Personnel	Name
Crew Chief	Jenrené Martel
Crew Chief	Alison McCleary
Crew Chief	Marianne McLeish
Data Processor	Joël Dubé
Data Processor	Monika Pal
Captain	Steve Gebhardt
Captain	Todd Svarckopf
Captain	Charles Dicks
Co-Pilot	Clinton Elliott
Aircraft Mechanic	Landen Coulas
Aircraft Mechanic	John Sevenhuysen
Aircraft Mechanic	John Burnham

The following personnel from TELLUS and GIS participated in field operations:

Field Personnel	Name
Tellus Border Project Manager	Mike Young
Tellus Border Deputy Project Manager	Marie Cowan
Tellus Border Assistant Project Manager	Mairead Glennon
Tellus Border Geophysicist	James Hodgson
Tellus Border Geophysicist	Mohammednur Desissa
Tellus Border Public Relations	Claire McGinn
GIS and Data Manager	Shane Carey
BGS Data Consultant	David Beamish

DIGITAL DATA COMPILATION

Preliminary processing for on-site quality control was performed in the field as each flight was completed. This included verifying the data on the computer screen, generating traces of all of the data channels, and creating preliminary data grids.

Frequency Domain Electromagnetic Data

The airborne electromagnetic data were recorded in volts at 40 Hz and later decimated to 10Hz in the processing. Data were recorded at four frequencies (912 Hz, 3005 Hz, 11962 Hz and 24510 Hz) each with two components, in-phase with the source pulse and out of phase "quadrature". The data were visually inspected for spikes and noise.

Lag

A +0.70 second static lag correction due to signal processing was applied to each data point. In addition a variable lag correction is applied that is a function of speed and the physical offset between the GPS antenna on the aircraft tail and the electromagnetic pods as measured along the long axis of the aircraft, known to be -8.4m. Therefore, the total lag applied is equal to (0.70 + (-8.4/v)) seconds where v is the instantaneous velocity of the aircraft in m/s. The aircraft speed dependent lag is calculated using SGL's Dynlag software.

Interactive single-flight, zero-level correction for non-linear (e.g. thermal) drift

The zero-level of the system can drift due to significant variations in air temperature and the data must be corrected for this effect. SGL uses a method similar to that described by Leväniemi et. al (2009, Journal of Applied Geophysics, 67, 219-233). The data should be zero when the survey aircraft is more than 200m above the ground, and we can use this fact to define a curve of corrections that brings the data to the correct level on a flight by flight basis. The start and end of the correction curve for each flight were set to coincide with the zero-level calibration pulse procedure that is performed at approximately 300m above ground before and after flying the survey lines. Intermediate points during production were determined when the aircraft ascended to flying heights of over 200 meters above ground, particularly when flying over obstacles or ferrying between sections of the survey block. The EM response data at the start, end and intermediate points are shifted until they are zero. Shifts between the known zero points are linearly interpolated to define the full correction curve. A separate correction curve is required for the in-phase and quadrature data of each frequency.

Interactive single-line, zero-level correction across adjacent lines

Grids of the in-phase and quadrature components were produced and studied. Lines, or groups of lines, that appeared high or low compared to their neighbours were given an additional zero-level shift to bring them into agreement.

Application of calibration coefficients

The in-phase and quadrature components were multiplied by a scaling factor to match the theoretical response of the system. The calibration coefficients were determined by test flights over Donegal Bay, as described in the Enniskillen Calibrations section. The coefficients used are displayed in the following table:

Flights	P (912Hz)	Q (912Hz)	P (3kHz)	Q (3 kHz)	P (12 khz)	Q (12 kHz)	P (25 kHz)	Q (25 kHz)
1 to 14	4.87	4.87	6.44	6.44	7.00	7.00	6.88	6.88
15 to 177	4.82	4.82	5.92	5.92	7.03	7.03	5.48	5.48

Differential polynomial levelling

Differential polynomial levelling following the method of Beiki et. al (2010, Geophysics, Vol. 75, No. 1, L13-L23) was used as an automatic method to apply non-linear levelling corrections to the data. The algorithm is based on polynomial fitting of data points in 1D and 2D sliding windows. The levelling error is taken as the difference between 1D and 2D polynomial fitted data at the center of the windows. Polynomials of order 1 were used along with a search radius of 600 meters for all components.

Micro-levelling

Micro-levelling was applied to remove residual levelling errors from the data. This was achieved by using a combined directional cosine filter and high pass Butterworth filter to identify and remove artefacts that are long wavelength parallel to survey lines and short wavelengths perpendicular to survey lines. A limit of +/-1000 ppm was set for all microlevelling corrections. The cut-off wavelength of the directional Butterworth filter was chosen to be 1600 meters for each frequency and component, and was designed to reduce remaining levelling errors while avoiding amplification of noise in areas of high signal gradient.

Conversion to resistivity

A look-up procedure was used that employs the in-phase and quadrature data components at each frequency to calculate resistivity. The process uses the same methods as the Airbeo program (http://www.electromag.com.au/csiro.php). The ground was modelled as a single layer with a constant lithology. Heights of the lookup table are modelled from 16 meters to 240 meters below the surface at 2 meter intervals, while the resistivity sampling was from 0.001 ohm.m to 79,432 ohm.m using a uniform logarithmic sampling interval of 20 points per decade.

Gridding

All grids were made using a minimum curvature algorithm to create a two-dimensional grid equally incremented in the X and Y directions. The algorithm produces a smooth grid by iteratively solving a set of difference equations minimizing the total second horizontal derivative while attempting to honour the input data (Briggs, I.C, 1974, Geophysics, v 39, no. 1). The final grids of the electromagnetic data were created with 50 m grid cell size appropriate for survey lines spaced at 200 m.

High-fly Zones

The EM system is most effective when survey altitude is as low as possible. When the flying height is increased, coupling with the ground is reduced, degrading results. At very high altitudes there is no coupling at all and results will be unreliable. High fly areas result when the terrain is sharp and pilots manoeuvre for safety, and also for obstacles such as towers, wind farms, and airports. In addition, high fly was required when requested by concerned members of the public. In general, data quality is degraded above 75 meters, and care must be taken when interpreting high fly data. A map of high-fly areas is shown in Figure 25.

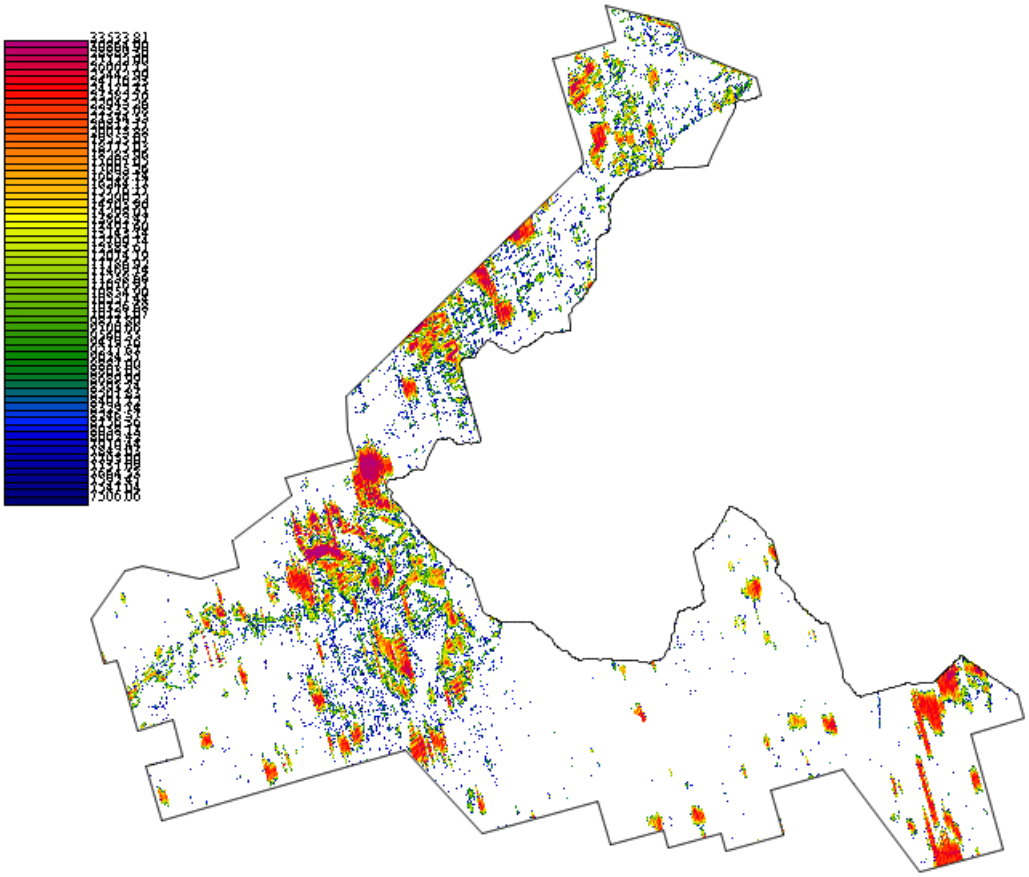

Figure 25: Map of High-fly Areas (>75 m above ground)

MAGNETOMETER DATA

The airborne magnetometer data, recorded at 160 Hz then later extracted to 10 Hz for processing, were plotted and checked for spikes and noise. A +0.25 second static lag correction due to signal processing was applied to each data point. In addition a variable lag correction is applied that is a function of speed and the physical offset between the GPS antenna on the aircraft tail and the wingtip magnetometer as measured along the long axis of the aircraft, known to be -8.4m. Therefore, the total lag applied is equal to (0.25 + (-8.4/v) seconds where v is the instantaneous velocity of the aircraft in m/s. The aircraft speed dependent lag is calculated using SGL's Dynlag software.

Ground magnetometer data were inspected for cultural interference and edited where necessary. The reference station magnetometer data were lightly filtered using a 121-point low pass filter to remove high frequency, low amplitude interference. All ground magnetometer data were corrected for the International Geomagnetic Reference Field (IGRF) using the year 2010 model extrapolated forwards to the present date and using the fixed ground station location and recorded date for each flight. The mean residual value of the ground station calculated to be 16.706 nT is subtracted to remove any bias from the local anomalous field. Diurnal variations in the airborne magnetometer data were then removed by subtracting the corrected ground station data.

The airborne magnetometer data were then corrected for the IGRF using the location, altitude, and date of each point. IGRF values were calculated using the year 2010 IGRF model extrapolated forwards to the present date. The altitude data used for the IGRF corrections are DGPS heights above the GRS-80 ellipsoid.

Height Adjustments

The survey was flown in radar guidance mode in order to stay as close to the target survey altitude of 59m as much as possible. This approach was adopted in order to optimize the acquisition of frequency domain electromagnetic (FEM) data which is known to drop off in signal strength rapidly. Little reliable FEM data is acquired at heights of 200 to 250 m above ground depending on the signal frequency and the conductivity of the ground, and the lower the survey is flown, the higher the signal to noise ratio for all frequencies.

By adopting a flying strategy optimized for FEM data, drape flying was not possible, resulting in survey lines flown at different altitudes in adjacent lines and at intersections between traverse and control lines. Inevitably this results in differences in the spectral content of airborne magnetic data where the survey height above ground is inconsistent. At low altitudes, even relatively small differences in altitude may result in significant changes in spectral content of the magnetic data. Amplitude of magnetic signal drops off with height at an exponential rate proportional to the frequency of the signal, so that high frequency signal in particular changes rapidly with small changes in altitude close to the ground. Correcting for such changes using traditional levelling methods can be challenging since there is no way to properly extrapolate corrections from miss-ties at intersections due to altitude differences. Therefore, there is an advantage to correcting the airborne data for height variation before attempting levelling for diurnal changes.

In order to correct magnetic data for altitude variation, we first need to define a consistent surface that will be used as a reference height. This can be a surface of constant height with respect to the ellipsoid or a drape surface that is similar to what would have been flown had a drape mode been employed instead of a radar mode. The drape surface approach has the advantage of retaining as much of the recorded signal content as possible whilst achieving consistency of height at intersections and smoothly varying heights between adjacent lines. Therefore the drape approach was adopted, and is based on a climb and decent rate of between 350 and 400 feet/nMile. The difference between the drape reference surface and the recorded altitude is the height difference to be accounted for.

The manner in which the magnetic signal changes with height can be predicted from the well known process of upward continuation. This concept is relatively easy to apply, but the reference surface is often below the recorded altitude. Therefore the correction to be applied often requires a downward continuation. Downward continuation is known to be problematic as it will tend to amplify the high frequency content of the data which is generally only noise, and it cannot recover true high frequency signal that was not originally recorded.

A better approach, and the one adopted in this case, is to predict the magnetic field intensity that would have been recorded at the different altitude based on a Taylor expansion that sums the derivatives of the field as follows:

$$T + (T' h)/1! + (T'' h2) / 2! + (T''' h3)/ 3! + (T'''' h4)/ 4! + ...$$

where

T is the total magnetic intensity (TMI) at any given point,
T' is the first vertical derivative of the TMI, T'' is the second vertical derivative etc.
1! is the factorial of 1, 2! is the factorial of 2 etc.

The series is infinite, but in practice we find no need to calculate the factors beyond the 4th derivative.

The calculation may be performed on the time series data in one dimension, but this does not account for the cross line gradients in the data. Therefore, it is preferable to derive a two dimensional grid, from which the derivatives may be calculated in the Frequency domain. In order to do this, a levelled grid of magnetic intensity must first be derived. This presents a quandary, since we wish to correct for height differences before levelling. The solution is to apply a heavy micro-levelling to the data for the purpose of calculating the height corrections only, and apply the corrections to the un-levelled data. It is then possible to iterate the process until the result is stable, but it is found that further iterations have negligible impact and the result is essentially stable after one cycle.

Levelling

Intersections between control and traverse lines were determined by a program which extracts the magnetic, altitude, and X and Y values of the traverse and control lines at each intersection point. Each control line was then adjusted by a constant value to minimize the intersection differences that were calculated using the following equation:

$\Sigma |i - a|$ summed over all traverse lines
where, i = (individual intersection difference)
a = (average intersection difference for that traverse line)

Adjusted control lines were further corrected locally to minimize the difference between individual corrections and the average correction for the control line that results from residual diurnal variations along the line. Traverse line levelling was then carried out by a program that interpolates and extrapolates levelling values for each point based on the two closest levelling values. After traverse lines have been levelled, the control lines are matched to them. This ensures that all intersections tie perfectly and permits the use of all data in the final products.

The levelling procedure was verified through inspection of Total Magnetic Intensity (TMI) contour maps, inspection of vertical derivative grids, plotting profiles of corrections along lines, and examining levelling statistics to check for steep correction gradients.

Micro-levelling

Micro-levelling was applied to remove residual diurnal effects from the data. This was achieved by using a combined directional cosine filter and high pass Butterworth filter to identify and remove artefacts that are long wavelength parallel to survey lines and short wavelengths perpendicular to survey lines. A limit of +/-2.00 nT was set for all micro-levelling corrections.

Gridding

The grid of the Total Magnetic Intensity was made using a minimum curvature algorithm to create a two-dimensional grid equally incremented in the X and Y directions. The algorithm produces a smooth grid by iteratively solving a set of difference equations minimizing the total second horizontal derivative while attempting to honour the input data (Briggs, I.C, 1974, Geophysics, v 39, no. 1).

The final grids of the magnetic data were created with 50 m grid cell size appropriate for survey lines spaced at 200 m. The strong geological trends on the grids were enhanced by SGL's Gtrend software, which places data values between survey lines along strong magnetic anomalies during the gridding procedure. This technique reduces the 'bubbling' affect which occurs when gridding short wavelength linear features that trend at a high angle to the traverse lines.

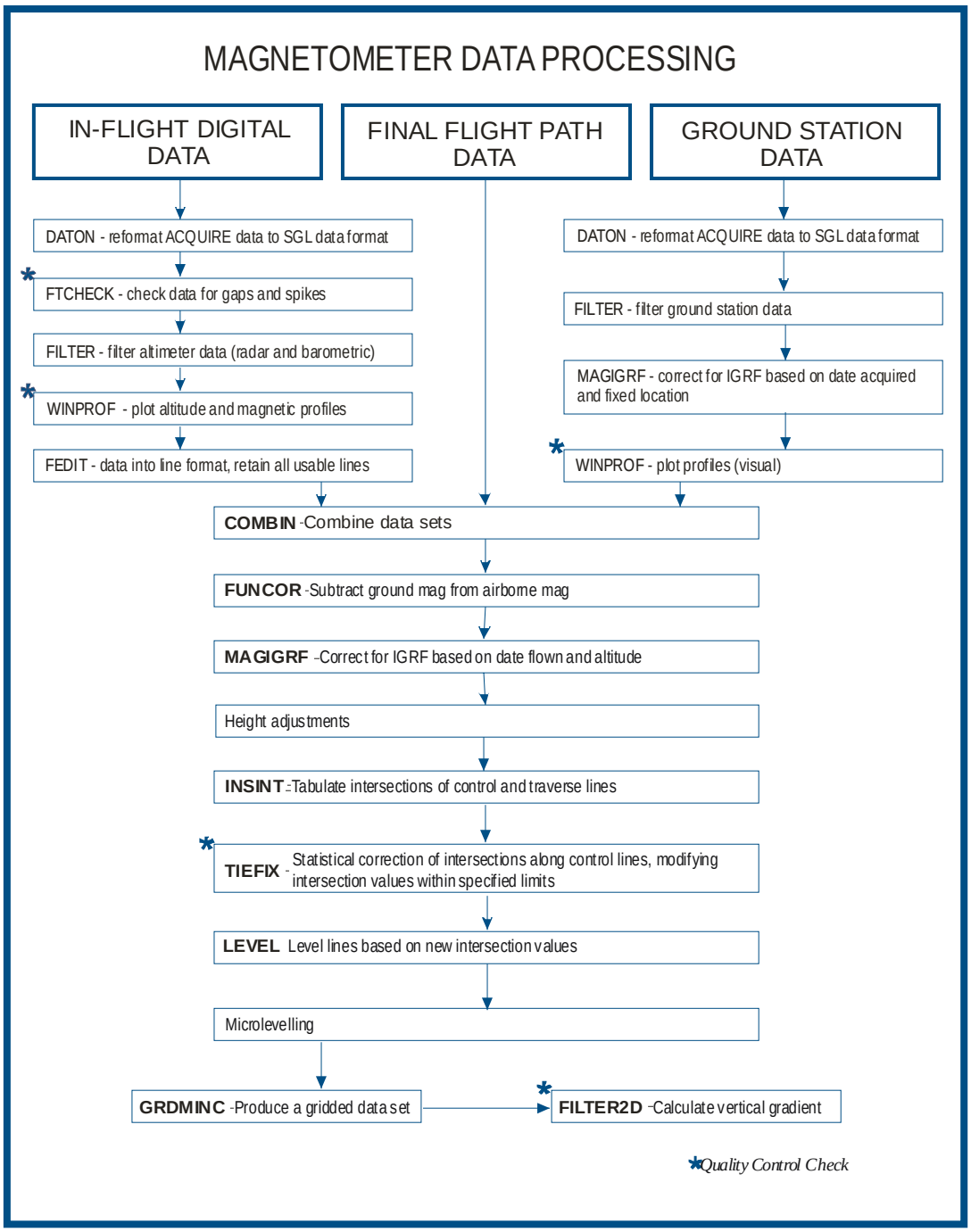

Figure 26: Magnetic Data Flow Chart

RADIOMETRIC DATA

A 0.5 second lag correction was applied to all data to correct for the time delay between detection and recording of the airborne data. The data were recorded at 1 Hz in asynchronous mode, and subsequently interpolated to 1 Hz synchronous data on the exact second.

Spectral Component Analysis

Raw 256 channel spectrometer data were analysed using noise adjusted singular value decomposition (NASVD; J. Hovgaard and R L. Grasty paper 98; Geophysics and

Geochemistry at the Millennium, Proceedings of the 4th Decennial International Conference on Mineral Exploration, 1997). Normalization with respect to the count rate is achieved by dividing each measured spectra by the square root of the best fit of the mean spectra, i.e. component zero. The NASVD method determines the components in order of significance with respect to the amount of variance in the data they describe. Each component is a spectrum with 256 channels. In theory, there are as many components as there are channels. Variation in the signal is accounted for by the low order components, and variation due to noise is accounted for by the higher order components. Inspection of the components allows us to determine which components describe the signal. It also facilitates the discarding of the noise components. Spectra are then reconstructed from the signal only components, and the count rates in the standard windows are recalculated.

Through such an analysis, the results suggest that components higher than order 19 are predominantly noise. The NASVD correction was applied to the entire dataset. Line data and grid based comparison with non-NASVD corrected data indicated that no geological signal was removed by applying NASVD.

A spectrometer data compilation flowchart is presented in Figure 27. Charts of the first 19 NASVD components are found in Appendix VI.

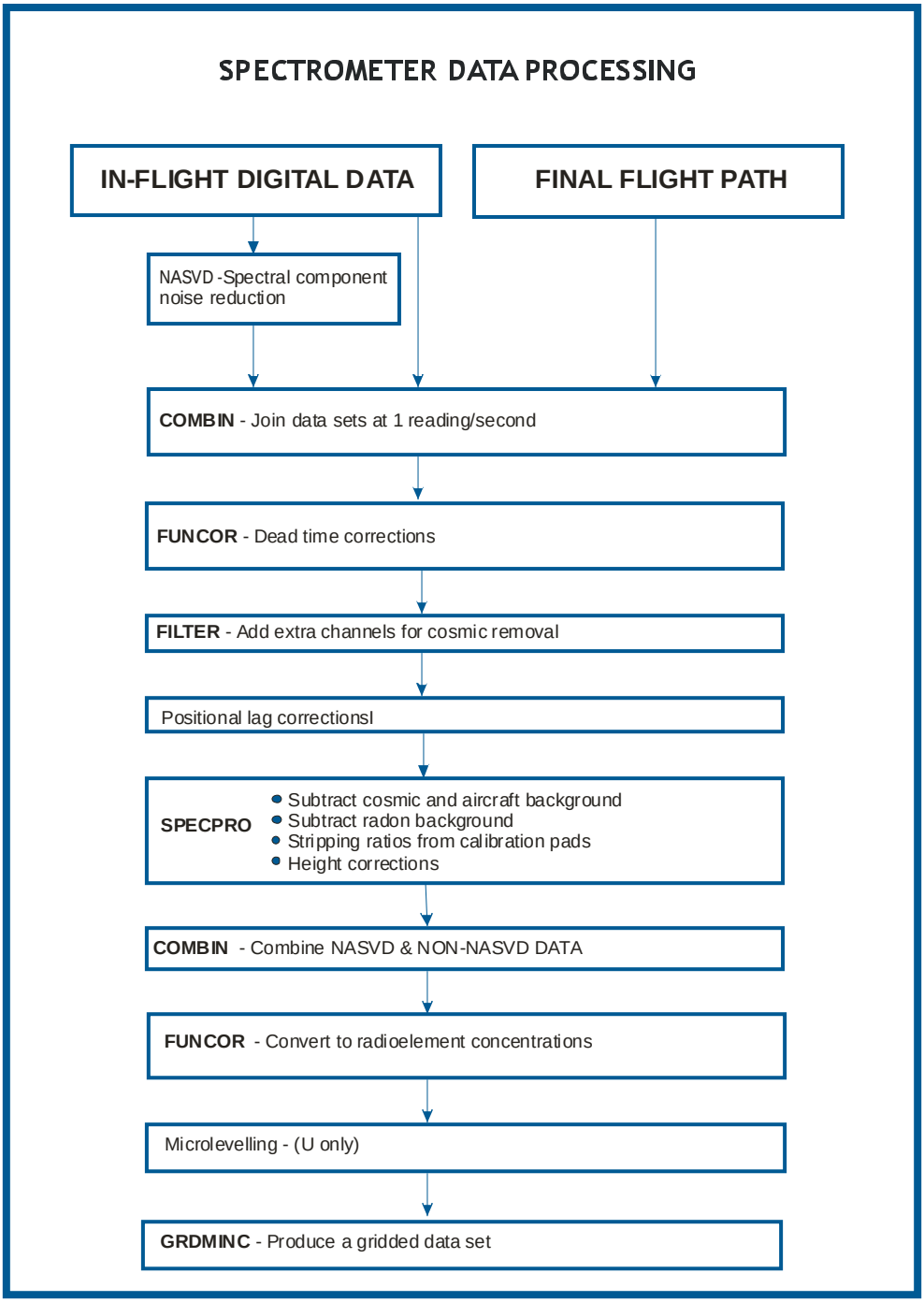

Figure 27: Spectrometer Data Compilation Flowchart

Standard Corrections

Spectrometer data were corrected as documented in the Geological Survey of Canada Open File No. 109 and the IAEA report "Airborne gamma-ray spectrometer surveying; Technical Report Series No. 323 (International Atomic Energy Agency, Vienna). The gamma-ray spectroscopy processing parameters are described in *Table X*. The parameters are predominately based on pre-survey test results but are further refined during data processing.

Table 4: Spectrometer Processing Parameters

Spectrometer Processing Parameters		
Spectrometer EXPLORANIUM, Model GR-820, S.N. 8245, 12 DOWN and 2 UP		
Window	Cosmic Stripping Ratio (b)	Aircraft Background (a)
Total	0.7012	51.99
Potassium	0.0426	7.11
Uranium	0.0336	0.47
Thorium	0.0365	0.31
Upward	0.0065	0.13
Radon Component	a	b
Total (I_r)	13.6258	6.104
Potassium (K_r)	0.7345	1.0177
Thorium (T_r)	0.0000	0.0000
Up (u_r)	0.2476	0.0428
Ground Component	a_1	a_2
Up (u_g)	0.04	0.01
Stripping Ratios	Contribution on the Ground	Effective Height Adjustment (m^{-1})
α	0.2555	0.00049
β	0.3806	0.00065
γ	0.7431	0.00069
a	0.0457	
b	0.0000	
g	0.0034	
Attenuation Coefficients (m^{-1})		
Total	-0.006905	
Potassium	-0.008507	
Uranium	-0.006983	
Thorium	-0.006722	
Sensitivities		
Potassium	105.4191 cps/%	
Uranium	12.1078 cps/eU ppm	
Thorium	5.6641 cps/eTh ppm	

Before gridding, the following corrections are applied to the spectrometer data in the order shown:

Dead time correction

The system live time is recorded by the spectrometer and represents the time that the system was available to accept incoming gamma radiation pulses. Live time is reduced, and dead time increased, as count rates increase and the time taken by the spectrometer to process measured pulses increases. The cosmic channel does not receive a dead-time correction as it is processed by separate circuitry in a GR820 spectrometer. The dead-time correction is applied to each window in both the upward and downward looking detector data using the following equation:

$$N = n / t$$

where: N = the corrected count rate in each channel
n = the raw count recorded in each second
t = the recorded live time (fraction of a second).

Calculation of effective height above ground level (AGL)

A moving average filter of 99 data points is applied to 10 Hz radar barometric and processed laser altimeter data. The barometric altimeter data is then converted to equivalent pressure, and used with the digitally recorded temperature to convert the radar altimeter data to effective height at standard pressure and temperature (STP) as follows:

$$h_e = h \times \frac{273.15}{T + 273.15} \times \frac{P}{101.325}$$

Correction for distance between GPS antenna and spectrometer (lag-correction)

A dynamic speed dependent lag correction was applied to the data for the 5.56m distance between spectrometer and GPS antenna. This provides a consistence time-stamp and positional match between spectrometer and positional data.

Height adaptive filter

Adaptive filters were applied to the gamma ray data to improve the signal-to-noise ratio. A moving average filter is applied to data of Total counts, Thorium and Potassium flown at 300 m and the degree of filtering applied increases gradually up to 400 m. For Uranium data, a moving average filter is applied to data flown at 150 m and the degree of filtering applied increases gradually up to 400 m. Data collected at a terrain clearance greater than 350 m for Total counts, Thorium and Potassium and 325 m for Uranium are considered unreliable due to the low count rates and consequent low signal to noise ratio and were removed from the data set and set as null.

Removal of cosmic radiation and aircraft background radiation

A 67-point low pass filter is applied to 1 Hz Cosmic data to reduce statistical noise. Cosmic radiation and aircraft background radiation are removed from each spectral window using the cosmic coefficients and aircraft background radiation values determined from test flight data using the following equation:

$N = a + bC$

where: N = the combined cosmic and aircraft background in each spectral window,
a = the aircraft background in the window,
b = the cosmic stripping factor for the window, and
C = the cosmic channel count.

Radon background corrections

A moving average filter of 99 data points is applied to 1 Hz downward uranium, downward thorium and upward uranium count data for the purposes of the radon correction only. The radon component in the uranium window is calculated using the radon coefficients determined from the survey data using the following equation:

$$U_r = \frac{u - a_1 U - a_2 T + a_2 b_T - b_u}{a_u - a_1 - a_2 a_T}$$

where: U_r = the radon background measured in the downward uranium window,
u = the filtered observed count in the upward uranium window,
U = the filtered observed count in the downward uranium window,
T = the filtered observed count in the downward thorium window,
a_1 and a_2 = the ground coefficients,
a_u and b_u = the radon coefficients for uranium,
a_T and b_T = the radon coefficients for thorium.

The radon counts in the total count, potassium and thorium downward windows are then calculated from U_r using the following equations:

$u_r = a_u U_r + b_u$
$K_r = a_K U_r + b_K$
$T_r = a_T U_r + b_T$
$I_r = a_I U_r + b_I$

Where u_r is the radon component in the upward uranium window, K_r, U_r, T_r and I_r are the radon components in the various windows of the downward detectors, and a and b are the radon calibration coefficients.

Radon background was monitored through the use of two upward looking detectors. Coefficients relating the count rate in the uranium window from the upward detectors to the count rate in the potassium, uranium, thorium and total count windows from the downward facing detectors were determined using 17 over-water test lines flown over Lower Lough Erne.

The cosmic and background corrected data from each of the Up (ur), Thorium (Tr), Potassium (Kr) and Total (Ir) windows are plotted against the counts in the Uranium (Ur) window for each over-water line flown. Linear regressions of these plots provide the radon coefficients to be used in the radiometric data processing. The results are shown in *Figure 28*. The coefficients determined for this survey are presented in *Table 4*.

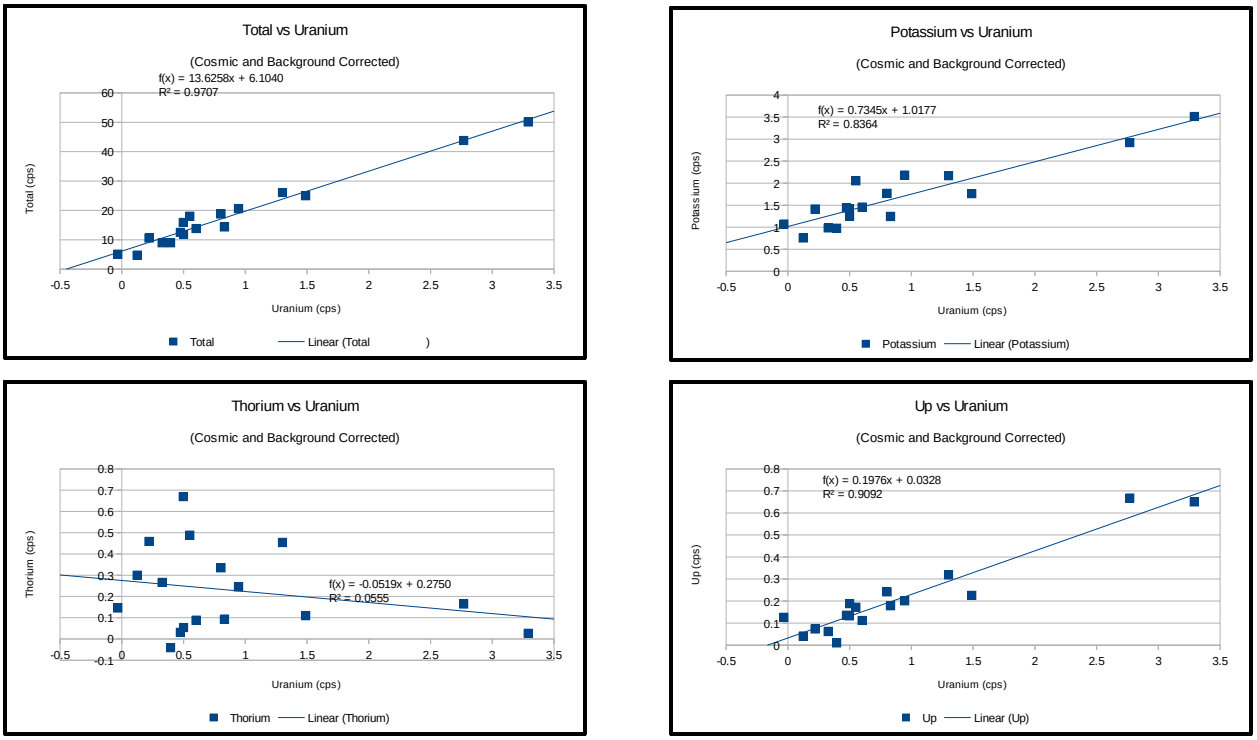

Figure 28: Radon Calibration Data

Stripping

The stripping ratios for the spectrometer system are determined experimentally. The stripped count rates for the potassium, uranium and thorium downward windows are calculated using the following equations:

$$N_K = \frac{n_{Th}(\alpha\gamma - \beta) + n_U(\alpha\beta - \gamma) + n_K(1 - a\alpha)}{A}$$

$$N_U = \frac{n_{Th}(g\beta - \alpha) + n_U(1 - b\beta) + n_K(b\alpha - g)}{A}$$

$$N_{Th} = \frac{n_{Th}(1 - g\gamma) + n_U(b\gamma - a) + n_K(ag - b)}{A}$$

where A has the value:

$$A = 1 - g\gamma - a(\gamma - gb) - b(\beta - \alpha\gamma)$$

and where:

n_K, n_U and n_{Th} = the unstripped potassium, uranium and thorium downward windows counts,

N_K, N_U and N_{Th} = the stripped potassium, uranium and thorium downward windows counts,

α, β, and γ = the forward stripping ratios, and

a, b and g = the reverse stripping ratios.

α, β, and γ are adjusted for effective height (as calculated above) by standard factors given in *Table 4 (Spectrometer Processing Parameters)*.

Altitude attenuation correction

This correction normalizes the data to a constant terrain clearance of 56 m above ground level (AGL) at standard temperature and pressure (STP). Attenuation coefficients for each of the downward windows are determined from test flights. The measured count rate is related to the actual count rate at the nominal survey altitude by the equation:

$$N_s = N_m(e^{\mu(h_o - h)})$$

where: N_s = the count rate normalized to the nominal survey altitude, h_o,
N = the background corrected, stripped count rate at effective height h,
μ = the attenuation coefficient for that window,
h_o = the nominal survey altitude, and
h = the effective height.

The effective height is determined in step 2.

Conversion to radio element concentration

Sensitivities are determined experimentally from the test flight data. The units of the count rates in each spectral window are converted to "Apparent Radio Element Concentrations" using the following equation:

where: C = the concentration of the element(s)
N = the count rate for the window after correction for dead time, background, stripping and attenuation
S = the broad source sensitivity for the window.

Potassium concentration is expressed as a percentage and equivalent uranium and thorium as parts per million of the accepted standards. Uranium and thorium are described as "equivalent" since their presence is inferred from gamma-ray radiation from daughter elements (Bi-214 for uranium, Tl-208 for thorium).

Data gridding

A minimum curvature gridding algorithm was considered most appropriate in order to preserve detail in the data. The method generates a 2-dimensional grid, equally incremented in x and y, from randomly placed data points. The algorithm (I.C.Briggs, 1974, Geophysics, v 39, no. 1) produces a smooth grid by iteratively solving a set of difference equations that minimize the total second horizontal derivative and attempt to honour input data. Spectrometer data within cells are combined with a cosine weighting

function before the minimum curvature surface is fitted.

The radiometric data were interpolated to a 50 m grid cell size appropriate for survey lines spaced at 200 m. Control and test lines were not included in the grids.

Correction for effects of precipitation

The survey test line averages for thorium were consistent throughout the duration of the survey (generally within +/- 10%), and no alterations to account for precipitation were applied.

Radar, Barometric, and Laser Altimeter Data

The terrain clearance measured by the radar altimeter and the barometric altitude, in metres, were recorded at 10 Hz.

The laser altimeter recorded terrain clearance at 3.3 Hz. Even though the laser altimeter can record returns up to 700 m above the ground with a high degree of certainty, some laser data dropouts occurred while flying over high hills and cliffs.

The radar altimeter records the first return within the footprint of its signal, and therefore tends to penetrate any tree cover less than the laser altimeter. The radar altimeter data were filtered to remove high-frequency noise using a 67-point low pass filter. The final data were plotted and inspected for quality.

A digital elevation model (DEM) was derived by subtracting the laser altimeter data from the differentially corrected DGPS altitude with respect to Mean Sea Level. Short sections of poor laser data due to high flying height when over flying cliffs were interpolated. The interpolated data was checked against the TRT radar data and the Shuttle Radar Terrain Mission (SRTM) data to ensure validity. Where variations arose between the interpolated DEM and SRTM data, minor levelling was applied.

Micro-levelling was also applied to a few isolated areas of the DEM. This was done to remove minor over water effects that occur due to tides and variable penetration of the radar into the water depending on wave conditions. Micro-levelling was achieved by using a combined directional cosine filter and high pass Butterworth filter to identify and remove artefacts that are long wavelength parallel to survey lines and short wavelengths perpendicular to survey lines. A limit of +/-2.50 m was set for all micro-levelling corrections. The DEM is provided as a grid with a 50 m cell size.

Positional Data

A number of programs were executed for the compilation of navigation data in order to reformat and recalculate positions in differential mode. SGL's GPS data processing package, GPSoft, was used to calculate DGPS positions from raw 10 Hz range data obtained from the moving (airborne) and stationary (ground) receivers using combinations of L1 and L2 phase signal.

The GPS data were processed using a number of different signal combinations resulting in multiple position solutions for each flight. The various solutions were automatically ranked based on accuracy and smoothness and the best solution for each individual line was

selected. This automatic selection process results in accuracy of greater than 1 m and good coherency between survey lines.

Accurate locations of the GPS antennas were determined by differentially correcting the SGL reference station position data using permanent GPS reference stations. This technique provides a final receiver location with an accuracy of better than 5 cm. The entire airborne data set was processed differentially using the calculated reference station location.

Positional data (X, Y, Z) were recorded and all data processing was performed in the WGS-84 datum. The delivered data were provided in X, Y locations with respect to the Irish National Grid 1975 datum. Please see Table 2 for datum conversion parameters to WGS-84 and Table 3 for projection parameters.

Table 5: Datum Parameters for Irish National Grid

Ellipsoid:	Airy-1849
Semi-major axis:	6 377 340.189
1/flattening:	299.3249646
Δx:	482.53 m
Δy:	-130.596 m
Δz:	564.557 m
x rotation:	5.05175856e-6 radians
y rotation:	1.03750128e-6 radians
z rotation:	3.05917433e-6 radians
Scale factor:	8.15e-6

Table 6: Projection Parameters for Irish National Grid

Map Projection	Transverse Mercator
True Origin	Latitude 53°30'00" Longitude 08°00'00"
False origin	200 000m West of true origin 250 000m South of true origin
Scale factor on Central Meridian	1.000035

Elevation data were recorded relative to the GRS-80 ellipsoid and transformed to mean sea level (MSL) using the Earth Gravity Model 2008.

FINAL PRODUCTS

Magnetic Line Data Format (sampling rate 10 Hz)

Profile data in ASCII format containing the following data channels:

Name	Format	Units	Description
DATE	A9	-	Date YYYYMMDD
DAY	A5	-	Day of year
FLIGHT	A7	-	Flight number
LINE	A10	-	Line number - LLLL.SR (L=line, S=segment, R=reflight)
TIME	A11	s	UTC seconds past midnight
FIDUCUAL	F11.2	-	Continuous seconds
RADAR_ALT	F11.2	m	Radar Altimeter height
RAW_RADAR	F11.2	m	Raw Radar Altimeter height
LASER_ALT	F11.2	m	Laser Altimeter height
RAW_LASER	F11.2	m	Raw Laser Altimeter height
X-IRISH-NG	F15.2	m	X coordinate, Irish National Grid
Y-IRISH-NG	F15.2	m	Y coordinate, Irish National Grid
X-IRISH-W	F15.2	m	X coordinate, Irish National Grid, WING mag
Y-IRISH-W	F15.2	m	Y coordinate, Irish National Grid, WING mag
MSLHGT	F11.2	m	Mean Sea Level Altitude
LAT	F13.7	degree	Latitude
LONG	F13.7	degree	Longtitude
LAT-W	F13.7	m	Latitude, WING mag
LONG-W	F13.7	m	Longitude, WING mag
WGSHGT	F11.2	m	WGS-84 Altitude
HEADING	F11.3	deg	Aircraft heading
DIURNAL	F11.3	nT	IGRF corrected and average removed ground station data
IGRF	F11.3	nT	Airborne IGRF correction
RAWMAG2	F11.3	nT	Raw compensated WING mag
DICMAG2	F11.3	nT	Diurnally and IGRF corrected WING mag
LEVMAG2	F11.3	nT	Levelled WING mag

Spectrometer Data Format (sampling rate 1 Hz)

Profile data in ASCII format containing the following data channels:

Name	Format	Units	Description
DATE	A9	-	Date YYYYMMDD
DAY	A5	-	Day of year
FLIGHT	A7	-	Flight number
LINE	A10	-	Line number - LLLL.SR (L=line, S=segment, R=reflight)
TIME	A11	s	UTC seconds past midnight
FIDUCIAL	F11.2	-	Continuous seconds
X-IRISH-NG	F15.2	m	X coordinate, Irish National Grid
Y-IRISH-NG	F15.2	m	Y coordinate, Irish National Grid
MSLHGT	F11.2	m	Mean Sea Level Altitude
WGSHGT	F11.2	m	WGS-84 Altitude
ALTIMETER	F11.2	m	Altimeter height
BARO	F11.1	m	Barometric Altitude
TEMP	F11.1	celsius	Temperature
LIVE	F11.3	msec	Live Time
COSMIC	F11.2	counts/s	Recorded Cosmic Count
UP	F11.2	counts/s	Recorded Upward Uranium Count
RAW_TOT	F11.2	counts/s	Recorded Total Count
RAW_K	F11.2	counts/s	Recorded Potassium Count
RAW_U	F11.2	counts/s	Recorded Uranium Count
RAW_TH	F11.2	counts/s	Recorded Thorium Count
COR_TOT	F11.2	counts/s	Corrected Total Count,de-lagged
E_Dose	F11.2	nGy/hr	Air absorbed dose rate,de-lagged
COR_K	F11.2	%	Corrected Potassium Concentration,de-lagged
COR_U	F11.2	ppm	Corrected Uranium Concentration,de-lagged
COR_TH	F11.2	ppm	Corrected Thorium Concentration,de-lagged
C_Uml	F11.2	ppm	Corrected Uranium Concentration, microlevelled and de-lagged
COR_TOTL	F11.2	counts/s	Corrected Total Count,de-lagged and minimum limited to 0
E_DoseL	F11.2	nGy/hr	Air absorbed dose rate,de-lagged and minimum limited to 0
COR_KL	F11.2	%	Corrected Potassium Concentration,de-lagged and minimum limited to 0
COR_UL	F11.2	ppm	Corrected Uranium Concentration,de-lagged and minimum limited to 0
COR_THL	F11.2	ppm	Corrected Thorium Concentration,de-lagged and minimum limited to 0
C_UmlL	F11.2	ppm	Corrected Uranium Concentration, microlevelled,de-lagged and minimum limited to 0
LAT	F13.7	degree	Latitude
LONG	F13.7	degree	Longtitude

Electromagnetic Data Format (sampling rate 1 Hz)

Profile data in ASCII format containing the following data channels:

Name	Format	Units	Description
DATE	A9	-	Date YYYYMMDD
DAY	A5	-	Day of year
FLIGHT	A7	-	Flight number
LINE	A10	-	Line number - LLLL.SR (L=line, S=segment, R=reflight)
TIME	A11	s	UTC seconds past midnight
FIDUCIAL	F11.2	-	Continuous seconds
X-IRISH-NG	F15.2	m	X coordinate, Irish National Grid
Y-IRISH-NG	F15.2	m	Y coordinate, Irish National Grid
LAT	F13.7	degree	Latitude
LONG	F13.7	degree	Longtitude
MSLHGT	F11.2	m	Mean Sea Level Altitude
WGSHGT	F11.2	m	WGS-84 Altitude
RRADAR	F11.1	m	Raw Radar altimeter
RADAR	F11.1	m	Final Radar altimeter
RLASER	F11.2	m	Raw Laser altimeter
LASER	F11.2	m	Final Laser altimeter
HEADING	F11.2	deg	Aircraft heading
P09	I11	ppm	In-phase coupling ratio, 912 Hz
Q09	I11	ppm	Quadrature coupling ratio, 912 Hz
P3	I11	ppm	In-phase coupling ratio, 3005 Hz
Q3	I11	ppm	Quadrature coupling ratio, 3005 Hz
P12	I11	ppm	In-phase coupling ratio, 11962 Hz
Q12	I11	ppm	Quadrature coupling ratio, 11962 Hz
P25	I11	ppm	In-phase coupling ratio, 24510 Hz
Q25	I11	ppm	Quadrature coupling ratio, 24510 Hz
P09L	I11	ppm	In-phase coupling ratio, 912 Hz, levelled
Q09L	I11	ppm	Quadrature coupling ratio, 912 Hz, levelled
P3L	I11	ppm	In-phase coupling ratio, 3005 Hz, levelled
Q3L	I11	ppm	Quadrature coupling ratio, 3005 Hz, levelled
P12L	I11	ppm	In-phase coupling ratio, 11962 Hz, levelled
Q12L	I11	ppm	Quadrature coupling ratio, 11962 Hz, levelled
P25L	I11	ppm	In-phase coupling ratio, 24510 Hz, levelled
Q25L	I11	ppm	Quadrature coupling ratio, 24510 Hz, levelled
PLM	F11.3	mV	Power line monitor
Res09	F11.3	Ohm-m	Apparent resistivity, half-space model, 912 Hz
Res3	F11.3	Ohm-m	Apparent resistivity, half-space model, 3005 Hz
Res12	F11.3	Ohm-m	Apparent resistivity, half-space model, 11962 Hz
Res25	F11.3	Ohm-m	Apparent resistivity, half-space model, 24510 Hz

Digital Grids

The following are provided as digital grids in Grid Exchange Format (GXF) and ASCII XYZ format, in the Irish National Grid datum, UTM Zone 29N:

Grid File Name	Units	Grid Cell Size	Description
tmit_ING	NT	50	Total Magnetic Intensity
tot-G	counts/s	50	Total Counts
pot-G	%	50	Potassium Concentration
ura-G	ppm	50	Equivalent Uranium Concentration
tho-G	ppm	50	Equivalent Thorium Concentration
P09	ppm	50	In-phase coupling ratio, 912 Hz, levelled
Q09	ppm	50	Quadrature coupling ratio, 912 Hz, levelled
P3	ppm	50	In-phase coupling ratio, 3005 Hz, levelled
Q3	ppm	50	Quadrature coupling ratio, 3005 Hz, levelled
P12	ppm	50	In-phase coupling ratio, 11962 Hz, levelled
Q12	ppm	50	Quadrature coupling ratio, 11962 Hz, levelled
P25	ppm	50	In-phase coupling ratio, 24510 Hz, levelled
Q25	ppm	50	Quadrature coupling ratio, 24510 Hz, levelled
Res09	Ohm-m	50	Apparent resistivity, half-space model, 912 Hz
Res3	Ohm-m	50	Apparent resistivity, half-space model, 3005 Hz
Res12	Ohm-m	50	Apparent resistivity, half-space model, 11962 Hz
Res25	Ohm-m	50	Apparent resistivity, half-space model, 24510 Hz

PROJECT SUMMARY

SURVEY TITLE:

Survey Location: Northern Ireland
Survey Duration: October 26, 2011 to July 15, 2012

Client: Geological Survey of Ireland and Geological Survey of Northern Ireland

Contact: Mike Young
mike.young@detini.gov.uk

Technical Inspector: James Hodgson
Jim.Hodgson@dcenr.gov.ie

Reference Station Location #1: GND1 54º23'49.60”N 7º38'47.73''W 105.71 m
Reference Station Location #2: GND2 54º26'52.00''N 7º39'08.11''W 112.72 m

Field Office Location: Enniskillen Airport

Airport Used: Enniskillen Airport (EGAB)

Digital Terrain source: SRTM (srtm.usgs.gov)

SURVEY SPECIFICATIONS

Magnetic Field in Survey Area: (54°24’ N 7° 39’ W)
Inclination (+ve down): 68.62°
Declination (+ve east): -4.87°
Total Magnetic Intensity: 49398 nT

Traverse lines:
Line numbers: 1001 to 1946
Line direction: N15ºW
Line spacing: 200 m

Control lines:
Line numbers: 101 to 201
Line direction: N75ºE
Line spacing: 2,000 m

Survey altitude: Radar guidance with target height of 59 m.

Flight numbers: 001 to 177
Datum: Irish National Grid
Projection: Transverse Mercator True origin N53.5

FIELD PERSONNEL

Project Manager: Reed Archer
Field Ops. Manager: Jenrené Martel, Alison McCleary, Marianne McLeish
Data Processors: Joël Dubé, Monika Pal
Pilots: Steve Gebhardt, Todd Svarckopf, Charles Dicks, Clinton Elliott
Aircraft Maintenance Engineer: Landen Coulas, John Sevenhuysen, John Burnham

DATA PROCESSING PERSONNEL

Manager: Martin Bates
Magnetic Data: Sara-Michèle Rochon, Marianne McLeish, Kristen Matsumoto
Electromagnetic Data: Monika Pal, Sol Meyer
Spectrometer Data: Andreas Prokoph
Report Compiled by: Monika Pal, B.Sc., Sol Meyer, B.Sc., Martin Bates, Ph.D., Alex Taylor